AD_____

Award Number: DAMD17-02-1-0457

TITLE: Evaluation of Novel Agents which Target Neovasculature of Breast Tumors

PRINCIPAL INVESTIGATOR: Michael Rosenblum, Ph.D.

CONTRACTING ORGANIZATION: The University of Texas
M.D. Anderson Cancer Center
Houston, TX 77030

REPORT DATE: April 2005

TYPE OF REPORT: Annual

PREPARED FOR: U.S. Army Medical Research and Materiel Command
Fort Detrick, Maryland 21702-5012

REPORT DOCUMENTATION PAGE

Form Approved
OMB No. 0704-0188

1. REPORT DATE *(DD-MM-YYYY)*	2. REPORT TYPE	3. DATES COVERED *(From - To)*
01-04-2005	Annual	1 Apr 2004 - 31 Mar 2005

4. TITLE AND SUBTITLE

Evaluation of Novel Agents which Target Neovasculature of Breast Tumors

5a. CONTRACT NUMBER

5b. GRANT NUMBER
DAMD17-02-1-0457

5c. PROGRAM ELEMENT NUMBER

6. AUTHOR(S)

Michael Rosenblum, Ph.D.

5d. PROJECT NUMBER

5e. TASK NUMBER

5f. WORK UNIT NUMBER

7. PERFORMING ORGANIZATION NAME(S) AND ADDRESS(ES)

The University of Texas
M.D. Anderson Cancer Center
Houston, TX 77030

8. PERFORMING ORGANIZATION REPORT NUMBER

9. SPONSORING / MONITORING AGENCY NAME(S) AND ADDRESS(ES)

U.S. Army Medical Research and Materiel Command
Fort Detrick, Maryland 21702-5012

10. SPONSOR/MONITOR'S ACRONYM(S)

11. SPONSOR/MONITOR'S REPORT NUMBER(S)

12. DISTRIBUTION / AVAILABILITY STATEMENT

Approved for Public Release; Distribution Unlimited

13. SUPPLEMENTARY NOTES

Original contains color plates: ALL DTIC reproductions will be in black and white

14. ABSTRACT – SEE ATTACHED PAGE

15. SUBJECT TERMS

Fusion Toxins, Co-Culture Studies, Hypoxia, MDA-MB-231, Gene Array Analysis, Vascular Targeting, Pharmacology

16. SECURITY CLASSIFICATION OF:			17. LIMITATION OF ABSTRACT	18. NUMBER OF PAGES	19a. NAME OF RESPONSIBLE PERSON
a. REPORT	b. ABSTRACT	c. THIS PAGE			19b. TELEPHONE NUMBER *(include area code)*
U	U	U	UU	169	

Abstract

The unique fusion toxin $VEGF_{121}$/rGel can specifically kill both log-phase and confluent vascular endothelial cells expressing the KDR receptor for VEGF(PNAS 99:7866,2002). We have discovered 22 unique genes consistently upregulated in endothelial cells treated with $VEGF_{121}$/rGel(confirmed by Western and RT-PCR).$VEGF_{121}$/rGel(i.v.) treatment had a dramatic cytotoxic effect in both orthotopic and metastatic human breast tumor models. Against the orthotopic model, tumor growth was significantly delayed by~50%. In addition, tumors completely regressed in 3/6 (50%) of treated mice. In the metastatic breast model, treatment with $VEGF_{121}$/rGel reduced both the number and area of lung foci by 58% and 50% respectively and we demonstrated $VEGF_{121}$/rGel(by IHC) on lung tumor vasculature but not normal vasculature. In addition, the number of blood vessels per mm^2 in metastatic foci was 198 $\pm$ 37 versus 388 $\pm$ 21 for treated and control respectively. Approximately 62% of metastatic colonies from the VEGF/rGel treated group had <10 vessels/colony compared to 23% in the control group. The flk-1 receptor on blood vessel endothelium was intensely expressed on control tumors, but not expressed on treated tumors. Metastatic foci had a 3 fold lower Ki-67 labeling index compared to control tumors. This suggests that $VEGF_{121}$/rGel has impressive antitumor activity in breast cancer.

Table of Contents

Evaluation of Novel Agents Which Target Neovasculature of Breast Tumors

Introduction

Biological studies examining the development of the vascular tree in normal development and in disease states have identified numerous cytokines and their receptors responsible for triggering and maintaining this process *(1-7)*. Tumor neovascularization is central not only to the growth and development of the primary lesion but appears to be a critical factor in the development and maintenance of metastases *(8-12)*. For example, clinical studies in bladder cancer *(9)* have demonstrated a correlation between micro-vessel density and metastases. In addition, studies of breast cancer metastases by Fox et al. and Aranda et al *(11-12)* have demonstrated that microvessel count in primary tumors appears to be related to the presence of metastases in lymph nodes and micrometastases in bone marrow.

The cytokine vascular endothelial growth factor-A (VEGF-A) and its receptors Flt-1(Receptor 1, R1) and KDR(Receptor 2, R2) have been implicated as one of the central mediators of normal angiogenesis and tumor neovascularization *(13-20)*. Up-regulation or over-expression of KDR or VEGF-A have been implicated as poor prognostic markers in various clinical studies of colon, breast and pituitary cancers *(21-23)*. Recently, Padro et al *(24)* have suggested that both VEGF-A and KDR may play a role in the neovascularization observed in bone marrow during AML tumor progression and may provide evidence that the VEGF/KDR pathway is important in leukemic growth particularly in the bone marrow.

For these reasons, there have been several groups interested in developing therapeutic agents and approaches targeting the VEGF-A pathway. Agents which prevent VEGF-A binding to its receptor, antibodies which directly block the KDR receptor itself and small molecules which block the kinase activity of the KDR and thereby block growth factor signaling are all under development *(25-37)*. Recently, our laboratory reported the development of a growth factor fusion construct of $VEGF_{121}$ and the recombinant toxin gelonin *(38)*. Our studies demonstrated that this agent was specifically cytotoxic only to cells expressing the KDR receptor and was not cytotoxic to cells over-expressing the Flt-1 receptor. In addition, this agent was shown to localize within tumor vasculature and caused a significant damage to vascular endothelium in both PC-3 prostate and MDA-MB-231 orthotopic xenograft tumor models.

The current study seeks to extend our original observations describing the in vitro biological effects of this novel fusion construct and we examined the effects of this agent in both orthotopic and metastatic tumor models.

Progress Report Body:

Original SOW:

1. **Establish In Vivo Activity of the $VEGF_{121}$/rGel Fusion Toxin in the MDA-MB231 Tumor Models**

Task 1: Radiolabeling

Numerous methods were employed initially to label the target protein. We settled on using Bolton-Hunter reagent which generated the highest yield of material capable of specific binding to purified, immobilized KDR receptor. Highly purified $VEGF_{121}$/rGel was radiolabeled using ^{125}I with this reagent and the material was adjusted to a specific activity of 602 Ci/mMol.

Task 2: Tissue Distribution

Mice bearing orthotopically-placed MDA-MB231 tumors were administered 4 μCi of $VEGF_{121}$/rGel(i.v., tail vein). At 24 and 48 hrs after administration, groups of 6 mice were sacrificed and various organs were excised, weighed and counted to determine ^{125}I activity.

As shown in this figure, the highest concentration of radiolabel was found in kidney> liver>tumor> spleen. At 48 hrs, the tissue:blood ratio in these organs increased particularly for kidney and tumor. The high levels found in kidney may be related to high levels of the flt-1 receptor found in this organ.

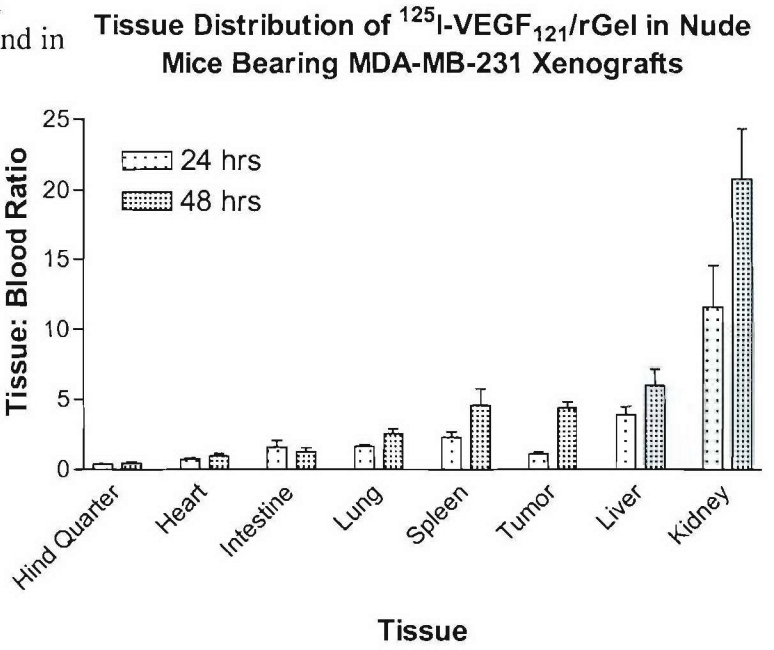

The pharmacokinetics of $VEGF_{121}$/rGel were additionally described using this radiolabeled material. Balb/c mice were injected with 1 μCi of labeled material and at various times after administration, groups of 3 mice were sacrificed and blood samples were removed and centrifuged. Aliquots of plasma were counted to determine radioactivity and the results were analyzed for conventional pharmacokinetic analyses using conventional mathematical modeling(pK Analyst from MicroMath, Inc). As shown in the figure below, the $VEGF_{121}$/rGel cleared from plasma with initial and terminal half-lives of 0.3 and 6h respectively. Therefore this agent has a relatively long half-life despite the significant uptake in kidney.

Clearance of $VEGF_{121}$/rGel From Plasma

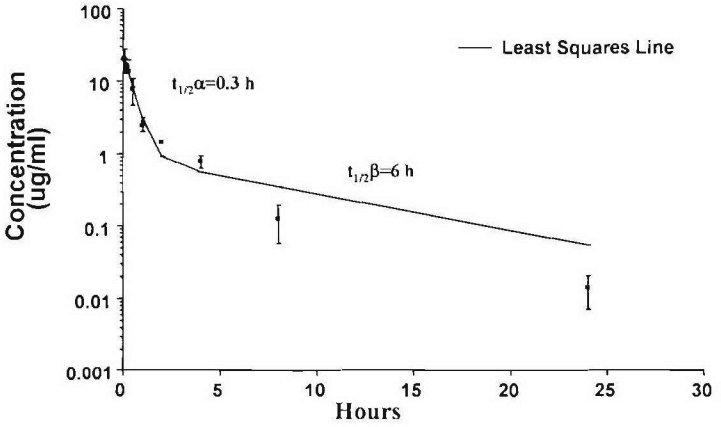

Task 3: Antitumor Effects-Orthotopic Model

Given the pharmacokinetic and tissue distribution data described above, we designed a treatment schedule comprised of 5 injections spaced 48 hrs apart(10 day course). Using this schedule, we delineated the Maximum Tolerated Dose as this schedule to be ~40 mg/kg. The effect of $VEGF_{121}$/rGel administration on orthotopically-placed MDA-MB-231 tumor bearing mice(6 per group) is shown in the Figure below. As shown, treatment significantly retarded tumor growth. In addition, 3/6 mice in the treated group demonstrated complete disappearance of the tumor compared to 0/6 in the saline-treated group.

Effect of $VEGF_{121}$/rGel on Orthotopically Placed MDA-MB-231 Tumor Cells in Nude Mice

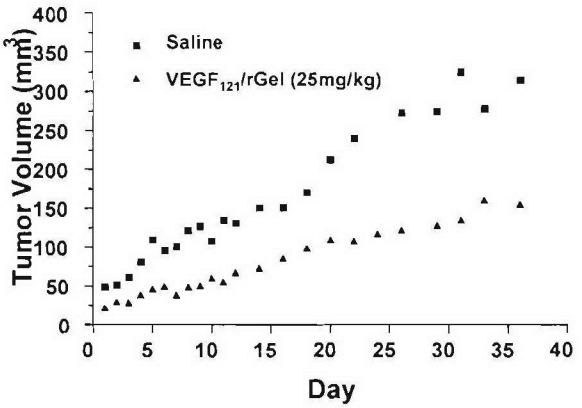

Task 4: Antitumor Effects-Metastatic Model

We evaluated the effect of $VEGF_{121}$/rGel fusion toxin treatment on the growth of metastatic MDA-MB-231 tumor cells in nude mice. Tumor cells ($0.5x10^6$ per mouse) were injected i.v. and 8 days after innoculation, mice (6 per group) were treated 6 times either with $VEGF_{121}$/rGel (100 μg/dose) or free gelonin. Three weeks after treatment, mice were sacrificed and the lungs were harvested and examined. The surface lung foci in the $VEGF_{121}$/rGel – treated mice were reduced by 58 % as compared to gelonin control animals (means were 22.4 and 53.3 for $VEGF_{121}$/rGel and control, respectively; $p<0.05$). The mean area of lung colonies from $VEGF_{121}$/rGel-treated mice was also 50% smaller than control mice (210 ± 37 μm versus 415 ± 10 μm for $VEGF_{121}$/rGel and control, respectively; $p< 0.01$). In addition, the vascularity of metastatic foci as assessed by the mean number of blood vessels per mm^2 in metastatic foci was significantly reduced (198 ± 37 versus 388 ± 21 for treated and control, respectively). Approximately 62% of metastatic colonies from the $VEGF_{121}$/rGel-treated group had fewer than 10 vessels per colony as compared to 23% in the control group. The VEGF receptor(Flk-1) was intensely detected on the metastatic vessels in the control but not on the vessels in the $VEGF_{121}$/rGel-treated group.

$VEGF_{121}$/rGel Localizes to Vasculature of Breast Tumor Foci in the Lungs of Mice

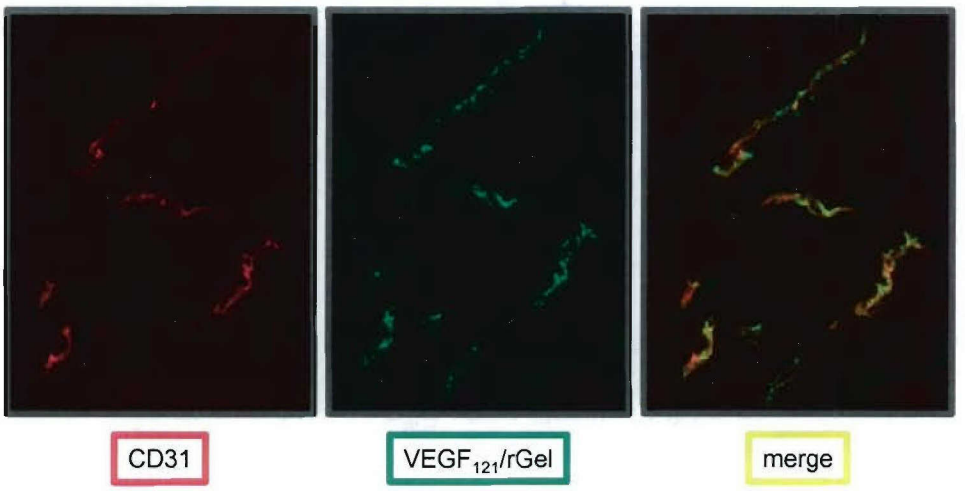

Mice bearing MDA-MB-435s lung tumor foci were injected i.v. with 50 μg of $VEGF_{121}$/rGel or 20μg of free rGel (only tissues from $VEGF_{121}$/rGel injected mice are shown). One hour later, mice were sacrificed and tissues excised. Lung sections were double-stained using an anti-CD31 antibody and an anti-gelonin antibody to detect blood vessels (red) and localized $VEGF_{121}$/rGel (green), respectively. Co-localization of the stains is indicated by a yellow color. Free rGel did not localize to the vasculature of lung tumor foci (not shown). No $VEGF_{121}$/rGel staining was detected in any of the normal tissues examined (lung, liver, kidney, heart, spleen, pancreas, brain).

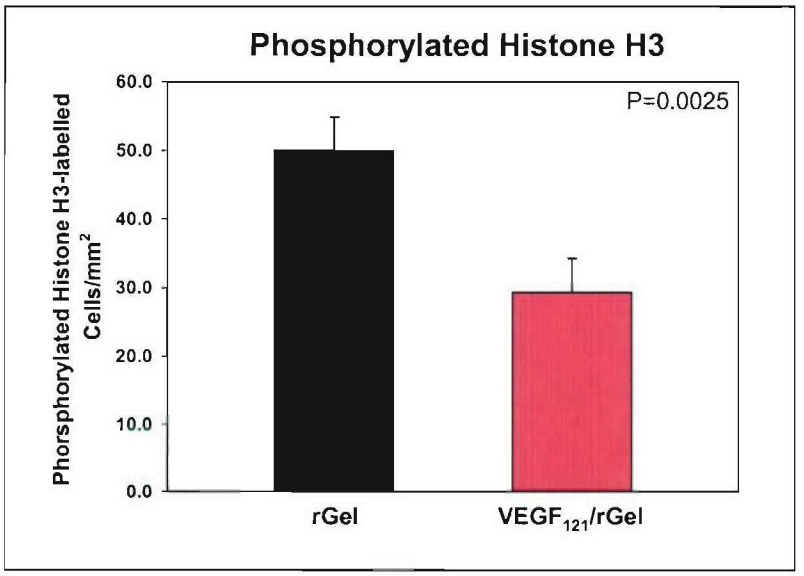

Frozen sections of lungs derived from $VEGF_{121}$/rGel- and rGel-treated mice bearing MDA-MB-231 lung tumor foci were stained with a phosphorylated histone H3 antibody. The number of tumor cells with phosphorylated histone H3 positive nuclei (mitotic cells) was counted in five high power fields of tumor sections from five mice per treatment group. The mean number per group ± SEM is presented and statistical significance was determined using the student's *t*-test.

Metastatic foci present in lung had a 3-fold lower Ki-67 labeling number compared to control tumors. These data strongly suggest that the anti-tumor vascular-ablative effect of $VEGF_{121}$/rGel could be utilized not only for treating primary tumors but also for inhibiting metastatic spread.

Task 5: Effects on Tissue Necrosis and Thrombosis:

Please note that a complete manuscript detailing the impressive anti-metastatic effects of $VEGF_{121}$/rGel in this breast tumor model is attached in the Appendix (The Vascular-Ablative Agent, $VEGF_{121}$/rGel, Inhibits Pulmonary Metastases of MDA-MB-231 Breast Tumors, by Ran et al (http://www.neoplasia.com/pdf/manuscript/neo04631.pdf).

Task 6: Effects on Vascular Permeability

Several studies have been performed to examine the effects of the $VEGF_{121}$/rGel fusion construct on vascular permeability. We performed the initial assessment on vascular permeability using ^{125}I labeled albumin exactly as described in the initial SOW. However, after several studies, we were unable to demonstrate an effect on tumor vasculature despite several other lines of histological evidence to the contrary. We therefore changed methodologies to assess in vivo vascular integrity to utilize the Evans Blue dye. In this method, MDA-MB-231 tumor cells (2 X 10^6) are placed in the mammary fat pad and allowed to develop into palpable tumors. The mice are treated with either $VEGF_{121}$/rGel (40 mg/kg, QOD X 5) or saline and 24 hrs after the final treatment, the mice are injected(i.v.) with 200 µl of dye(20 mg/ml). After 0.5 hr, the mice are

sacrificed, blood is collected and the mice are perfused with 5 ml of PBS/heparin. The various tissues(including tumor) are harvested and weighed into glass test tubes. A sample(0.5 ml) or N-N-DMF is added to each tube and allowed to incubate at room temp for 48 h. The concentration of Evans Blue dye is assessed spectrophotometrically(A_{630}) against a standard curve for the dye. The results are then expressed as either % of control or as ng dye/mg tissue.

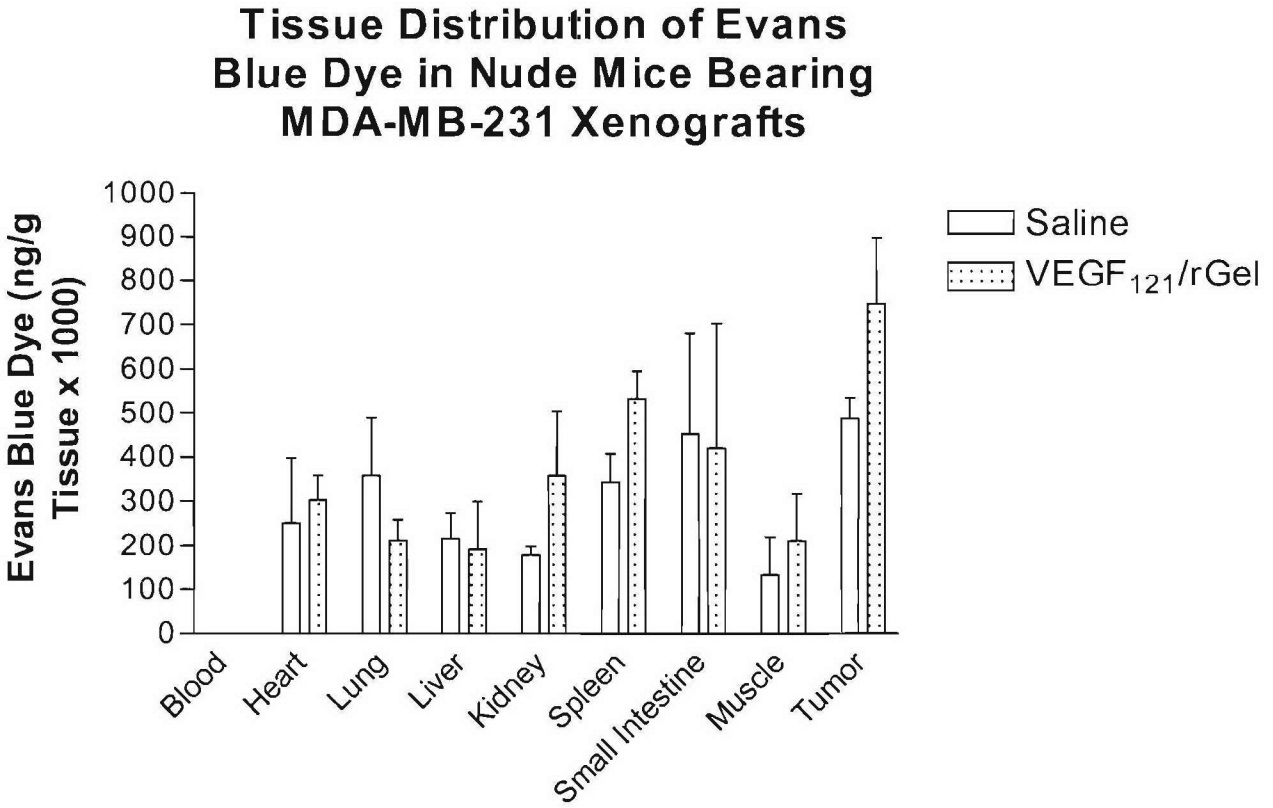

As shown in the figure above, we found a small(25%) but statistically-significant increase in the vascular permeability in tumor tissue, normal spleen and kidney with a concomitant small decrease(not statistically significant) in the vascular permeability of normal lung tissue. Histology and pathology studies are currently ongoing to evaluate the effects of $VEGF_{121}$/rGel on normal tissues as a part of the pre-IND evaluation package on this agent and these studies on vascular permeability may be evaluated in concert with observed effects on histology. In addition, in this next (unfunded) year, we plan to extend these observations on vascular permeability to evaluate the magnitude and timeline for these effects. We believe these observations may be of critical importance in developing the timing of imaging studies for the Phase I/II trial of this agent.

Task 7: Effects on Tumor Hypoxia

These studies are presently ongoing at UT Southwestern. However, we present initial studies with the construct. We treated mice bearing MDA-MB-231 tumors with saline, rGel of VEGF/rGel every other day(i.v.) for 5 days. Twenty-four hrs after the last administration, the animals were administered a dose of hydroxyprobe and the animals were then sacrificed and tumor specimens were obtained and snap-frozen. Immunohistochemical analyses were performed to stain for regions of hypoxia. In addition, we stained for VEGFR2 and blood vessels(MECA32). As shown in the figure below, we were unable to detect an increase in the hypoxia staining with treatment with the fusion construct compared to PBS or treatment with free rGel. Studies to repeat this experiment are ongoing.

Effects of Various Treatments on Tumor Hypoxia

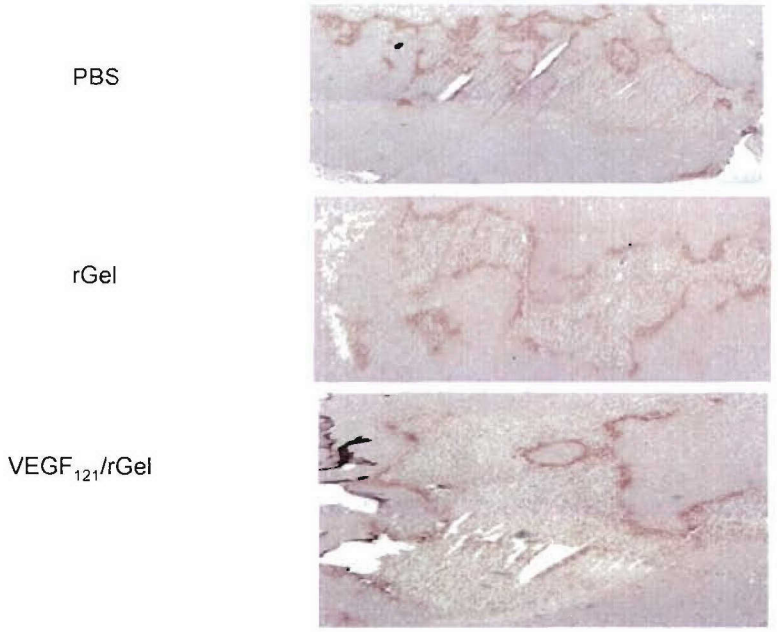

Task 8: Co-Culture of Endothelial Cells and MDA-MB231 Tumor Cells

We utilized the Falcon multi-well culture plates to culture the MDA-MB-231 tumor cells. Suspended above these cells, we placed an insert containing log-phase PAE/KDR cells. The 2 cell lines are cultured in the same DMEM/F-12 growth media, so no adaptation was required.

Task 9: Studies of $VEGF_{121}$/rGel Effects on Endothelial and Breast Tumor Cells

In the co-culture chambers, the 2 cell lines were treated with various doses of the $VEGF_{121}$/rGel fusion construct targeting the KDR receptor on endothelial cells. The MDA-MB-231 cells lack this receptor and were not affected by the doses utilized. At various times after drug administration, both cell lines were harvested, the RNA extracted and analyzed using the Gene Chip as described to assess the impact of treatment on over 7,000 genes including proteins involved in signal transduction, stress response, cell cycle control and metastasis. As shown below, we demonstrate the cytotoxic effects of the fusion construct on endothelial cells. Initial studies demonstrated that the initially-proposed PAE/KDR endothelial cells would be utilized,

however, Gene Chip analysis showed no hybridization to isolated RNA samples. Troubleshooting demonstrated that there is insufficient homology of the porcine cell RNA to that of the human probes on the Gene Chip, therefore, HUVEC cells were substituted for this phase of study. As shown below, HUVECs showed specific cytotoxicity of the fusion construct compared to rGel itself although the magnitude of the differential is lower than that of the PAE/KDR cells.

Cytotoxicity of $VEGF_{121}$/rGel on HUVECs

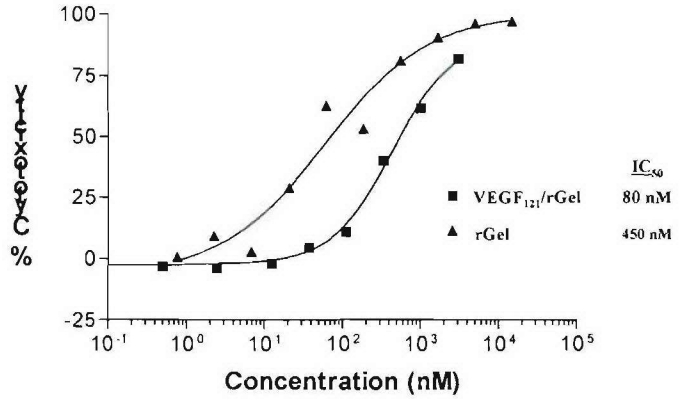

As shown below, extensive micro-array analyses were performed on breast tumor cells as well as on endothelial cells as described in the original SOW. We identified a total of 22 unique genes upregulated (>2-fold in at least 3 out of 4 arrays) by treatment with $VEGF_{121}$/rGel. These include genes involved in the control of cell adhesion, apoptosis, transcription regulation, chemotaxis and inflammatory response. These micro-array data were confirmed using Western analysis and RT-PCR and are further detailed in the attached manuscript(appendix) submitted to the Journal of Biological Chemistry

Genes overexpressed in HUVECs by 24 hr treatment with VEGF121/rGel:

E Selectin (endothelial adhesion molecule 1)
Small inducible cytokine A2 (monocyte chemotactic protein 1)
Tumor necrosis factor, alpha-induced protein 3
Nuclear factor of kappa light polypeptide gene enhancer in B-cells inhibitor, alpha
Kinesin-like 5 (mitotic kinesin-like protein 1)
Small inducible cytokine A4
Jun B proto-oncogene
Nidogen 2
Prostaglandin-endoperoxide synthase 2
Dual specificity phosphatase 5
Small inducible cytokine subfamily A (Cys-Cys), member 11 (eotaxin)
Plasminogen activator, urokinase
Vascular cell adhesion molecule 1

H2A histone family, member L
Small inducible cytokine A7 (monocyte chemotactic protein 3)
Spermidine/spermine N1-acetyltransferase
Syndecan 4 (amphiglycan, ryudocan)
Chemokine (C-X-C motif), receptor 4 (fusin)
Nuclear factor of kappa light polypeptide gene enhancer in B-cells 1 (p105)
Baculoviral IAP repeat-containing 3
Kruppel-like factor 4
Early growth response 1

All of the genes described above are known in the literature, however their association with cytotoxic events related to toxins such as rGel and activity on endothelial cells was previously unsuspected. To confirm these observations, these studies were repeated and RT-PCR was also employed(figure below) to more closely assess the timelines for gene modulation. As shown below, our RT-PCR essentially confirmed the upregulation of E-selectin, TNF AIP3, NFkB and SCYA2 genes in control(C) versus treated(T) samples at 4 and 24 hrs after exposure which confirms the results of the Gene Chip analysis of the 5 most highly upregulated genes.

Up-regulation of mRNA in HUVECs treated with $VEGF_{121}$/rGel

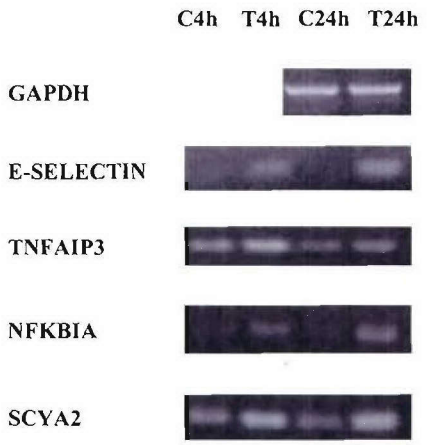

C: No Treatment Controls

Task 10: Effects of $VEGF_{121}$/rGel Exposure on Endothelial Cells Followed by Hypoxia

This past year, we performed extensive studies of the cellular response and concomitant gene regulation of endothelial and tumor(MDA-MD-231) cells exposed to $VEGF_{121}$/rGel.

Modulation of gene expression was assessed using an mRNA micro-array analysis as described in the Original SOW. We also looked at various times at the genes modified in tumor cells treated with the construct in the presence of endothelial cells and under both hypoxic and normoxic conditions as an approximation of intratumoral conditions in vivo. Tables 1-3 describe the various genes upregulated and downregulated in both tumor cells alone and in co-culture with endothelial cells exposed to $VEGF_{121}$/rGel or $VEGF_{121}$ under both normoxic and hypoxic conditions.

TABLE 1

Change in Gene Regulation of MDA-MB-231 cells (> 3-fold) Hypoxic Conditions

24h treatment with $VEGF_{121}$

Gene Designation	Name	Fold over Control
Upregulated		
NM_006993	Nucleoplosmin/Nucleoplasmin 3	4.1
NM_003341	Ubiquitin-conjugating enzyme E2E 1 (UBE2E1)	4.0
NM_021939	FK506 binding protein 10	3.6
Downregulated		
AK055846	Similar to Actin interacting protein 2	17.0
NM_000587	Complement component 7	5.3

24h treatment with $VEGF_{121}$/rGel

Upregulated		
NM_003528	Histone 2, H2be	4.0
NM_000584	Interleukin 8 (IL-8)	3.7
NM_006993	Nucleoplosmin/Nucleoplasmin 3	3.7
NM_001875	Carbamoyl-phosphate synthetase 1	3.2
NM_021939	FK506 binding protein 10	3.1
NM_025195	Tribbles homolog 1	3.1
Downregulated		
AK055846	Similar to Actin interacting protein 2	25.2
NM_000587	Complement component 7	4.6

24h treatment with $VEGF_{121}$/rGel vs $VEGF_{121}$

Upregulated		
AL137326	Genomic DNA; cDNA DKFZp434B0650	5.8
NM_003528	Histone 2, H2be	4.8
NM_000584	Interleukin 8 (IL-8)	4.7
NM_002260	Killer cell lectin-like receptor subfamily C, member 2	3.9
NM_025195	Tribbles homolog 1	3.9

Downregulated
None observed

TABLE 2

Change in Gene Regulation of MDA-MB-231 cells (> 3-fold) in Co-culture with PAE/KDR cells under Normoxic Conditions

72h treatment with $VEGF_{121}$

Upregulated

D86978	KIAA0225	8.4
AB001915	NG,NG-dimethylarginine dimethylaminohydrolase	5.7
NM_018191	Regulator of chromosome condensation (RCC1) and BTB (POZ) domain containing protein 1 (RCBTB1)	4.0
NM_004517	Integrin-linked kinase (ILK)	3.5

Downregulated

NM_032799	Zinc finger, DHHC domain containing 12 (ZDHHC12)	16.0
NM_005798	Ret finger protein 2 (RFP2), transcript variant 1	15.9
D87446	KIAA0257	13.5
AF038440	phospholipase D2 (PLD2)	6.5
AJ251973	Steerin-1	5.2
AL050041	Genomic DNA; cDNA DKFZp566L0424	4.4
NM_004391	Cytochrome P450 (CYP8B1)	4.0
NM_014736	KIAA0101	3.9
NM_002309	leukemia inhibitory factor (LIF)	3.6
NM_007150	zinc finger protein 185 (LIM domain) (ZNF185)	3.6
Y17456	LSFR2	3.5
NM_005597	nuclear factor I/C (NFIC)	3.5
AK025003	FLJ21350 fis	3.3
AF178669	p34	3.2
AK057059	Similar to K+ channel protein, beta subunit	3.0
NM_007076	Huntingtin interacting protein E (HYPE)	3.0

72h treatment with $VEGF_{121}$/rGel

Upregulated

D86978	KIAA0225	8.8
AK024586	FLJ20933 fis	5.0
AB001915	NG,NG-dimethylarginine dimethylaminohydrolase	4.9
NM_018191	Regulator of chromosome condensation (RCC1) and BTB (POZ) domain containing protein 1 (RCBTB1)	4.1
NM_024680	Likely ortholog of mouse E2F transcription factor 8 (E2F8)	3.3
NM_033084	Fanconi anemia, complementation group D2 (FANCD2)	3.0
NM_003937	Kynureninase (L-kynurenine hydrolase) (KYNU)	3.0

Downregulated

NM_032799	Zinc finger, DHHC domain containing 12 (ZDHHC12)	10.4
NM_003486	Solute carrier family 7, member 5 (SLC7A5)	5.4
NM_017801	Chemokine-like factor super family 6 (CKLFSF6)	4.8

NM_002621	Properdin P factor, complement (PFC)	4.8
AL122088	cDNA DKFZp564C0671 (from clone DKFZp564C0671)	4.8
NM_004207	Solute carrier family 16, member 3 (SLC16A3)	4.7
NM_015700	HIRA interacting protein 5 (HIRIP5)	4.5
AJ251973	Steerin-1	4.2
NM_012155	Echinoderm microtubule associated protein like 2 (EML2)	4.1
NM_004295	TNF receptor-associated factor 4 (TRAF4)	4.0
NM_024111	MGC4504	4.0
AK025003	FLJ21350 fis	3.9
NM_007324	Zinc finger, FYVE domain containing 9 (ZFYVE9)	3.9
NM_144726	FLJ31951	3.8
NM_021158	Tribbles homolog 3 (TRIB3)	3.8
NM_002928	Regulator of G-protein signalling 16 (RGS16)	3.8
NM_005717	Actin related protein 2/3 complex, subunit 5 (ARPC5)	3.7
NM_024567	FLJ21616	3.6
NM_003341	Ubiquitin-conjugating enzyme E2E 1 (UBE2E1)	3.6
NM_133436	Asparagine synthetase (ASNS)	3.6
NM_001348	Death-associated protein kinase 3 (DAPK3)	3.5
BC010350	TAF9-like RNA polymerase II, TATA box binding protein (TBP)-associated factor	3.5
NM_130469	Jun dimerization protein 2 (JDP2)	3.4
NM_001517	General transcription factor IIH, polypeptide 4 (GTF2H4)	3.4
NM_003275	Tropomodulin 1 (TMOD1)	3.4
NM_033332	CDC14 cell division cycle 14 homolog B (CDC14B)	3.3
NM_007076	Huntingtin interacting protein E (HYPE)	3.1
NM_017816	FLJ20425 (LYAR)	3.1
NM_000050	Argininosuccinate synthetase (ASS)	3.1
AB010067	RBP56/hTAFII68	3.1
X02160	Insulin receptor precursor	3.0

72h treatment with $VEGF_{121}$/rGel vs $VEGF_{121}$

Upregulated

NM_005798	Ret finger protein 2 (RFP2), transcript variant 1	10.7
D87446	KIAA0257	5.4
NM_001336	Cathepsin Z (CTSZ)	3.5
AK024586	FLJ20933 fis	3.2
NM_003548	Histone 2, H4 (HIST2H4)	3.1
NM_006290	Tumor necrosis factor, alpha-induced protein 3 (TNFAIP3)	3.1
NM_004454	Ets variant gene 5 (ets-related molecule) (ETV5)	3.1
NM_013282	Ubiquitin-like 1 (UHRF1)	3.1
NM_002260	Killer cell lectin-like receptor (KLRC2)	3.1
NM_0147736	KIAA0101	3.1

Downregulated

NM_004207	Solute carrier family 16 (SLC16A3)	5.7
NM_001282	Adaptor-related protein (AP2B1)	5.1

NM_144726	FLJ31951	4.5
NM_007324	Zinc finger, FYVE domain containing 9 (ZFYVE9)	4.3
NM_004295	TNF receptor-associated factor 4 (TRAF4)	4.0
M80899	AHNAK	3.7
NM_012155	Echinoderm microtubule associated protein like 2 (EML2)	3.3
NM_001517	General transcription factor IIH, polypeptide 4 (GTF2H4)	3.3
NM_024111	MGC4504	3.2
NM_016333	Serine/arginine repetitive matrix 2 (SRRM2)	3.1
NM_014437	Solute carrier family 39 (SLC39A1)	3.1
NM_001348	Death-associated protein kinase 3 (DAPK3)	3.1
NM_003341	Ubiquitin-conjugating enzyme E2E 1 (UBE2E1)	3.1
NM_018113	Lipocalin-interacting membrane receptor (LIMR)	3.0

TABLE 3

Change in Gene Regulation of MDA-MB-231 cells (> 3-fold) in Co-culture with PAE/KDR cells under Hypoxic Conditions

72h treatment with $VEGF_{121}$

Upregulated

NM_032023	Ras association (RalGDS/AF-6) domain family 4 (RASSF4)	96.1
NM_024531	G protein-coupled receptor 172A (GPR172A)	8.0
AK001020	FLJ10158 fis	3.9

Downregulated

AF083386	Putative WHSC1 protein (WHSC1)	31.4
NM_015271	Tripartite motif-containing 2 (TRIM2)	4.1

72h treatment with $VEGF_{121}$/rGel

Upregulated

NM_016073	Hepatoma-derived growth factor, related protein 3 (HDGFRP3)	8.4
BC010926	Histone 1, H4h	7.6
NM_003543	Histone 1, H4h (HIST1H4H)	4.3
L40326	Hepatitis B virus X-associated protein 1	4.0
AL049965	cDNA DKFZp564A232 (from clone DKFZp564A232)	4.0
R85474	Soares adult brain N2b4HB55Y	4.0
NM_005658	TNF receptor-associated factor 1 (TRAF1)	3.8
AP000557	genomic DNA, chromosome 22q11.2, BCRL2 region	3.8
NM_016113	Transient receptor potential cation channel (TRPV2)	3.7
BI462740	603202190F1 NIH_MGC_97 cDNA clone IMAGE:5268046	3.5
NM_004521	Kinesin family member 5B (KIF5B)	3.5
NM_014890	Downregulated in ovarian cancer 1 (DOC1)	3.2
NM_003452	Zinc finger protein 189 (ZNF189)	3.0
AB037770	KIAA1349	3.0

Downregulated

NM_144726	FLJ31951	4.8
NM_006874	E74-like factor 2 (ets domain transcription factor) (ELF2)	4.6
AK026965	FLJ23312 fis	3.7
NM_015271	Tripartite motif-containing 2 (TRIM2)	3.4
NM_001282	Adaptor-related protein complex 2, beta 1 subunit (AP2B1)	3.1

72h treatment with $VEGF_{121}$/rGel vs $VEGF_{121}$

Upregulated

NM_016073	Hepatoma-derived growth factor, related protein 3 (HDGFRP3)	9.4
BC010926	Histone 1, H4h	8.0
NM_005658	TNF receptor-associated factor 1 (TRAF1)	5.1
NM_004521	Kinesin family member 5B (KIF5B)	4.7
NM_014890	Downregulated in ovarian cancer 1 (DOC1)	4.4

BC015134	Clone IMAGE:3934391	3.7
L40326	Hepatitis B virus X-associated protein 1	3.6
AB037770	KIAA1349	3.2
NM_030965	ST6 (alpha-N-acetyl-neuraminyl-2,3-beta-galactosyl-1,3)-N-acetylgalactosaminide alpha-2,6-sialyltransferase 5 (ST6GALNAC5)	3.1
NM_003452	Zinc finger protein 189 (ZNF189)	3.1
NM_006807	Chromobox homolog 1(CBX1)	3.0
X07289	HF.10	3.0
NM_018137	HMT1 hnRNP methyltransferase-like 6 (HRMT1L6)	3.0

Downregulated

NM_032023	Ras association (RalGDS/AF-6) domain family 4 (RASSF4)	88.6
NM_024531	G protein-coupled receptor 172A (GPR172A)	8.9
NM_144726	FLJ31951	5.2
NM_006874	E74-like factor 2 (ets domain transcription factor) (ELF2)	4.3
U57645	Helix-loop-helix proteins Id-1 (ID-1) and Id-1' (ID-1)	4.2
NM_003341	Ubiquitin-conjugating enzyme E2E 1 (UBE2E1)	3.5
AK001020	FLJ10158 fis	3.3
NM_020353	Phospholipid scramblase 4 (PLSCR4),	3.2
NM_016518	Pipecolic acid oxidase (PIPOX),	3.2
NM_000484	Amyloid beta (A4) precursor protein (protease nexin-II, Alzheimer disease) (APP)	3.1
NM_001282	Adaptor-related protein complex 2, beta 1 subunit (AP2B1)	3.0
AL163284	Chromosome 21 segment HS21C084	3.0

As shown in the tables above, both $VEGF_{121}$ and $VEGF_{121}$/rGel induce and suppress a different subset of genes on breast tumor cells, as expected. Treatment of breast tumor cells in co-culture with endothelial cells with $VEGF_{121}$/rGel for 72 hrs in hypoxic conditions appeared to significantly downregulate(89 fold) Ras family protein and the G-coupled receptor 172A. In contrast, histone 1 and hepatoma-derived growth factor-related protein 3(HDGFRP3) were both highly upregulated. The effects of VEGF/rGel on MDA-MB-231 tumor cells appears to be significantly different under normoxic conditions was significantly different as shown in Table 2. Both Ret finger protein 2 and KIA were upregulated while SLC16A3 and AP2B1 were downregulated in response to VEGF/rGel.

Original SOW Tasks still to be accomplished in the requested (no-cost) extension year 2005-2006:

Task 11: Confirmation of In Vitro Gene Chip Findings With PCR Analysis of Tumor Samples

This information is critical to confirm our co-culture studies with actual data from xenograft MDA-MB-231 models. We now have RT-PCR confirmation of the findings using the Gene Chip analysis. This narrows the gene search and we can focus on the specific genes using conventional RT-PCR in tumor xenograft specimens. In addition, we plan an extensive analysis

to determine the temporal nature of these potential changes. This data will be critical for our planned clinical trials of this agent in breast cancer patients and may allow a more complete understanding of the molecular profile for cellular changes induced by this agent.

Task 12: Use of $VEGF_{121}$/rGel in combination with chemotherapeutic agents against MDA-MB231

We believe that combination of various modalities is critical to successful therapeutic approaches. Recent impressive data presented at ASCO(2005) demonstrate the power of combination of Herceptin antibody with conventional chemotherapy in an adjuvant setting in breast cancer patients. Much of the design for the adjuvant study with Herceptin was derived from combination therapy studies in xenograft models. Our original proposal SOW also included a final task to perform combination studies of $VEGF_{121}$/rGel with conventional agents. For the original reasons outlined we plan to continue combination studies in this next year. We believe this data may be eventually useful to identify potential synergistic/additive combinations for eventual clinical trials.

Unanticipated, Novel Findings of related to $VEGF_{121}$/rGel and This Proposal

Breast cancer metastases to bone are associated with significant morbidity and mortality. Patients with advanced breast cancer experience frequent bone metastasis. However, the pathophysiological processes leading to the development of breast skeletal metastases remains poorly understood. Since breast skeletal metastases are essentially untreatable, improvements in our understanding of the biological mechanisms behind breast cancer metastases to bone could enhance the development of regimens to treat this disease. Therefore, we have initiated studies to improve our understanding of the development of breast skeletal metastases by examining how breast tumors remodel bone, which result in both osteoblastic and osteolytic lesions. Osteoclastogenesis plays a central role in the development and maintenance of normal bone tissue, which requires osteoblastic matrix deposition and osteoclastic resorption to be closely coordinated. Interference with the process of osteoclastogenesis alters the kinetics of bone remodeling resulting in abnormal bone development. There is general consensus that the hematopoietically derived osteoclast is the pivotal cell in the degradation of the bone matrix. Osteoclast pre-cursor cells have been shown to be recruited to the future site of resorption by VEGF-A and RANKL, two cytokines that are expressed in the immediate vicinity of the bone surface. In addition, both of the major receptors of VEGF-A have been observed in osteoclasts, although some reports cite only the presence of Flt-1. The VEGF-Flt-1 interaction has been implicated in the recruitment process of osteoclast pre-cursor cells from hematopoietic tissue to the site of bone resorption. However, the role of each receptor, and its regulation, has yet to be established.

It has been hypothesized that osteoclasts play a critical role in the establishment of osteoblastic bone metastases by inducing bone resorption, which allows breast tumor cells to invade the bone and therefore promote tumor growth. VEGF plays an important role in the vascularization of bone tissues, as a mitogen for endothelial cells and as a chemo-attractant for both osteoblasts and osteoclasts. Therefore, establishing the precise role that each VEGF receptor plays in the maturation of osteoclast pre-cursor cells to osteoclasts is a critical step towards understanding the interaction that occurs between breast tumor cells and the bone microenvironment.

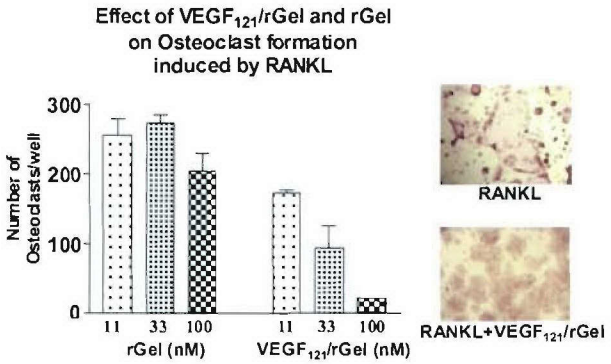

Figure 1. Effect of $VEGF_{121}$/rGel and rGel on RANKL-mediated osteoclast formation. Raw 264.7 cells were cultured overnight in 24-well plates. Osteoclast formation was induced by addition of 100 ng/ml RANKL with increasing concentrations of $VEGF_{121}$/rGel or rGel. Cells were allowed to differentiate for 96 hours followed by determination of the number of osteoclasts per well. Each experiment was performed in triplicate. The data shown is representative of three separate experiments. RANKL or RANKL + rGel-treated Raw 264.7 cells differentiate into large multi-nucleated TRAP-positive osteoclasts. In contrast, RANKL + $VEGF_{121}$/rGel-treated cells do not differentiate and do not stain for TRAP.

We have begun preliminary experiments examining the effect of $VEGF_{121}$/rGel on osteoclast formation in two model systems: (1) RAW 264.7 cells, cultured mouse osteoclast precursor cells that differentiate into mature osteoclasts upon stimulation with RANKL and (2) Bone marrow-derived macrophages (BMM), mouse primary cells that require stimulation with macrophage colony stimulating factor (MCSF) followed by RANKL for differentiation into osteoclasts. $VEGF_{121}$/rGel dramatically reduces osteoclastogenesis of both RAW 264.7 (Figure 1) and bone marrow-derived macrophages (Figure 2). Interestingly, a significantly lower concentration of $VEGF_{121}$/rGel is required to inhibit osteoclastogenesis in the primary bone marrow-derived cells than in RAW264.7 cells.

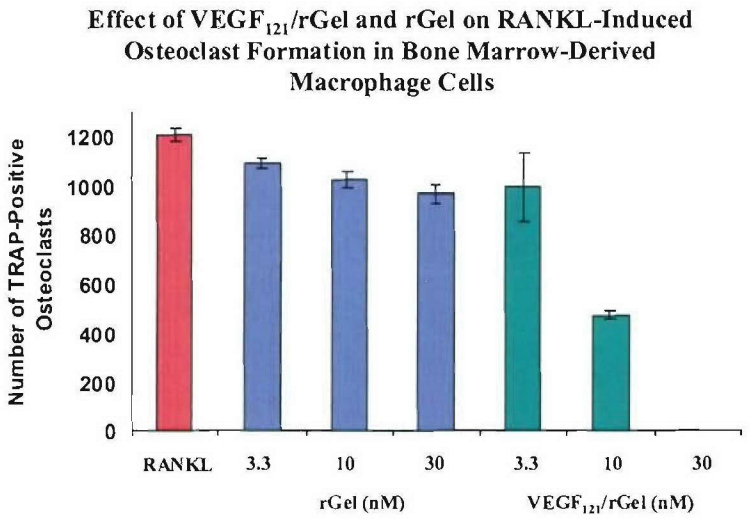

Figure 2. Effect of $VEGF_{121}$/rGel and rGel on RANKL-mediated osteoclast formation in bone marrow-derived macrophages (BMM). BMM cells were cultured overnight in 24-well plates with MCSF. Osteoclast formation was induced by addition of 100 ng/ml RANKL with increasing concentrations of $VEGF_{121}$/rGel or rGel. Cells were allowed to differentiate for 96 hours followed

by determination of the number of osteoclasts per well. Each experiment was performed in duplicate. RANKL or RANKL + rGel-treated BMM cells differentiate into large multi-nucleated TRAP-positive osteoclasts. In contrast, RANKL + $VEGF_{121}$/rGel-treated cells do not differentiate and do not stain for TRAP.

Treatment of Raw 264.7 cells with $VEGF_{121}$/rGel and rGel for 24 hours

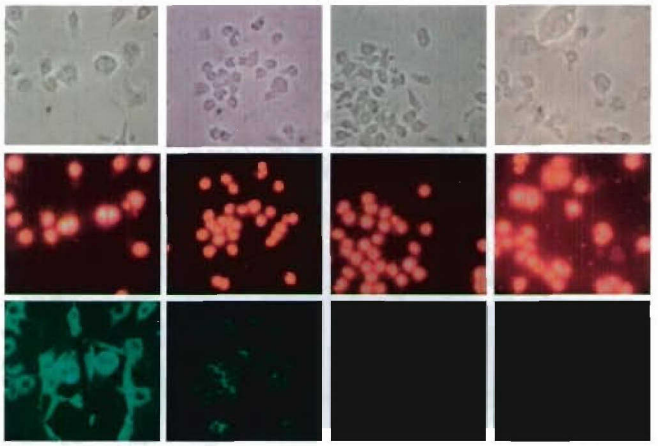

[$VEGF_{121}$/rGel] (nM)	**10**	**-**	**-**	**100**
[rGel] (nM)	**-**	**1000**	**-**	**-**
Primary Ab	**Yes**	**Yes**	**Yes**	**No**
Secondary Ab	**Yes**	**Yes**	**Yes**	**Yes**

Figure 3. $VEGF_{121}$/rGel is internalized into RAW 264.7 cells. One thousand RAW 264.7 cells were plated into chamber slides and cultured overnight. Cells were then treated with $VEGF_{121}$/rGel and rGel for 24 hours. After the cell surface was stripped of membrane-bound $VEGF_{121}$/rGel or rGel, non-specific binding sites were blocked with 5% BSA and cells were permeabilized. Cells were treated with rabbit anti-gelonin (1:100) overnight followed by FITC-conjugated secondary antibody (1:80). Nuclei were stained with Propidium Iodide (middle row). $VEGF_{121}$/rGel is specifically internalized into RAW 264.7 cells (Column 1) as a 100-fold increase in rGel results in significantly lower internalization. Columns 3 and 4 serve as negative controls without antigen or primary antibody respectively.

We next examined whether the inhibition of osteoclastogenesis by $VEGF_{121}$/rGel is mediated by entry of the molecule into the cell or solely by disruption via cell signaling, we performed immunohistochemistry experiments on RAW 264.7 cells. Our results, shown in Figure 3, indicate that $VEGF_{121}$/rGel is internalized into the osteoclast pre-cursor cells within 24 hours, and that the internalization is due to the presence of $VEGF_{121}$, not gelonin. Thus, it is likely that inhibition of osteoclastogenesis is mediated(at least in part) by one of the receptors for $VEGF_{121}$, Flt-1 (VEGFR-1) or Flk-1/KDR (VEGFR-2).

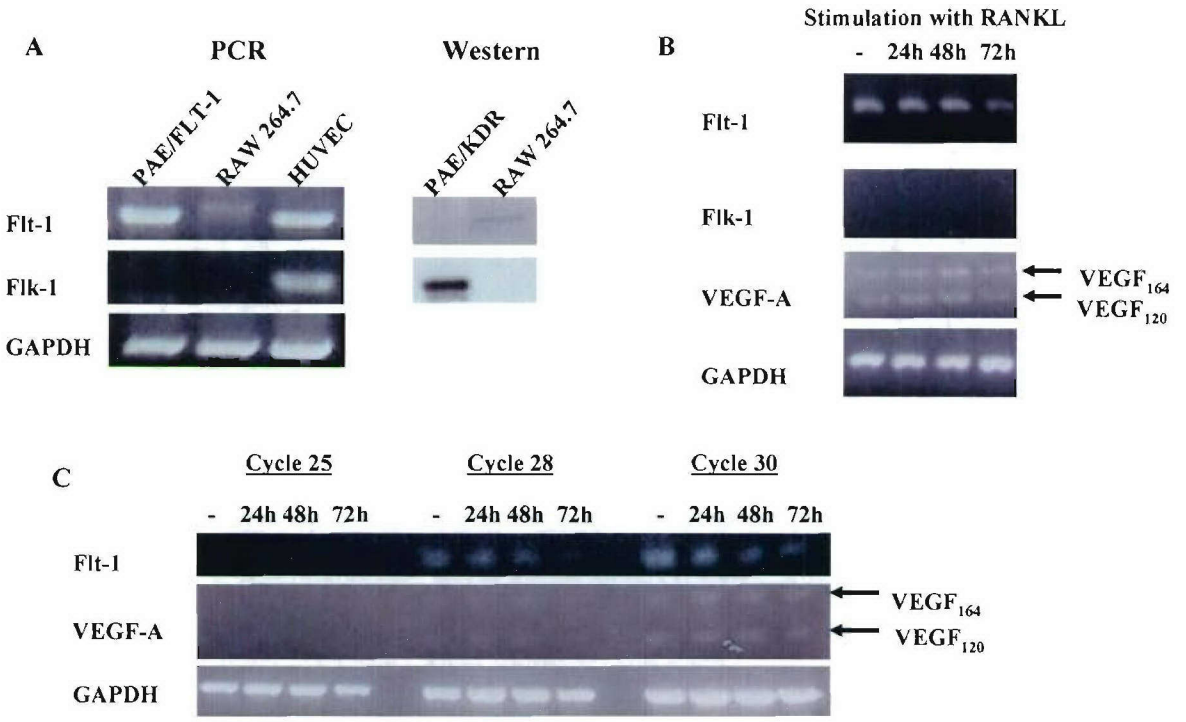

Figure 4

Figure 4. Flt-1 levels are down-regulated during osteoclastogenesis. The osteoclast precursor cell line RAW 264.7 cell line was cultured for 72 hours with MCSF with or without stimulation with RANKL for 24, 48 and 72 hours. Total RNA was harvested and subjected to PCR analysis using primers specific for Flk-1, Flt-1 and two isoforms of VEGF-A(164 and 120). RAW cells do not express Flk-1 but do express levels of Flt-1 receptor at levels lower than that of HUVEC. PCR analysis also suggests that Flt-1 is expressed by RAW cells, and that these levels decline during RANKL-stimulated osteoclastogenesis. RAW cells also express $VEGF_{120}$ and $VEGF_{164}$ isoforms, but not the $VEGF_{189}$ and $VEGF_{144}$ isoforms(not shown), (similar to MDA-MB-231 cells).

In order to understand whether the effect of $VEGF_{121}$/rGel is receptor-mediated, we have begun experiments to identify the presence of $VEGF_{121}$ receptors, and their role during osteoclastogenesis. This information is critical because the receptor target through which $VEGF_{121}$/rGel effects are mediated on osteoclasts is not known. This is significant because $VEGF_{121}$/rGel may inhibit breast cancer osteoblastic and osteolytic lesions in bone as a result of osteoclastogenesis inhibition. We have identified the presence of Flt-1, but not Flk-1, in BMM cells by PCR analysis (Figure 4). Interestingly, the levels of Flt-1 appear to decrease during osteoclast formation. We will examine the role of Flt-1 in this process by testing whether $VEGF_{121}$/rGel affects the level of Flt-1 during osteoclastogenesis, both by PCR and by Western

blot. We also plan on performing co-culture experiments with breast tumor cells for the same reasons.

Key Research Accomplishments

- **Described the Pharmacokinetics and Tissue Distribution of $VEGF_{121}$/rGel to allow rational development of an optimal therapeutic schedule on which to base both murine and eventual clinical studies.**
- **Described significant in vivo antitumor effects of $VEGF_{121}$/rGel against orthotopicially-placed breast tumor xenografts. Demonstrated complete regression of primary orthotopic breast tumors in 50% of treated mice(3/6).**
- **Identified significant vascular-ablative effects of $VEGF_{121}$/rGel on breast metastatic foci present in lung. Identified the impact this agent appears to have in suppressing the development of tumor metastases by destruction of tumor vascular endothelium and drug-induced downregulation of flk-1 receptors in tumor endothelium.**
- **Identified a unique aspect of therapy using $VEGF_{121}$/rGel in that lung metastases of treated mice have virtually no vasculature and appear to grow to the approximate limit of oxygen diffusion for avascular tissues.**
- **Identified 22 unique genes associated with the development cytotoxic effects of the rGel toxin component on vascular endothelial cells.**
- **Confirmed the Gene Chip results via RT-PCR and Western analysis. Provided a unique gene "fingerprint" for intoxication of cells by $VEGF_{121}$/rGel which provides information as to the exact molecular mechanism of action of this agent and may provide a molecular rationale for combinations with other therapeutic agents.**
- **Identified a unique set of genes upregulated and downregulated in MDA-MB-231 breast tumor cells co-cultured with endothelial cells in response to treatment with $VEGF_{121}$/rGel and under both normoxic and hypoxic conditions.**
- **Provided significant rationale for continued pre-clinical development of $VEGF_{121}$/rGel as a vascular-ablative agent in breast cancer.**
- **Described the unique ability of this fusion construct to inhibit skeletal tumor metastases in vivo. The mechanism of action appears to be through direct inhibition of normal osteoclast function which appears to be essential for bone remodeling in the development of skeletal metastases.**
- **Identified an unanticipated mechanism of action of this fusion construct which indicates a role for VEGF in development of skeletal metastases.**

Reportable Outcomes:

Abstracts:

1. Mohamedali K, Poblenz A, Sikes C, Luster T, Navone N, Thorpe P, Darnay B, Rosenblum MG. The Vascular Targeting Agent $VEGF_{121}$/rGel Inhibits Bone Remodeling and Skeletal Metastases through a Unique Mechanism. AACR, Abstract# 4624, 2005 (See Appendices #1).

Manuscripts:

1. Mohamedali KA, Poblenz AT, Sikes C, Novone N, Thorpe P, Darnay B and Rosenblum M. Inhibition of Bone Remodeling and Prostate Skeletal Metastases by the Vasulcar Targeting Agent $VEGF_{121}$/rGel. Nature Medicine, submitted (See Appendices #2).

2. Ran S, Mohamedali K, Thorpe P, Rosenblum M. The vascular-ablative agent $VEGF_{121}$/rGel inhibits pulmonary metastases of MDA-MB-231 breast tumors. Neoplasia 7(5):486-496, 2005 (See Appendices #3).

3. Lyu M-A, Kurzrock R, Rosenblum M. Targeting Human Pancreatic Tumor Cells with the anti-HER-2/neu Immunocytokine scFv23/TNF. Molecular Cancer Therapeutics, submitted (See Appendices #4).

4. Mohamedali K, Gomez-Manzano C, Ramdas L, Xu J, Cheung L, Zhang W, Thorpe P, Rosenblum M. $VEGF_{121}$/rGel fusion toxin targets the KDR receptor to inhibit vascular endothelial growth *in vitro* and *in vivo*: specific effects assessed using microarray analysis. Journal of Biological Chemistry, submitted (See Appendices #5).

Conclusions:

Vascular targeting as an approach to tumor therapy holds significant promise for the treatment of solid tumors. However, many current approaches attempting to inhibit the neovascularization process through small molecule inhibitors of VEGFR signaling, antibodies to VEGF itself or to the VEGFR2 have not met with success. This is due in part to the multiply-redundant and robust process which tumor vascularization represents. On the other hand, lethal damage to tumor endothelium using the $VEGF_{121}$/rGel fusion toxin is a comparatively unique approach. This construct has remarkable and long-term antitumor effects in xenograft models as opposed to other agents that have limited activity in their own right. Dr. Louise Gorchow, Head of CTEP has indicated in a public presentation that the $VEGF_{121}$/rGel fusion toxin is one of a very few agents with these properties. The data presented above and in the attached Appendix demonstrates that this agent can reduce the growth of both orthotopic breast tumors and can significantly limit the metastatic spread of a breast metastatic model. In addition, the lung metastases that do survive appear to have a much lower vascular supply and a limited tumor cell turnover rate suggesting a reduced growth and metastatic potential. No other vascular targeting agents have thus far demonstrated such unique effects in an in vivo model. Of interest will be to examine the impact this fusion toxin will have on survival in this metastatic model. In addition, our findings examining the mechanism of direct action of the fusion construct on endothelial cells has significance in more exactly understanding how toxins work at the molecular level and may be an important first step in understanding how to more effectively employ these agents for therapeutic advantage. Furthermore, the importance of understanding how vascular targeting agents affect tumor cells indirectly may also have therapeutic significance in understanding the rationale for combinations of these vascular targeting agents with conventional chemotherapeutic agents, or with radiotherapeutic or biological agents. Finally, we have identified that development of breast tumor skeletal metastases apparently require VEGF and the VEGF-

receptor pathway. Our studies have demonstrated that the $VEGF_{121}$/rGel fusion construct can significantly inhibit skeletal metastases through a unique inhibition of osteoclast maturation and function in vitro and probably in vivo. This suggests that the $VEGF_{121}$/rGel fusion construct may therefore be useful for the prevention and treatment of skeletal metastases in breast cancer and perhaps for skeletal metastases in other types of cancers as well.

References

1. Birnbaum, D. VEGF-FLT1 receptor system: a new ligand-receptor system involved in normal and tumor angiogenesis. Jpn.J.Cancer Res., *86*: 1, 1995.

2. Kerbel, R. S. Tumor angiogenesis: past, present and the near future. Carcinogenesis, *21*: 505-515, 2000.

3. Bando, H. and Toi, M. Tumor angiogenesis, macrophages, and cytokines. Adv.Exp.Med.Biol., *476*: 267-284, 2000.

4. Falterman, K. W., Ausprunk, H., and Klein, M. D. Role of tumor angiogenesis factor in maintenance of tumor-induced vessels. Surg.Forum, *27*: 157-159, 1976.

5. Patt, L. M. and Houck, J. C. Role of polypeptide growth factors in normal and abnormal growth. Kidney Int., *23*: 603-610, 1983.

6. Ravi, R., Mookerjee, B., Bhujwalla, Z. M., Sutter, C. H., Artemov, D., Zeng, Q., Dillehay, L. E., Madan, A., Semenza, G. L., and Bedi, A. Regulation of tumor angiogenesis by p53-induced degradation of hypoxia-inducible factor 1alpha. Genes Dev., *14*: 34-44, 2000.

7. Folkman, J. Proceedings: Tumor angiogenesis factor. Cancer Res., *34*: 2109-2113, 1974.

8. Strugar, J., Rothbart, D., Harrington, W., and Criscuolo, G. R. Vascular permeability factor in brain metastases: correlation with vasogenic brain edema and tumor angiogenesis. J.Neurosurg., *81*: 560-566, 1994.

9. Jaeger, T. M., Weidner, N., Chew, K., Moore, D. H., Kerschmann, R. L., Waldman, F. M., and Carroll, P. R. Tumor angiogenesis correlates with lymph node metastases in invasive bladder cancer. J.Urol., *154*: 69-71, 1995.

10. Melnyk, O., Zimmerman, M., Kim, K. J., and Shuman, M. Neutralizing anti-vascular endothelial growth factor antibody inhibits further growth of established prostate cancer and metastases in a pre-clinical model. J.Urol., *161*: 960-963, 1999.

11. Aranda, F. I. and Laforga, J. B. Microvessel quantitation in breast ductal invasive carcinoma. Correlation with proliferative activity, hormonal receptors and lymph node metastases. Pathol.Res.Pract., *192*: 124-129, 1996.

12. Fox, S. B., Leek, R. D., Bliss, J., Mansi, J. L., Gusterson, B., Gatter, K. C., and Harris, A. L. Association of tumor angiogenesis with bone marrow micrometastases in breast cancer patients. J.Natl.Cancer Inst., *89*: 1044-1049, 1997.

13. Senger, D. R., Van de, W. L., Brown, L. F., Nagy, J. A., Yeo, K. T., Yeo, T. K., Berse, B., Jackman, R. W., Dvorak, A. M., and Dvorak, H. F. Vascular permeability factor (VPF, VEGF) in tumor biology. Cancer Metastasis Rev., *12*: 303-324, 1993.

14. McMahon, G. VEGF receptor signaling in tumor angiogenesis. Oncologist., *5 Suppl 1*: 3-10, 2000.

15. Obermair, A., Kucera, E., Mayerhofer, K., Speiser, P., Seifert, M., Czerwenka, K., Kaider, A., Leodolter, S., Kainz, C., and Zeillinger, R. Vascular endothelial growth factor (VEGF) in human breast cancer: correlation with disease-free survival. Int.J.Cancer, *74*: 455-458, 1997.

16. Miyoshi, C. and Ohshima, N. Vascular endothelial growth factor (VEGF) expression regulates angiogenesis accompanying tumor growth in a peritoneal disseminated tumor model. In Vivo, *15*: 233-238, 2001.

17. Neufeld, G., Cohen, T., Gengrinovitch, S., and Poltorak, Z. Vascular endothelial growth factor (VEGF) and its receptors. FASEB J., *13*: 9-22, 1999.

18. Shibuya, M. Role of VEGF-flt receptor system in normal and tumor angiogenesis. Adv.Cancer Res., *67*: 281-316, 1995.

19. Detmar, M. The role of VEGF and thrombospondins in skin angiogenesis. J.Dermatol.Sci., *24 Suppl 1*: S78-S84, 2000.

20. Verheul, H. M. and Pinedo, H. M. The Role of Vascular Endothelial Growth Factor (VEGF) in Tumor Angiogenesis and Early Clinical Development of VEGF-Receptor Kinase Inhibitors. Clin.Breast Cancer, *1 Suppl 1*: S80-S84, 2000.

21. McCabe, C. J., Boelaert, K., Tannahill, L. A., Heaney, A. P., Stratford, A. L., Khaira, J. S., Hussain, S., Sheppard, M. C., Franklyn, J. A., and Gittoes, N. J. Vascular endothelial growth factor, its receptor KDR/Flk-1, and pituitary tumor transforming gene in pituitary tumors. J.Clin.Endocrinol.Metab, *87*: 4238-4244, 2002.

22. Kranz, A., Mattfeldt, T., and Waltenberger, J. Molecular mediators of tumor angiogenesis: enhanced expression and activation of vascular endothelial growth factor receptor KDR in primary breast cancer. Int.J.Cancer, *84*: 293-298, 1999.

23. Harada, Y., Ogata, Y., and Shirouzu, K. Expression of vascular endothelial growth factor and its receptor KDR (kinase domain-containing receptor)/Flk-1 (fetal liver kinase-1) as prognostic factors in human colorectal cancer. Int.J.Clin.Oncol., *6*: 221-228, 2001.

24. Padro, T., Bieker, R., Ruiz, S., Steins, M., Retzlaff, S., Burger, H., Buchner, T., Kessler, T., Herrera, F., Kienast, J., Muller-Tidow, C., Serve, H., Berdel, W. E., and Mesters, R. M. Overexpression of vascular endothelial growth factor (VEGF) and its cellular receptor KDR (VEGFR-2) in the bone marrow of patients with acute myeloid leukemia. Leukemia, *16*: 1302-1310, 2002.

25. Wedge, S. R., Ogilvie, D. J., Dukes, M., Kendrew, J., Curwen, J. O., Hennequin, L. F., Thomas, A. P., Stokes, E. S., Curry, B., Richmond, G. H., and Wadsworth, P. F. ZD4190: an orally active inhibitor of vascular endothelial growth factor signaling with broad-spectrum antitumor efficacy. Cancer Res., *60*: 970-975, 2000.

26. Laird, A. D., Vajkoczy, P., Shawver, L. K., Thurnher, A., Liang, C., Mohammadi, M., Schlessinger, J., Ullrich, A., Hubbard, S. R., Blake, R. A., Fong, T. A., Strawn, L. M., Sun, L., Tang, C., Hawtin, R., Tang, F., Shenoy, N., Hirth, K. P., McMahon, G., and Cherrington SU6668 is a potent antiangiogenic and antitumor agent that induces regression of established tumors. Cancer Res., *60*: 4152-4160, 2000.

27. Haluska, P. and Adjei, A. A. Receptor tyrosine kinase inhibitors. Curr.Opin.Investig.Drugs, *2*: 280-286, 2001.

28. Fabbro, D., Ruetz, S., Bodis, S., Pruschy, M., Csermak, K., Man, A., Campochiaro, P., Wood, J., O'Reilly, T., and Meyer, T. PKC412--a protein kinase inhibitor with a broad therapeutic potential. Anticancer Drug Des, *15*: 17-28, 2000.

29. Fabbro, D., Buchdunger, E., Wood, J., Mestan, J., Hofmann, F., Ferrari, S., Mett, H., O'Reilly, T., and Meyer, T. Inhibitors of protein kinases: CGP 41251, a protein kinase inhibitor with potential as an anticancer agent. Pharmacol.Ther., *82*: 293-301, 1999.

30. Sun, L. and McMahon, G. Inhibition of tumor angiogenesis by synthetic receptor tyrosine kinase inhibitors. Drug Discov.Today, *5*: 344-353, 2000.

31. Solorzano, C. C., Baker, C. H., Bruns, C. J., Killion, J. J., Ellis, L. M., Wood, J., and Fidler, I. J. Inhibition of growth and metastasis of human pancreatic cancer growing in nude mice by PTK 787/ZK222584, an inhibitor of the vascular endothelial growth factor receptor tyrosine kinases. Cancer Biother.Radiopharm., *16*: 359-370, 2001.

32. Drevs, J., Hofmann, I., Hugenschmidt, H., Wittig, C., Madjar, H., Muller, M., Wood, J., Martiny-Baron, G., Unger, C., and Marme, D. Effects of PTK787/ZK 222584, a specific inhibitor of vascular endothelial growth factor receptor tyrosine kinases, on primary tumor, metastasis, vessel density, and blood flow in a murine renal cell carcinoma model. Cancer Res., *60*: 4819-4824, 2000.

33. Dimitroff, C. J., Klohs, W., Sharma, A., Pera, P., Driscoll, D., Veith, J., Steinkampf, R., Schroeder, M., Klutchko, S., Sumlin, A., Henderson, B., Dougherty, T. J., and Bernacki, R. J. Anti-angiogenic activity of selected receptor tyrosine kinase inhibitors, PD166285 and PD173074: implications for combination treatment with photodynamic therapy. Invest New Drugs, *17*: 121-135, 1999.

34. Mendel, D. B., Schreck, R. E., West, D. C., Li, G., Strawn, L. M., Tanciongco, S. S., Vasile, S., Shawver, L. K., and Cherrington, J. M. The angiogenesis inhibitor SU5416 has long-lasting effects on vascular endothelial growth factor receptor phosphorylation and function. Clin.Cancer Res., *6*: 4848-4858, 2000.

35. Prewett, M., Huber, J., Li, Y., Santiago, A., O'Connor, W., King, K., Overholser, J., Hooper, A., Pytowski, B., Witte, L., Bohlen, P., and Hicklin, D. J. Antivascular endothelial growth factor receptor (fetal liver kinase 1) monoclonal antibody inhibits tumor angiogenesis and growth of several mouse and human tumors. Cancer Res., *59*: 5209-5218, 1999.

36. Chen, Y., Wiesmann, C., Fuh, G., Li, B., Christinger, H. W., McKay, P., de Vos, A. M., and Lowman, H. B. Selection and analysis of an optimized anti-VEGF antibody: crystal structure of an affinity-matured Fab in complex with antigen. J.Mol.Biol., *293*: 865-881, 1999.

37. Ryan, A. M., Eppler, D. B., Hagler, K. E., Bruner, R. H., Thomford, P. J., Hall, R. L., Shopp, G. M., and O'Neill, C. A. Preclinical safety evaluation of rhuMAbVEGF, an antiangiogenic humanized monoclonal antibody. Toxicol.Pathol., *27*: 78-86, 1999.

38. Veenendaal, L. M., Jin, H., Ran, S., Cheung, L., Navone, N., Marks, J. W., Waltenberger, J., Thorpe, P., and Rosenblum, M. G. In vitro and in vivo studies of a VEGF121/rGelonin chimeric fusion toxin targeting the neovasculature of solid tumors. Proc.Natl.Acad.Sci.U.S.A, *99*: 7866-7871, 2002.

Appendices:

1. Mohamedali K, Poblenz A, Sikes C, Luster T, Navone N, Thorpe P, Darnay B, Rosenblum MG. The Vascular Targeting Agent $VEGF_{121}$/rGel Inhibits Bone Remodeling and Skeletal Metastases through a Unique Mechanism. AACR, Abstract# 4624, 2005.
2. Mohamedali KA, Poblenz AT, Sikes C, Novone N, Thorpe P, Darnay B and Rosenblum M. Inhibition of Bone Remodeling and Prostate Skeletal Metastases by the Vasulcar Targeting Agent $VEGF_{121}$/rGel. Nature Medicine, submitted.
3. Ran S, Mohamedali K, Thorpe P, Rosenblum M. The vascular-ablative agent $VEGF_{121}$/rGel inhibits pulmonary metastases of MDA-MB-231 breast tumors. Neoplasia 7(5):486-496, 2005.
4. Lyu M-A, Kurzrock R, Rosenblum M. Targeting Human Pancreatic Tumor Cells with the anti-HER-2/neu Immunocytokine scFv23/TNF. Molecular Cancer Therapeutics, submitted.
5. Mohamedali K, Gomez-Manzano C, Ramdas L, Xu J, Cheung L, Zhang W, Thorpe P, Rosenblum M. $VEGF_{121}$/rGel fusion toxin targets the KDR receptor to inhibit vascular endothelial growth *in vitro* and *in vivo*: specific effects assessed using microarray analysis. Journal of Biological Chemistry, submitted.

#1

96th Annual Meeting
April 16-20, 2005
Anaheim/Orange County, CA

Print this Page for Your Records Close Window

Abstract Number: 4624

Presentation Title: The vascular targeting agent $VEGF_{121}$/rGel inhibits bone remodeling and skeletal metastases through a unique mechanism

Presentation Start/End Time: Tuesday, Apr 19, 2005, 1:00 PM - 5:00 PM

Board Number: Board #1

Author Block: *Khalid A. Mohamedali, Ann T. Poblenz, Chuck Sikes, Troy Luster, Nora Navone, Philip Thorpe, Bryant Darnay, Michael G. Rosenblum.* UT M.D. Anderson Cancer Center, Houston, TX, UT Southwestern Medical Center, Dallas, TX

Cancer metastases to bone are associated with significant morbidity and mortality and patients with advanced cancer experience frequent bone metastasis. The pathophysiological processes leading to the development of skeletal metastases remains poorly understood. We developed a novel fusion construct designated $VEGF_{121}$/rGel, composed of $VEGF_{121}$ and the plant toxin gelonin (rGel), which targets the tumor neovasculature and exerts impressive cytotoxic effects by inhibiting cellular protein synthesis in target cells. We tested the ability of $VEGF_{121}$/rGel treatment to inhibit the growth of prostate cancer cells in a bone metastases model. $VEGF_{121}$/rGel inhibited tumor growth and enhanced survival of mice by targeting the tumor vasculature as well as normalizing the number of mature osteoclasts found in bone. Treatment of mice bearing PC-3 intrafemoral tumor xenografts with $VEGF_{121}$/rGel was shown to dramatically suppress PC-3 skeletal metastases. All control mice developed lytic lesions and were sacrificed by day 67. In contrast, 50% of the $VEGF_{121}$/rGel-treated mice survived past day 140 without any sign of skeletal tumor lesions. In vitro studies showed that $VEGF_{121}$/rGel but not rGel could dramatically suppress RANKL-induced osteoclast differentiation of RAW cells into $TRAP^+$ multi-nucleated osteoclasts. The observed effect was not mediated by either $VEGF_{121}$ or gelonin alone but is a characteristic unique to the combined fusion protein. The IC_{50} of $VEGF_{121}$/rGel on dividing RAW cells was 40 nM as compared with 900 nM for rGel itself, indicating the presence of a receptor for $VEGF_{121}$. Similar results were obtained for $VEGF_{121}$/rGel-treated bone marrow-derived monocytes. While immunofluorescence studies clearly show $VEGF_{121}$/rGel penetration into osteoclast precursor (RAW) cells, the receptor responsible for mediating the cellular entry of $VEGF_{121}$/rGel is unknown. RT-PCR analysis of RAW cells indicates the presence of only VEGFR-1 (Flt-1). In addition, Flt-1 levels are downregulated following stimulation of osteoclastogenesis by RANKL demonstrating that mature osteoclasts express comparatively low levels of Flt-1 and are insensitive to $VEGF_{121}$/rGel cytotoxic effects. These studies suggest an important role for VEGF and its receptors in tumor-mediated osteoclastogenesis and demonstrate that $VEGF_{121}$/rGel appears to suppress osteolytic lesions by acting directly on osteoclast precursor cells as well as on suppression of tumor vasculature. This suggests a previously unrecognized role for this unique agent in the treatment of skeletal metastases. Research conducted, in part, by the Clayton Foundation for Research.

96th Annual Meeting
April 16-20, 2005
Anaheim/Orange County, CA

Citation format: Proc Amer Assoc Cancer Res 2005;46:[Abstract #].

Manuscript Submitted to Nature Medicine

Inhibition of Bone Remodeling and Prostate Skeletal Metastases by the Vascular Targeting Agent $VEGF_{121}$/rGel

Khalid A. Mohamedali[1], Ann T. Poblenz[1], Chuck Sikes[2], Nora Navone[2], Philip Thorpe[3], Bryant Darnay[1] and Michael G. Rosenblum[1]

[1]Department of Experimental Therapeutics, The University of Texas M. D. Anderson Cancer Center, Houston, Texas 77030, USA. [2]Department of Genitourinary Medical Oncology, The University of Texas M. D. Anderson Cancer Center, Houston, TX 77030, USA. [3]Department of Pharmacology, Simmons Comprehensive Cancer Center, The University of Texas Southwestern Medical Center, Dallas, Texas 75390, USA.

Correspondence to: Michael G. Rosenblum, Ph. D., The University of Texas M. D. Anderson Cancer Center, Department of Experimental Therapeutics, Unit 44, 1515 Holcombe Blvd., Houston, Texas 77030. Tel: 713-792-3554; Fax: 713-794-4261 or 713-745-3916; E-mail: mrosenbl@mdanderson.org.

Research supported in part by the Clayton Foundation for Research and The Department of Defense (DAMD-17-02-1-0457).

Abstract

The pathophysiological processes underlying the development of skeletal metastases remain incompletely understood and these lesions respond poorly to therapeutic intervention. Vascular endothelial growth factor A (VEGF-A) and its receptors are known to play a role in both osteoclastogenesis and in tumor growth. We previously described a fusion toxin composed of $VEGF_{121}$ and the toxin gelonin and its ability to target cells overexpressing VEGF receptors. Systemic treatment of nude mice bearing skeletal prostate (PC-3) tumors with $VEGF_{121}$/rGel dramatically inhibited the growth of prostate bone metastases and 50% percent of treated mice demonstrated complete regression of bone tumors with no development of lytic bone lesions. Immunohistochemical analysis additionally demonstrated that $VEGF_{121}$/rGel treatment suppressed tumor-mediated osteoclastogenesis in vivo. In vitro treatment of murine osteoclast precursors obtained from either bone marrow or cell lines (RAW264.7) revealed that $VEGF_{121}$/rGel was selectively cytotoxic to osteoclast precursor cells rather than mature osteoclasts. Maturation of precursor cells by treatment with RANKL resulted in down-regulation of Flt-1 receptors and resistance to the cytotoxic effects of $VEGF_{121}$/rGel. Analysis by flow cytometry and RT-PCR showed that both bone marrow-derived monocytes (BMM) and RAW264.7 cells both display high levels of Flt-1 but low levels of Flk-1 receptors for VEGF. Internalization of $VEGF_{121}$/rGel into osteoclast precursor cells was suppressed by pre-treatment with an Flt-1 neutralizing antibody or by PlGF, but not with an Flk-1 neutralizing antibody. $VEGF_{121}$/rGel not only inhibits neovascularization of tumor bone lesions, but also inhibits osteoclast maturation/recruitment in vivo and it appears that both processes are important in the

resulting suppression of skeletal osteolytic lesions. This is a novel and unique mechanism of action for this class of agents and suggests a potentially new approach to treatment or prevention of skeletal metastases. In addition, these data demonstrate that $VEGF_{121}$/rGel is a useful probe to investigate the role of VEGF and its cognate receptors in the development of skeletal metastases.

Introduction

Osteoclastogenesis differentiation and activation plays a central role in the development and maintainence of normal bone tissue, which requires osteoblastic matrix deposition and osteoclastic resorption to be closely coordinated (for review, see [1]). Interference with the process of osteoclastogenesis alters the kinetics of bone remodeling resulting in abnormal bone development[2-5]. There is general consensus that the hematopoietically-derived osteoclast is the pivotal cell in the degradation of the bone matrix[6] and stimulation of osteoclastic bone resorption is the primary mechanism responsible for bone destruction in metastatic cancer[7-9].

The progression of osteolytic metastases requires the establishment of close functional interactions between tumor cells and bone cells[10-12]. Osteoclast precursor cells may be stimulated to differentiate or activated directly by tumor-secreted soluble factors such as GM-CSF, M-CSF, interleukins, TGF-β and VEGF among others[7,9,13-15]. The secretion of some of these factors by cancer cells regulates expression of RANKL on the surface of stromal osteoblasts, thereby increasing osteoclast-mediated bone resorption[16,17].

While there is now little doubt that the VEGF-A cytokine family has an essential role in the regulation of embryonic and postnatal physiologic angiogenic processes, their role in skeletal growth, endochondral bone formation and differentiation of osteoclast pre-cursor cells is substantially less well-understood. Osteoclast pre-cursor cells have been shown to be recruited to the future site of resorption by VEGF-A and RANKL, two cytokines that are expressed in the immediate vicinity of the bone surface[18,19]. VEGF mRNA is expressed by hypertrophic chondrocytes in the epiphyseal growth plate, suggesting that a VEGF gradient is needed for directional growth and cartilage invasion

by metaphyseal blood vessels[20]. Treatment with a soluble VEGFR-1 antibody to block VEGF results in almost complete suppression of blood vessel invasion and impaired trabecular bone formation[20], a development that is reversed by cessation of the anti-VEGF treatment. A similar phenotype is observed when *Vegf* is deleted in the cartilage of developing mice by means of Cre-*lox*P-mediated, tissue-specific gene ablation[21]. In addition, examination of $VEGF^{120/120}$ mice shows delayed recruitment of blood vessels into the perichondrium as well as delayed invasion of vessels into the primary ossification center, indicating a significant role of VEGF at both early and late stages of cartilage vascularization[22].

VEGF plays an important role in the vascularization of bone tissues[23,24]; increases osteoclast-mediated bone resorption[25,26]; induces osteoclast chemotaxis and recruits osteoclasts to the site of bone remodeling[19,27]; and can partially rescue M-CSF deficiency in op/op mice[26].

While VEGF receptors have been the increasing focus of attention as therapeutic targets, both by us[28,29] and others[30-32], the context has usually been in terms of vascular targeting and anti-angiogenic therapy. The VEGF receptors Flt-1/FLT-1 (VEGFR-1) and Flk-1/KDR (VEGFR-2) are over-expressed on the endothelium of tumor vasculature[33-39] including lung, brain, breast, colon, prostate, skin and ovarian cancers. In contrast, these receptors are almost undetectable in the vascular endothelium of adjacent normal tissues[40] and, therefore, appear to be excellent targets for the development of therapeutic agents that inhibit tumor growth and metastatic spread through inhibition of tumor neovascularization.

Both of the major receptors of VEGF-A have been observed in osteoclasts[20,26,41], although some reports cite only the presence of Flt-1[41,42]. The VEGF-Flt-1 interaction has been implicated in the recruitment process of osteoclast pre-cursor cells from hematopoietic tissue to the site of bone resorption[41,43,44]. However, the role of each receptor, and its regulation, has yet to be established. Osteoclasts play a critical role in the establishment of osteoblastic bone metastases by inducing bone resorption, which allows cancer cells to invade the bone and therefore promote tumor growth. Therefore, establishing the precise role that each VEGF receptor plays in the maturation of osteoclast pre-cursor cells to osteoclasts is a critical step towards understanding the interaction that occurs between tumor cells and the bone microenvironment.

We previously developed and characterized a novel growth factor fusion construct composed of $VEGF_{121}$ and the highly cytotoxic plant toxin gelonin (rGel)[29]. Our previous studies have demonstrated an impressive vascular targeting and vascular ablative activity of $VEGF_{121}$/rGel against tumor neovasculature in a variety of soft-tissue tumor xenograft models. In the current study, we used the $VEGF_{121}$/rGel fusion toxin to inhibit growth of tumor cells in a prostate cancer skeletal metastasis model and as a probe to investigate the role of VEGF and its cognate receptors in the development of skeletal metastases.

Results

$VEGF_{121}$/rGel inhibits growth of intrafemoral PC-3 tumors and reduces the number of tumor-induced osteoclasts.

The anti-tumor effect of the fusion protein $VEGF_{121}$/rGel was evaluated in a prostate cancer bone model by injecting PC-3 tumor cells into the distal epiphysis of the right femur of athymic nude mice. The mice were treated every other day (five total treatments) with a total dose of 45 mg/kg of $VEGF_{121}$/rGel or saline. Tumor growth was monitored by X-ray analysis and animals with large osteolytic lesions or bone lysis were sacrificed. One hundred percent (100%) of tumor-innoculated mice treated with saline developed osteolytic lesions (Fig. 1a, left panels) and 50% survival occurred 40 days after tumor placement (Fig. 1b). In contrast, treatment with $VEGF_{121}$/rGel resulted in suppression of intrafemoral growth of tumor osteolytic lesions as assessed radiologically (Fig. 1a, right panels) and 50% of the $VEGF_{121}$/rGel-treated mice survived past 140 days without sign of osteolysis (Fig. 1b). H&E staining showed nests of PC-3 cells in bone marrow of mice treated with saline (Fig. 1c, top panel) and isolated pockets of PC-3 cells in some bone marrow sections from $VEGF_{121}$/rGel-treated mice (Fig.1c, arrows, middle panel), as well as bone sections without any visible tumor cells from mice treated with $VEGF_{121}$/rGel (Fig. 1c, bottom panel).

We next examined PC-3 tumor cells to identify whether the observed $VEGF_{121}$/rGel-mediated inhibition of PC-3- induced osteolysis was a direct effect on the tumor cells. As shown in Fig 2a, the $VEGF_{121}$/rGel fusion construct was not specifically cytotoxic to tumor cells compared to the rGel toxin alone suggesting that these cells

express an insufficient number of VEGF receptors to mediate specific $VEGF_{121}$/rGel cytotoxicity. This was confirmed by RT-PCR analysis (Fig. 2a, inset).

Immunohistochemical analysis of tissue sections for osteoclasts (TRAP staining) revealed a dramatic increase in the number of osteoclasts in the tumor-bearing leg of mice treated with saline (Fig. 2b). In contrast, bone sections of $VEGF_{121}$/rGel-treated mice showed the same number of osteoclasts as those present in the contralateral (control) leg, suggesting that $VEGF_{121}$/rGel may play a role in inhibiting tumor-mediated osteoclast proliferation and/or differentiation.

$VEGF_{121}$/rGel affects osteoclast pre-cursor cells but not terminally differentiated osteoclasts

To understand the effect of $VEGF_{121}$/rGel in the bone microenvironment and test if $VEGF_{121}$/rGel may be directly targeting osteoclast pre-cursor cells *in vivo*, we next evaluated the effect of $VEGF_{121}$/rGel on RANKL-induced osteoclast differentiation of RAW264.7 cells and bone marrow-derived monocytes (BMM) *in vitro*. Treatment with increasing concentrations of $VEGF_{121}$/rGel, but not rGel, showed a dramatic decrease of $TRAP^+$ multi-nucleated osteoclasts in both RAW264.7 (Fig. 3a and 3b) and BMM (Fig. 3d and 3e) cells. The observed effect was not mediated by either $VEGF_{121}$ or gelonin alone but is a characteristic unique to the combined fusion protein. The IC_{50} of $VEGF_{121}$/rGel on undifferentiated RAW264.7 cells was 40 nM compared to 900 nM for rGel, indicating that the cytotoxicity of $VEGF_{121}$/rGel was mediated through $VEGF_{121}$ and suggested the presence of a receptor recognizing $VEGF_{121}$ (Fig. 3c). Similar to the RAW264.7 cells, the IC_{50} of $VEGF_{121}$/rGel (8 nM) on undifferentiated BMM cells was

substantially lower than that of rGel (Fig. 4f, exact IC_{50} not determined). $VEGF_{121}$/rGel demonstrated a greater cytotoxic effect on BMM compared to undifferentiated RAW264.7 cells. In addition, we observed that $VEGF_{121}$/rGel, but not rGel, inhibited the M-CSF-dependent survival of monocytes (data not shown). Thus, $VEGF_{121}$/rGel not only inhibited RANKL-mediated differentiation of osteoclast precursors, but also exhibited cytotoxicity towards undifferentiated cells in a targeted manner.

The observed inhibitory effect of $VEGF_{121}$/rGel on osteoclastogenesis could be due to a reduced density of osteoclast progenitor cells. Insufficient number of osteoclast progenitor cells may lead to impaired contact between committed progenitors, leading to inability to form multi-nucleated osteoclasts. We next investigated the susceptibility of primary mouse monocytes and their terminally differentiated counterparts to $VEGF_{121}$/rGel cytotoxicity. BMM cells were treated with VEGF/rGel or rGel at various times after RANKL stimulation. Cells treated with $VEGF_{121}$/rGel simultaneously with RANKL stimulation showed a dose-dependent inhibition of osteoclastogenesis (Fig. 4a, b and d) as described above. However, osteoclastogenesis proceeded normally if BMM cells were allowed to differentiate for 60 h prior to the addition of $VEGF_{121}$/rGel (Fig. 4c and d). The apparent cytotoxicity of $VEGF_{121}$/rGel to osteoclast pre-cursor cells but not to mature osteoclasts was further investigated by adding $VEGF_{121}$/rGel at different time points after RANKL stimulation of both RAW264.7 and BMM cells (Table 1). The increase in the IC_{50} of $VEGF_{121}$/rGel corresponded to the length of time following RANKL stimulation of both RAW264.7 (Table 1a) and BMM (Table 1b) cells. In RAW264.7 cells, the IC_{50} of $VEGF_{121}$/rGel increased from 30 nM when added simultaneously with RANKL to 300 nM when added 96 h after RANKL stimulation,

whereas the IC_{50} of rGel did not change significantly. The change in IC_{50} of $VEGF_{121}$/rGel on BMM cells was more dramatic, increasing from 8 nM to 100 nM if $VEGF_{121}$/rGel was added 24 h post RANKL stimulation. Addition of $VEGF_{121}$/rGel 48 h post RANKL stimulation increased the IC_{50} to > 400 nM.

$VEGF_{121}$/rGel but not rGel is internalized into RAW264.7 cells and BMM cells through a specific mechanism

Based on our previous studies, specific VEGF-driven cytotoxicity is receptor-dependant and we next examined by immunostaining whether $VEGF_{121}$/rGel was delivered into the cytoplasm of the osteoclast pre-cursor cells. $VEGF_{121}$/rGel, but not rGel, localized in the cytoplasm of RAW264.7 cells and this internalization data is consistent with our studies on the cytotoxic effect of this agent (Fig. 5a). We assessed if internalization of $VEGF_{121}$/rGel was mediated by a VEGF receptor by examining by Western blot analysis if $VEGF_{121}$/rGel activated pp44/42, a known down-stream target of VEGF receptor activation. Treatment with$VEGF_{121}$/rGel resulted in similar activation of pp44/42, as did treatment with equimolar amounts of $VEGF_{121}$ alone (Fig. 5b). rGel did not induce stimulation of pp44/42, indicating that the effect of $VEGF_{121}$/rGel is mediated by a $VEGF_{121}$ receptor, rather than a non-specific mechanism (Fig.5b). Treatment with PlGF, an Flt-1-specific ligand, resulted in pp44/42 activation underscoring the presence of this receptor on the surface of osteoclast pre-cursor cells.

RAW264.7 and BMM cells express Flt-1

Because $VEGF_{121}$/rGel cytotoxicity on both RAW264.7 and BMM cells appears to be mediated by receptors for $VEGF_{121}$, we determined the levels of Flk-1 and Flt-1 in these cells. RT-PCR analysis indicated low levels of Flt-1, but no Flk-1 transcript, in RAW264.7 cells (Fig. 6a, lanes 1-3). Western blot analysis of RAW264.7 cells confirmed this observation (Fig. 6b). FACS analysis indicated that 99% of the RAW264.7 cells expressed Flt-1 (Fig. 6c) and 8% expressed Flk-1 (Fig. 6d). RT-PCR analysis of BMM cells showed an amplification of both Flt-1 and Flk-1 (Fig. 6a, lanes 4-6) and FACS analysis showed that 41.9% of the CD11b positive BMM cells expressed Flt-1 and 5.4% expressed Flk-1 (Fig. 6e-g). RT-PCR analysis of BMM cells following stimulation of RANKL-mediated osteoclastogenesis showed no change in the levels of Flk-1, but treatment appeared to downregulate the Flt-1 transcript (Fig. 6h). RT-PCR analysis of mVEGF isoforms detected low levels of $VEGF_{164}$ and $VEGF_{120}$ transcript but no $VEGF_{188}$ (data not shown). The downregulation of Flt-1 mRNA in BMM cells following stimulation of osteoclastogenesis by RANKL was confirmed by testing samples at different cycles of the RT-PCR analysis (data not shown) and further validated by densitometric analysis as described in Methods. All bands were individually compared to its internal GAPDH standard loaded in the same fashion in order to normalize the data. Flk-1 did not show a significant change in expression 96 h post RANKL stimulation whereas Flt-1 did exhibit a down-regulation of 3.4 fold 96 h post RANKL stimulation compared to untreated BMM (Fig. 6i).

Localization of $VEGF_{121}$/rGel into RAW264.7 and BMM cells may be mediated by Flt-1

To determine the role of $VEGF_{121}$ receptors in $VEGF_{121}$/rGel-mediated cytotoxicity of osteoclast precursor cells, we pre-incubated RAW264.7 and BMM cells with neutralizing antibodies to Flt-1 and Flk-1 for one hour prior to addition of $VEGF_{121}$/rGel, and monitored internalization of $VEGF_{121}$/rGel. Pretreatment of RAW264.7 cells and BMM cells with neutralizing antibodies to Flt-1, but not Flk-1 inhibited the localization of $VEGF_{121}$/rGel into these cells (Fig 7a). We assessed the role of each receptor in $VEGF_{121}$/rGel –mediated cytotoxicity by pre-incubating RAW264.7 and BMM cells with Flt-1 or Flk-1 neutralizing antibodies or with PlGF for 1h prior to the addition of $VEGF_{121}$/rGel. PlGF was able to inhibit the $VEGF_{121}$/rGel-mediated cytotoxicity in both RAW264.7 and BMM cells (Fig. 7b). Taken together, this indicates that the Flt-1 receptor, but not the Flk-1 receptor, is responsible for mediating $VEGF_{121}$/rGel- induced cytotoxicity in osteoclast progenitor cells.

Discussion

Prostate cancer is highly metastatic and the primary site of prostate cancer metastases is bone. The survival rate of patients with prostate cancer metastases is about 31%, compared to a nearly 100% 5-year survival rate if the cancer is locally confined. Several reports[45-50] have implicated VEGF in prostate carcinogenesis and metastatic spread in addition to its well-established role in angiogenesis. VEGF is also produced by tumor cells to facilitate nesting of metastatic cells in bone and to promote neovascularization[20] which are two critical events necessary to the successful formation of skeletal metastases.

Receptor kinase inhibitors, antibodies targeting the receptors for VEGF and other strategies are all under development as strategies to disrupt tumor angiogenesis[51-56]. Growth factor fusion constructs such as $VEGF_{121}$/rGel have a tremendous potential to interfere with tumor angiogenesis by targeted destruction of tumor endothelium. However, our observation that the anti-angiogenic $VEGF_{121}$/rGel construct can significantly impact skeletal prostate metastases is a novel finding for agents in this class although studies by Dai et al[57] and Shariat et al[58] have suggested a link between VEGF expression and metastatic spread (including skeletal metastases) in prostate tumors. Another unanticipated finding is that this agent can disrupt osteoclast activity and a third finding is that the cytotoxic effect of the $VEGF_{121}$/rGel construct on osteoclasts can be mediated through interaction with the Flt-1 receptor. These observations provide a potentially new series of pathways, which may be exploited not only for prostate metastases to bone but theoretically for treatment of other osteolytic tumors as well.

Previous studies in our laboratory have clearly demonstrated that the cytotoxicity and cellular internalization of $VEGF_{121}$/rGel on vascular endothelial cells is mediated through binding to the Flk-1/KDR receptor and not the Flt-1 receptor. However, the current study demonstrates that Flt-1 and not Flk-1 on osteoclast precursor cells appears to be primarily responsible for mediating the cytotoxic effects of $VEGF_{121}$/rGel. Using competition assays with specific blocking antibodies against either Flt-1 or Flk-1, as well as using the Flt-1-specific ligang PlGF, our data suggests that Flt-1 may be the receptor utilized for internalization by $VEGF_{121}$/rGel in this system. PlGF may recruite Flt-1 positive cells from the bone-marrow microenvironment[59]. This indicates that $VEGF_{121}$/rGel may also intervene with monocyte migration/activation as this event is mediated by Flt-1[43]. Taken together, our studies suggest that the biological role and character of the two receptors for VEGF is different on osteoclasts compared to vascular endothelial cells[60-62]. Our results imply a more complex biology for these receptors than has been previously appreciated. $VEGF_{121}$/rGel appears to be an excellent probe to investigate the biology of Flt-1 and Flk-1/KDR receptors and their interaction in complex systems.

Of the VEGF receptors, Flt-1 was the first to be discovered[63], and yet its function is not understood as well as other VEGF receptors. It was originally suggested that Flt-1 merely functions as a decoy receptor, tempering the activation of Flk-1/KDR[64]. Conflicting data at the present suggests that the function and signaling of Flt-1 is complex and appears to be dependent on developmental stage and on cell type[60-62]. Importantly Flt-1, but not Flk-1/KDR, is associated with inhibition of hematopoietic stem cell cycling, differentiation, and hematopoietic recovery in adults[65], and hematopoietic cell

motility[43,59] and since $VEGF_{121}$/rGel targets osteoclast precursor cells specifically expressing Flt-1, this may suggest that the Flt-1 receptor may be an overlooked therapeutic target to specifically modulate osteolytic bone diseases.

The dual ability of $VEGF_{121}$/rGel to target neovasculature as well as osteoclast precursor cells, represents a novel application of this fusion protein with significant clinical potential. Because VEGF is involved in both angiogenesis and osteolysis (Fig. 8), $VEGF_{121}$/rGel may disrupt tumor growth both by preventing angiogenesis and by inhibiting the process of bone remodeling. This, in turn, prevents further tumor invasion and osteolytic penetration of tumor into bone. Since osteolysis is an integral component of osteoblastic lesions as well, it remains to be seen if $VEGF_{121}$/rGel is as efficacious in these models and xenograft model studies are currently under way to address this issue. Based on our data, the "trojan horse" approach employed by $VEGF_{121}$/rGel might be useful for the treatment of bone-related malignancies such as bone metastases, and may also be useful in treating other bone-related malignancies such as the osteoclast component of Pagets disease and hematopoietic diseases such as multiple myeloma. Our study clearly shows that the Flt-1 receptor may be of equal if not greater importance in bone biology and warrants further study regarding its importance in the normal bone remodeling process and in various pathological states.

Methods

Materials

Bacterial strains, pET bacterial expression plasmids and recombinant enterokinase were obtained from Novagen (Madison, WI). All other chemicals were from Sigma Chemical Company (St. Louis, MO) or Fisher Scientific (Pittsburgh, PA). TALON metal affinity resin was obtained from Clontech laboratories (Palo Alto, CA). Other chromatography resin and materials were from Pharmacia Biotech (Piscataway, NJ). Tissue culture reagents were from Gibco BRL (Gaithersburg, MD) or Mediatech Cellgro (Herndon, VA). Rabbit anti-gelonin antisera were obtained from the Veterinary Medicine Core Facility at MDACC. Anti-Flt-1 (sc-9029), and anti-Flk-1 (sc-315,sc-19530) polyclonal antibodies were purchased from Santa Cruz Biotechnology, Inc. (Santa Cruz, CA). R-Phycoerythrin (R-PE)-conjugated Flk-1 monoclonal antibody and Alexa Fluor 488-conjugated CD11b (Mac-1) monoclonal antibody were purchased from BD Pharmingen (San Diego, CA). R-Phycoerythrin-conjugated secondary antibodies were purchased from Jackson ImmunoResearch Laboratories Inc. (West Grove, PA). Neutralizing antibodies to Flt-1 (AF471) and Flk-1 (AF644), recombinant mM-CSF and rPlGF were purchased from R&D Systems (Minneapolis, MN).

Cell lines

All media were supplemented with 100 units/ml penicillin, 100 units/ml streptomycin, and 10% fetal bovine serum (FBS). Porcine aortic endothelial cells transfected with the human KDR (PAE/KDR) or FLT-1 (PAE/FLT-1) receptors were a

generous gift from Dr. J. Waltenberger. Cells were maintained as a monolayer in F12 nutrient medium (HAM). Mouse brain endothelial (bEnd3) cells and the prostate cancer cell line PC-3 were maintained as monolayer cultures in DMEM with 10% non-essential amino acids. The cultured mouse osteoclast precursor cells RAW264.7 was maintained in DMEM-F12 medium. BMM cells were maintained in α-MEM medium with M-CSF (R&D Systems Inc., Minneapolis MN). Cells were harvested by treatment with Versene (0.02% EDTA/PBS) or Trypsin/EDTA (0.025%/0.01%).

Primary Bone Marrow Cell Culture

Bone marrow cells from the tibiae and femora were aseptically dissected from mice 8-12 weeks of age. Bone ends were cut off, and marrow was forced out in α-MEM supplemented with 10% FBS and 100 units/ml penicillin (α-MEM). The marrow suspension was filtered through a fine meshed sieve to remove bone particles and gentle pipetting was used to obtain a single cell suspension. The bone marrow cells were washed and plated at 1.5-2 x 10^7 cells/10 cm dish with 10 ml of α -MEM and cultured for 24h in the presence of M-CSF (10ng/ml). Non-adherent cells were then washed and re-suspended in α -MEM, plated at 2.5 x 10^4 cells per well in a 96 well dish for cyto-toxicity assays or 5 x 10^3 pre well in a 96 well plate for osteoclast assays, RNA extraction and Western blot analysis. Cells were then cultured for 3 days in the presence of 10 ng/ml M-CSF before they were used for further experiments.

Animals

Male athymic BALB/c nude mice were obtained from the Animal Production Area of the National Cancer Institute, Frederick Cancer Research Facility (Frederick, MD). Black 6 mice (C57BL/6J) were obtained from Charles River (Wilmington, MA). Mice were maintained in a laminar air-flow cabinet under specific pathogen-free conditions and used at 8-12 weeks of age. All facilities were approved by the American Association for Accreditation of Laboratory Animal Care (AAALAC) in accordance with the current regulations and standards of the United States Department of Agriculture, the Department of Health and Human Services, and the NIH. Mice were fed Purina rodent chow and tap water ad libitum.

Expression and purification of $VEGF_{121}$/rGel

The construction, expression and purification of $VEGF_{121}$/rGel has been previously described[29]. The fusion toxin was stored in sterile PBS at -20°C.

Cytoxicity of $VEGF_{121}$/rGel and rGel

Cytotoxicity of $VEGF_{121}$/rGel and rGel against log phase PC-3, RAW264.7 and BMM cells was performed as described[29]. Log phase cells (3×10^3 PC-3, 5×10^3 RAW264.7 or 2.5×10^4 BMM) were plated in 96-well flat-bottom tissue culture plates and allowed to attach overnight. Purified $VEGF_{121}$/rGel and rGel were diluted in culture media and added to the wells in 5-fold serial dilutions. Cells were incubated for 72 h. The remaining adherent cells were stained with crystal violet (0.5% in 20% methanol) and

solubilized with Sorenson's buffer (0.1 M sodium citrate, pH 4.2, in 50% ethanol). Absorbance was measured at 630 nm.

In Vitro Osteoclast Differentiation

BMM and RAW 264.7 cells were cultured in 96-well dishes at a density of 5 x 10^3 cells per well and 3 x 10^3 cells per well, respectively. Cell cultures were initially treated with 100 ng/ml RANKL and 10ng/ml M-CSF (for BMM) and also subject to a medium change on day 3. We assessed osteoclast differentiation by counting the total number of multinucleated (>3 nuclei), TRAP-positive cells per well 96 h post-treatment using the Leucocyte Acid phosphatase kit (Sigma-Aldrich , St. Louis, MO, USA).

Time-dependent cytotoxicity

Non-adherent, primary monocytes (50 x 10^3 /well) were cultured overnight in 24-well plates. Cells were then treated with RANKL (100 ng/ml) in the absence or presence of increasing concentrations of $VEGF_{121}$/rGel or rGel added either with RANKL stimulation and TRAP stained at 96h post-treatment, added with RANKL stimulation and TRAP stained at 60h post treatment, or added at 60h post RANKL stimulation and TRAP stained at 96h. Cells were fixed, stained for TRAP and TRAP+ multinucleated cells were counted in each condition.

RNA extraction

BMM and RAW cells were treated with their respective IC_{50} $VEGF_{121}$/rGel doses in the presence and absence of RANKL (and M-CSF for BMM cells) for 24 to 96 h.

Control cells, including bEnd3, PAE/KDR and PAE/FLT-1 cells, were treated with PBS. Total RNA was extracted using the RNeasy mini-kit (Qiagen, Valencia, CA) and its integrity verified by electrophoresis on a denaturing formaldehyde-agarose gel and on a 2100 Bioanalyzer (Agilent, Foster City, CA).

RT-PCR analysis

Levels of Flt-1/FLT-1, Flk-1/KDR and VEGF-A were assessed by RT-PCR analysis. GAPDH primers were used as controls. The primers were as follows: Flk-1/KDR forward – 5' ATTACTTGCAGGGGACAG; Flk-1/KDR reverse – 5' GGAACAAATCTCTTTTCTGG; Flk-1 forward – 5' CATGCACAGTCTACGCCAACC; Flk-1 reverse – 5' CGCAACATGTTTACACTTCGGT; Flt-1/FLT-1 forward – 5' CAAATGCAACGTACAAAGA; Flt-1/FLT-1 reverse – 5' AGAGTGGCAGTGAGGTTTTTT; Flt-1 forward – 5' ACTGAAACTAGGCAAATCGCTCG; Flt-1 reverse – 3' GCGGATCTGTCACAGTCGTCG; VEGF-A forward – 5' TGAAGTGATCAAGTTCATGGACGT; VEGF-A reverse – 5' TCACCGCCTTGGCTTGTC; GAPDH forward - 5' GTCTTCACCACCATGGAG; and GAPDH reverse - 5' CCACCCTGTTGCTGTAGC. Isolated RNA was subjected to first-strand cDNA synthesis as described by the manufacturer of the Superscript First Strand synthesis system (Invitrogen, Carlsbad, CA). RT-PCR was performed using a Robocyclet Gradient 96 machine (Stratagene, La Jolla, CA). Negative controls (samples without Taq polymerase or with water instead of RNA) were included. Amplified RT-PCR products were analyzed on 2% agarose gels containing ethidium bromide and

subjected to densitometric analysis using Alpha Innotech FluorChem8900 (San Leandro, CA).

Western blot analysis

Total cell extracts of PAE/KDR and PAE/FLT-1 cells were obtained by lysing cells in Cell Lysis buffer (50 mM Tris, pH 8.0, 0.1 mM EDTA, 1 mM DTT, 12.5 mM $MgCl_2$, 0.1 M KCl, 20% glycerol) supplemented with protease inhibitors (leupeptin (0.5%), aprotinin (0.5%) and PMSF (0.1%). Protein samples were separated by SDS-PAGE under reducing conditions and electrophoretically transferred to a PVDF memberane overnight at 4°C in transfer buffer (25 mM Tris-HCl, pH 7.6, 190 mM glycine, 20% HPLC-grade methanol). The membranes were incubated overnight with appropriate antibodies (1:200 in 5% milk) followed by incubation with goat-anti-rabbit IgG horseradish peroxidase, developed using the Amersham ECL detection system and exposed to X-ray film.

FACS Analysis

RAW246.7 and BMM cells were harvested and washed with PBS, resuspended in staining buffer (PBS + 2% FBS) at a concentration of $10x10^6$ cells/ml. One hundred microliter aliquots of RAW264.7 and BMM cells were incubated with 2 μg and 0.5 μg anti-Flt-1 or R-PE conjugated anti-Flk-1 antibody respectively. Cells were incubated with primary antibodies for 1 h at 4°C. In addition, BMM cells were incubated for 1 h (4°C) with 0.2 μg Alexa Fluor 488-conjugated CD11b antibody for detection of the monocyte/macrophage population. 0.5 μg R-PE conjugated secondary antibody (Jackson

Immunoresearch, West Grove, PA) was employed to detect anti Flt-1. Samples were analyzed on a BD FACS Calibur flow cytometer (BD, San Jose, CA), using CellQuest Pro acquisition software (BD, San Jose, CA). Instrumentation set-up and electronic compensation for spectral overlap was performed using cell samples single-stained with FITC or R-PE. At least 10,000 events were collected for each sample.

Internalization of $VEGF_{121}$/rGel into RAW264.7 and BMM cells

Cells were incubated with various concentrations of $VEGF_{121}$/rGel or rGel at the timepoints indicated. To demonstrate receptor specificity, Cells were pre-treated with Flt-1 or Flk-1 neutralizing antibodies for one hour prior to treatment with $VEGF_{121}$/rGel or rGel. Glycine buffer (500 mM NaCl, 0.1 glycine, pH 2.5) was used to strip the cell surface of non-internalized $VEGF_{121}$/rGel. Cells were fixed with 3.7% formaldehyde and permeabilized with 0.2% Triton X-100. Non-specific binding sites were blocked with 5% BSA in PBS. Cells were then incubated with a rabbit anti-gelonin polyclonal antibody (1:200) followed by a TRITC-conjugated anti-rabbit secondary antibody (1:80). Nuclei were stained with propidium iodide (1μg/ml) in PBS. The slides were fixed with DABCO media, mounted and visualized under fluorescence (Nikon Eclipse TS1000) and confocal (Zeiss LSM 510) microscopes. Competition assays were performed by plating RAW264.7 (5×10^3) and BMM (2.5×10^4) cells in 96 well plates and pre-incubating the cells for 1 h with increasing doses of PlGF (prior to addition of 20 nM $VEGF_{121}$/rGel. Results were analyzed by staining the remaining adherent cells with crystal violet as described above.

Intrabone injections

The PC-3 cells were harvested by a 1 min treatment with Trypsin/EDTA. The culture flask was tapped to detach the cells. The cells were washed in PBS and resuspended in PBS in preparation for implantation into the mice. Animals were anesthetized with intramuscular injections of ketamine (100 mg/kg) plus acepromazine (2.5 mg/kg). Aliquots of 5×10^4 of PC-3 cells were diluted in 5 μl of growth medium and then injected into the distal epiphysis of the right femur of each mouse using a 28-gauge Hamilton needle. The contralateral femur was used as an internal control. Twenty mice were randomized into two treatment groups. Treatment began one week after tumor placement. The animals were treated (i.v.) with the following protocol: Group 1 - 200 μl saline every other day for nine days (5 treatments); Group 2 - 180 μg $VEGF_{121}$/rGel in 200 μl saline every other day for nine days (5 treatments). Mice were monitored weekly for tumor bulk and bone loss. Mice were killed in case of excessive bone loss as per AAALAC guidelines and pathologic examination of the subject bones was performed.

Processing of bone tissue samples

Formalin-fixed, paraffin-embedded tissue samples from the tumors were prepared by the Department of Veterinary Medicine at M. D. Anderson Cancer Center. The subject bones were dissected free of muscle, fixed in 10% buffered formalin, decalcified in 5% formic acid, and then embedded in paraffin. Longitudinal 3-μm thick sections were obtained from each sample and stained with H&E. TRAP staining was performed as described by the manufacturer of the kit (Sigma Aldrich, St. Louis, MO).

Figure Legends

Figure 1 $VEGF_{121}$/rGel inhibits tumor growth and osteolysis in the PC-3 xenograft model and increases the survival of mice. **(a)** Effect of $VEGF_{121}$/rGel in nude mice with PC-3 tumors in bone. Mice were injected with 5 x 10^4 PC-3 cells into the distal epiphysis of the right femur, using the contralateral femur as an internal control. Mice received 5 treatments with either saline or 180μg $VEGF_{121}$/rGel 2 days apart, starting 2 days post PC-3 tumor placement. Animals were analyzed by X-ray, and radiograms shown are representative of 20 mice. Arrows indicate location of osteolytic lesion, which were only found in the saline-treated animals (left panels), but not in the majority of $VEGF_{121}$/rGel treated animals (right panels). (**b**) A survival curve of the mice in this study. All control mice were sacrificed by day 67. Asterisk one mouse (without tumor) that did not recover from anesthesia. Sections of femurs two weeks after injection of PC-3 tumor cells were stained for H&E to analyze the presence of PC-3 cell burden (c). Mice treated with saline show proliferation of PC-3 tumor cells (upper panel). In contrast, mice treated with $VEGF_{121}$/rGel show isolated pockets of PC-3 tumor cells (middle panel). Shown in the lower panel is a representative bone section in which PC-3 tumor cells had been placed from a mouse treated with $VEGF_{121}$/rGel, showing absence of tumor.

Figure 2 PC-3 cells are not specifically targeted by $VEGF_{121}$/rGel. **(a)** Cytotoxicity of $VEGF_{121}$/rGel and rGel on PC-3 cells. PC-3 cells (5 x 10^3) were plated in 96- well plates and the cytotoxicity of increasing concentrations of $VEGF_{121}$/rGel and rGel were evaluated by crystal violet staining following incubation for 72 h. Values represent the mean of three separate experiments. (**a,** inset) Expression of KDR and FLT-1 RNA was

evaluated by RT-PCR. Total RNA was isolated as desribed in "Methods" and 500ng RNA of each sample was subject to RT-PCR prior to separation on a 2% agarose gel containing ethidium bromide for visualization of RNA. **(b)** Effect of $VEGF_{121}$/rGel on the number of osteoclasts in bone sections of nude mice with PC-3 tumor cells. $VEGF_{121}$/rGel reduces the number of osteoclasts and inhibits tumor growth *in vivo*.

Figure 3 $VEGF_{121}$/rGel inhibits RANKL-mediated osteoclastogenesis in RAW264.7 cells and mouse primary monocytes. Each experiment was performed in triplicate. The data shown is representative of three separate experiments. **(a)** RAW264.7 cells (1×10^4 /well) were cultured overnight in 24-well plates. Cells were treated with RANKL (100 ng/ml) in the absence or presence of increasing concentrations of $VEGF_{121}$/rGel or rGel. After 4 days, cells were fixed, TRAP stained, and the total number of multinucleated (>3 nuclei) $TRAP^+$ osteoclasts was counted. **(b)** Appearance of TRAP stained RAW264.7 cells following incubation with RANKL without or with $VEGF_{121}$/rGel or rGel. **(c)** Cytotoxicity of $VEGF_{121}$/rGel and rGel was assessed in 96-well plates. 5×10^3 RAW264.7 cells were plated in 96-well plates and incubated over night. Cells were then subjected to increasing concentrations of $VEGF_{121}$/rGel and rGel for 72 h, followed by staining with crystal violet. **(d)** Non-adherent mouse bone marrow-derived monocytes were isolated from the tibia and femur of mice and plated in 24-well plates (5×10^4 /well) and incubated with M-CSF (10 ng/ml). After 3 days, the cells were washed and stimulated with M-CSF (10 ng/ml) in the absence or presence of increasing concentrations of $VEGF_{121}$/rGel or rGel and RANKL (100 ng/ml). Medium was changed on day 3. On day 5 the cells were fixed, stained for TRAP, and the total number of

$TRAP^+$ osteoclasts was counted. **(e)** Appearance of TRAP stained BMM cells following incubation with RANKL and M-CSF without or with $VEGF_{121}$/rGel or rGel. **(f)** Cytotoxicity of $VEGF_{121}$/rGel and rGel was assessed in 96-well plates. Non-adherent mouse bone marrow-derived monocytes isolated from the tibia and femur of mice were plated (25×10^4 /well) and incubated with M-CSF (10 ng/ml) for three days. Cells were then washed and subjected to increasing concentrations of $VEGF_{121}$/rGel and rGel for 72 h, followed by staining with crystal violet.

Figure 4 $VEGF_{121}$/rGel is cytotoxic to mouse primary monocytes, but not mature osteoclasts. The effect of $VEGF_{121}$/rGel and rGel on primary monocytes was investigated at various time-points after RANKL stimulation. The data shown is representative of three separate experiments. Non-adherent, primary monocytes (50×10^3/well) were cultured overnight in 24-well plates. Cells were then treated with RANKL (100 ng/ml) in the absence or presence of increasing concentrations of $VEGF_{121}$/rGel or rGel added either with RANKL stimulation and TRAP stained at 96 h post-treatment **(a)**, added with RANKL stimulation and TRAP stained at 60 h post treatment **(b)**, or added at 60 h post RANKL stimulation and TRAP stained at 96 h **(c)**. **(d)** Cells were fixed, stained for TRAP and multinucleated (>3 nuclei), TRAP+ cells were counted in each condition. The data shown is representative of three separate experiments and error bars represent mean ± s.e.m. for each sample done in triplicate. RL: RANKL

Figure 5 $VEGF_{121}$/rGel is internalized into RAW264.7 cells and stimulates ERK activation. **(a)** Intracellular delivery of $VEGF_{121}$/rGel in RAW264.7 cells. RAW264.7 cells were treated with either $VEGF_{121}$/rGel or rGel for 24 hrs. The cells were fixed, acid-washed to remove surface-bound material, permeabilized, and immunostained for the presence of rGel (green). The cells were counterstained with propidium iodide (red) to identify nuclei. **(b)** 0.6 x 10^6 RAW264.7 cells were plated in 6 well plates and incubated for 24 hours. Cells were then serum starved over night prior to incubation of 7nM $VEGF_{121}$, 7 nM $VEGF_{121}$/rGel, 1 nM PlGF or 100nM rGel for the indicated time points. 5nM RANKL was used as a control. Cells were then harvested and 50ug of the whole cell lysate was subjected to SDS-PAGE Western blot analysis with the indicated antibodies. Data show is representative of 3 separate experiments.

Figure 6 Expression of Flt-1 and Flk-1 in RAW264.7 and BMM cells. **(a)** RT-PCR analysis. Total RNA was extracted from RAW264.7, BMM, and bEnd3 cells were subject to RT-PCR analysis using 500ng RNA and primers for Flt-1, Flk-1/KDR and GAPDH. bEnd3 cells (lanes 7-9) express both Flt-1 and Flk-1 and were used as a control. RAW264.7 cells (lanes 1-3) express Flt-1 but not Flk-1. BMM cells (lanes 4-6) express Flt-1 and low levels of Flk-1. **(b)** Western blot analysis of RAW264.7 cells. Expression of Flt-1, but not Flk-1, is confirmed. **(c-g)** FACS analysis of RAW264.7 and BMM cells for Flt-1 and Flk-1 receptors. 1 x 10^6 cells were used per sample. RAW264.7 cells incubated with antibodies recognizing the extracellular portion of Flt-1 **(c)** or Flk-1 **(d)** revealed that 99% of the cells expressed Flt-1 but only 8% of the cells expressed Flk-1. **(e)** BMM cells were identified with an antibody recognizing CD11b and double stained

with antibodies to Flt-1 (f) or Flk-1 (g). Approximately 42% of the positively identified BMM cells expressed Flt-1 but only 5.4% of the cells expressed Flk-1. Data show is representative of four separate experiments. **(h)** BMM cells stimulated to differentiate by RANKL (100 ng/ml) were harvested at the time points indicated and analyzed by RT-PCR. Flt-1 mRNA is down-regulated during RANKL-mediated differentiation of bone marrow-derived cells of monocyte/macrophage lineage to osteoclasts. GAPDH was utilized as a loading control. **(i)** Densitometric analysis of Flt-1 and Flk-1 expression in BMM cells during osteoclastogenesis. After RT-PCR, 5, 10, and 20 ul of each sample was loaded on a 2% agarose gel and evaluated densiometrically. Each sample was normalized with its individual GAPDH control within its own group and then compared to each other. The Flt-1 transcript was downregulated by 3.4-fold during differentiation of osteoclast pre-cursor cells whereas Flk-1 trancript levels did not change. Data shown represent three separate RNA preparations and is representative of 3 separate experiments.

Figure 7 Flt-1, but not Flk-1, mediates the cytotoxic effect of $VEGF_{121}$/rGel. **(a)** Cells were pre-treated for one hour with 10 μg/ml of neutralizing antibodies to either Flt-1 or Flk-1 prior to the addition of 10 nM $VEGF_{121}$/rGel . The cells were fixed, acid-washed to remove surface-bound material, permeabilized, and immunostained for the presence of rGel (green). The cells were counterstained with propidium iodide (red) to identify nuclei. **(b)** 5×10^3 RAW264.7 cells were plated in 96-well plates and incubated over night. Cells were then incubated with increasing concentrations of recombinant mouse PlGF for 1 hour prior to the addition of 30nM $VEGF_{121}$/rGel 72 h. **(c)** Non-adherent mouse bone marrow-derived monocytes were isolated from the tibia and femur of mice

and plated in 96-well plates (25 x 10^4 /well) and incubated with M-CSF (10 ng/ml). After 3 days, the cells were washed subjected to increasing concentrations of recombinant mouse PlGF for 1 hour prior to the addition of 8nM $VEGF_{121}$/rGel for 72 h. After 3 days, the remaining RAW264.7 and BMM cells were stained with crystal violet to evaluate cytotoxicity of $VEGF_{121}$/rGel and rGel. Data show is representative of two separate experiments and error bars represent mean ± s.e.m. for each concentration done in quadruplets.

Figure 8 Proposed dual role for $VEGF_{121}$/rGel in invasion and osteolytic penetration in bone. Tumor growth following skeletal metastases requires the proliferation of new blood vessels as well as resorption of bone. VEGF and its receptors play a critical role in both pathways and in the development of skeletal metastases in breast cancer. The fusion protein $VEGF_{121}$/rGel is a useful molecule to probe the roles of VEGF and its receptors, as it can prevent both angiogenesis and bone resorption by competing with VEGF as well as exerting cytotoxic effects.

Table 1

a) Cytoxicity of $VEGF_{121}$/rGel and rGel over 72 hours on RAW264.7 cells after treatment with RANKL

Agent	Treatment with RANKL (h)	IC_{50} (nM)
$VEGF_{121}$/rGel	0	30
	24	30
	72	200
	96	300
rGel	0	450
	24	500
	72	500
	96	500

b) Cytoxicity of $VEGF_{121}$/rGel and rGel over 72 hours on BMM cells after treatment with RANKL and M-CSF

Agent	Treatment with RANKL (h)	IC_{50} (nM)
$VEGF_{121}$/rGel	0	8
	24	100
	48	>400
	72	>400

Reference List

1. Boyle,W.J., Simonet,W.S. & Lacey,D.L. Osteoclast differentiation and activation. *Nature* 423, 337-342 (2003).

2. Dai,J. *et al.* Chronic alcohol ingestion induces osteoclastogenesis and bone loss through IL-6 in mice. *J. Clin. Invest* 106, 887-895 (2000).

3. Kim,S. *et al.* Stat1 functions as a cytoplasmic attenuator of Runx2 in the transcriptional program of osteoblast differentiation. *Genes Dev.* 17, 1979-1991 (2003).

4. Naruse,M. *et al.* Inhibition of osteoclast formation by 3-methylcholanthrene, a ligand for arylhydrocarbon receptor: suppression of osteoclast differentiation factor in osteogenic cells. *Biochem. Pharmacol.* 67, 119-127 (2004).

5. Odgren,P.R. *et al.* The role of RANKL (TRANCE/TNFSF11), a tumor necrosis factor family member, in skeletal development: effects of gene knockout and transgenic rescue. *Connect. Tissue Res.* 44 Suppl 1, 264-271 (2003).

6. Karsenty,G. The genetic transformation of bone biology. *Genes Dev.* 13, 3037-3051 (1999).

7. Francini,G. *et al.* Production of parathyroid hormone and parathyroid-hormone-related protein by breast cancer cells in culture. *J. Cancer Res. Clin. Oncol.* 119, 421-425 (1993).

8. Roodman,G.D. Biology of osteoclast activation in cancer. *J. Clin. Oncol.* 19, 3562-3571 (2001).

9. Taube,T., Elomaa,I., Blomqvist,C., Beneton,M.N. & Kanis,J.A. Histomorphometric evidence for osteoclast-mediated bone resorption in metastatic breast cancer. *Bone* 15, 161-166 (1994).

10. Boyce,B.F., Yoneda,T. & Guise,T.A. Factors regulating the growth of metastatic cancer in bone. *Endocr. Relat Cancer* 6, 333-347 (1999).

11. Mbalaviele,G. *et al.* Cadherin-6 mediates the heterotypic interactions between the hemopoietic osteoclast cell lineage and stromal cells in a murine model of osteoclast differentiation. *J. Cell Biol.* 141, 1467-1476 (1998).

12. Mundy,G.R. & Yoneda,T. Facilitation and suppression of bone metastasis. *Clin. Orthop. Relat Res.* 34-44 (1995).

13. Guise,T.A. & Chirgwin,J.M. Transforming growth factor-beta in osteolytic breast cancer bone metastases. *Clin. Orthop. Relat Res.* S32-S38 (2003).

14. Kumta,S.M. *et al.* Expression of VEGF and MMP-9 in giant cell tumor of bone and other osteolytic lesions. *Life Sci.* 73, 1427-1436 (2003).

15. Nakata,A. *et al.* Inhibition by interleukin 18 of osteolytic bone metastasis by human breast cancer cells. *Anticancer Res.* 19, 4131-4138 (1999).

16. Bendre,M.S. *et al.* Expression of interleukin 8 and not parathyroid hormone-related protein by human breast cancer cells correlates with bone metastasis in vivo. *Cancer Res.* 62, 5571-5579 (2002).

17. Thomas,R.J. *et al.* Breast cancer cells interact with osteoblasts to support osteoclast formation. *Endocrinology* 140, 4451-4458 (1999).

18. Engsig,M.T. *et al.* Matrix metalloproteinase 9 and vascular endothelial growth factor are essential for osteoclast recruitment into developing long bones. *J. Cell Biol.* 151, 879-889 (2000).

19. Henriksen,K., Karsdal,M., Delaisse,J.M. & Engsig,M.T. RANKL and vascular endothelial growth factor (VEGF) induce osteoclast chemotaxis through an ERK1/2-dependent mechanism. *J. Biol. Chem.* 278, 48745-48753 (2003).

20. Gerber,H.P. *et al.* VEGF couples hypertrophic cartilage remodeling, ossification and angiogenesis during endochondral bone formation. *Nat. Med.* 5, 623-628 (1999).

21. Haigh,J.J., Gerber,H.P., Ferrara,N. & Wagner,E.F. Conditional inactivation of VEGF-A in areas of collagen2a1 expression results in embryonic lethality in the heterozygous state. *Development* 127, 1445-1453 (2000).

22. Zelzer,E. *et al.* Skeletal defects in VEGF(120/120) mice reveal multiple roles for VEGF in skeletogenesis. *Development* 129, 1893-1904 (2002).

23. Carlevaro,M.F., Cermelli,S., Cancedda,R. & Descalzi,C.F. Vascular endothelial growth factor (VEGF) in cartilage neovascularization and chondrocyte differentiation: auto-paracrine role during endochondral bone formation. *J. Cell Sci.* 113 (Pt 1), 59-69 (2000).

24. Horner,A. *et al.* Immunolocalisation of vascular endothelial growth factor (VEGF) in human neonatal growth plate cartilage. *J. Anat.* 194 (Pt 4), 519-524 (1999).

25. Nakagawa,M. *et al.* Vascular endothelial growth factor (VEGF) directly enhances osteoclastic bone resorption and survival of mature osteoclasts. *FEBS Lett.* 473, 161-164 (2000).

26. Niida,S. *et al.* Vascular endothelial growth factor can substitute for macrophage colony-stimulating factor in the support of osteoclastic bone resorption. *J. Exp. Med.* 190, 293-298 (1999).

27. Min,J.K. *et al.* Vascular endothelial growth factor up-regulates expression of receptor activator of NF-kappa B (RANK) in endothelial cells. Concomitant increase of angiogenic responses to RANK ligand. *J. Biol. Chem.* 278, 39548-39557 (2003).

28. Liu,Y., Cheung,L.H., Thorpe,P. & Rosenblum,M.G. Mechanistic studies of a novel human fusion toxin composed of vascular endothelial growth factor (VEGF)121 and the serine protease granzyme B: directed apoptotic events in vascular endothelial cells. *Mol. Cancer Ther.* 2, 949-959 (2003).

29. Veenendaal,L.M. *et al.* In vitro and in vivo studies of a VEGF121/rGelonin chimeric fusion toxin targeting the neovasculature of solid tumors. *Proc. Natl. Acad. Sci. U. S. A* 99, 7866-7871 (2002).

30. Arora,N. *et al.* Vascular endothelial growth factor chimeric toxin is highly active against endothelial cells. *Cancer Res.* 59, 183-188 (1999).

31. Olson,T.A., Mohanraj,D., Roy,S. & Ramakrishnan,S. Targeting the tumor vasculature: inhibition of tumor growth by a vascular endothelial growth factor-toxin conjugate. *Int. J. Cancer* 73, 865-870 (1997).

32. Ramakrishnan,S., Olson,T.A., Bautch,V.L. & Mohanraj,D. Vascular endothelial growth factor-toxin conjugate specifically inhibits KDR/flk-1-positive endothelial cell proliferation in vitro and angiogenesis in vivo. *Cancer Res.* 56, 1324-1330 (1996).

33. Fine,B.A., Valente,P.T., Feinstein,G.I. & Dey,T. VEGF, flt-1, and KDR/flk-1 as prognostic indicators in endometrial carcinoma. *Gynecol. Oncol.* 76, 33-39 (2000).

34. Gille,H. *et al.* Analysis of biological effects and signaling properties of Flt-1 (VEGFR-1) and KDR (VEGFR-2). A reassessment using novel receptor-specific vascular endothelial growth factor mutants. *J. Biol. Chem.* 276, 3222-3230 (2001).

35. McMahon,G. VEGF receptor signaling in tumor angiogenesis. *Oncologist.* 5 Suppl 1, 3-10 (2000).

36. Neufeld,G., Tessler,S., Gitay-Goren,H., Cohen,T. & Levi,B.Z. Vascular endothelial growth factor and its receptors. *Prog. Growth Factor Res.* 5, 89-97 (1994).

37. Senger,D.R. *et al.* Vascular permeability factor (VPF, VEGF) in tumor biology. *Cancer Metastasis Rev.* 12, 303-324 (1993).

38. Shibuya,M. Role of VEGF-flt receptor system in normal and tumor angiogenesis. *Adv. Cancer Res.* 67, 281-316 (1995).

39. Takahashi,A. *et al.* Markedly increased amounts of messenger RNAs for vascular endothelial growth factor and placenta growth factor in renal cell carcinoma associated with angiogenesis. *Cancer Res.* 54, 4233-4237 (1994).

40. Peters,K.G., De Vries,C. & Williams,L.T. Vascular endothelial growth factor receptor expression during embryogenesis and tissue repair suggests a role in endothelial differentiation and blood vessel growth. *Proc. Natl. Acad. Sci. U. S. A* 90, 8915-8919 (1993).

41. Matsumoto,Y. *et al.* Possible involvement of the vascular endothelial growth factor-Flt-1-focal adhesion kinase pathway in chemotaxis and the cell proliferation of osteoclast precursor cells in arthritic joints. *J. Immunol.* 168, 5824-5831 (2002).

42. Sawano,A. *et al.* Flt-1, vascular endothelial growth factor receptor 1, is a novel cell surface marker for the lineage of monocyte-macrophages in humans. *Blood* 97, 785-791 (2001).

43. Barleon,B. *et al.* Migration of human monocytes in response to vascular endothelial growth factor (VEGF) is mediated via the VEGF receptor flt-1. *Blood* 87, 3336-3343 (1996).

44. Clauss,M. *et al.* The vascular endothelial growth factor receptor Flt-1 mediates biological activities. Implications for a functional role of placenta growth factor in monocyte activation and chemotaxis. *J. Biol. Chem.* 271, 17629-17634 (1996).

45. Casanova,M.L. *et al.* A critical role for ras-mediated, epidermal growth factor receptor-dependent angiogenesis in mouse skin carcinogenesis. *Cancer Res.* 62, 3402-3407 (2002).

46. Kelavkar,U.P. *et al.* Overexpression of 15-lipoxygenase-1 in PC-3 human prostate cancer cells increases tumorigenesis. *Carcinogenesis* 22, 1765-1773 (2001).

47. Wong,Y.C., Wang,Y.Z. & Tam,N.N. The prostate gland and prostate carcinogenesis. *Ital. J. Anat. Embryol.* 103, 237-252 (1998).

48. Chen,J., De,S., Brainard,J. & Byzova,T.V. Metastatic properties of prostate cancer cells are controlled by VEGF. *Cell Commun. Adhes.* 11, 1-11 (2004).

49. Zeng,Y. *et al.* Expression of vascular endothelial growth factor receptor-3 by lymphatic endothelial cells is associated with lymph node metastasis in prostate cancer. *Clin. Cancer Res.* 10, 5137-5144 (2004).

50. Ismail,A.H., Altaweel,W., Chevalier,S., Kassouf,W. & Aprikian,A.G. Expression of vascular endothelial growth factor-A in human lymph node metastases of prostate cancer. *Can. J. Urol.* 11, 2146-2150 (2004).

51. Paz,K. & Zhu,Z. Development of angiogenesis inhibitors to vascular endothelial growth factor receptor 2. current status and future perspective. *Front Biosci.* 10, 1415-1439 (2005).

52. Ueda,Y. *et al.* VGA1155, a novel binding antagonist of VEGF, inhibits angiogenesis in vitro and in vivo. *Anticancer Res.* 24, 3009-3017 (2004).

53. Ruan,G.R. *et al.* Effect of antisense VEGF cDNA transfection on the growth of chronic myeloid leukemia K562 cells in vitro and in nude mice. *Leuk. Res.* 28, 763-769 (2004).

54. O'Farrell,A.M. *et al.* Effects of SU5416, a small molecule tyrosine kinase receptor inhibitor, on FLT3 expression and phosphorylation in patients with refractory acute myeloid leukemia. *Leuk. Res.* 28, 679-689 (2004).

55. Verheul,H.M. & Pinedo,H.M. Vascular endothelial growth factor and its inhibitors. *Drugs Today (Barc.)* 39 Suppl C, 81-93 (2003).

56. Ferrara,N., Hillan,K.J., Gerber,H.P. & Novotny,W. Discovery and development of bevacizumab, an anti-VEGF antibody for treating cancer. *Nat. Rev. Drug Discov.* 3, 391-400 (2004).

57. Dai,J. *et al.* Vascular endothelial growth factor contributes to the prostate cancer-induced osteoblast differentiation mediated by bone morphogenetic protein. *Cancer Res.* 64, 994-999 (2004).

58. Shariat,S.F. *et al.* Association of preoperative plasma levels of vascular endothelial growth factor and soluble vascular cell adhesion molecule-1 with lymph node status and biochemical progression after radical prostatectomy. *J. Clin. Oncol.* 22, 1655-1663 (2004).

59. Hattori,K. *et al.* Placental growth factor reconstitutes hematopoiesis by recruiting VEGFR1(+) stem cells from bone-marrow microenvironment. *Nat. Med.* 8, 841-849 (2002).

60. Fong,G.H., Zhang,L., Bryce,D.M. & Peng,J. Increased hemangioblast commitment, not vascular disorganization, is the primary defect in flt-1 knock-out mice. *Development* 126, 3015-3025 (1999).

61. Hiratsuka,S., Minowa,O., Kuno,J., Noda,T. & Shibuya,M. Flt-1 lacking the tyrosine kinase domain is sufficient for normal development and angiogenesis in mice. *Proc. Natl. Acad. Sci. U. S. A* 95, 9349-9354 (1998).

62. Matsumoto,T. & Claesson-Welsh,L. VEGF receptor signal transduction. *Sci. STKE.* 2001, RE21 (2001).

63. De Vries,C. *et al.* The fms-like tyrosine kinase, a receptor for vascular endothelial growth factor. *Science* 255, 989-991 (1992).

64. Park,J.E., Chen,H.H., Winer,J., Houck,K.A. & Ferrara,N. Placenta growth factor. Potentiation of vascular endothelial growth factor bioactivity, in vitro and in vivo, and high affinity binding to Flt-1 but not to Flk-1/KDR. *J. Biol. Chem.* 269, 25646-25654 (1994).

65. Gerber,H.P. *et al.* VEGF regulates haematopoietic stem cell survival by an internal autocrine loop mechanism. *Nature* 417, 954-958 (2002).

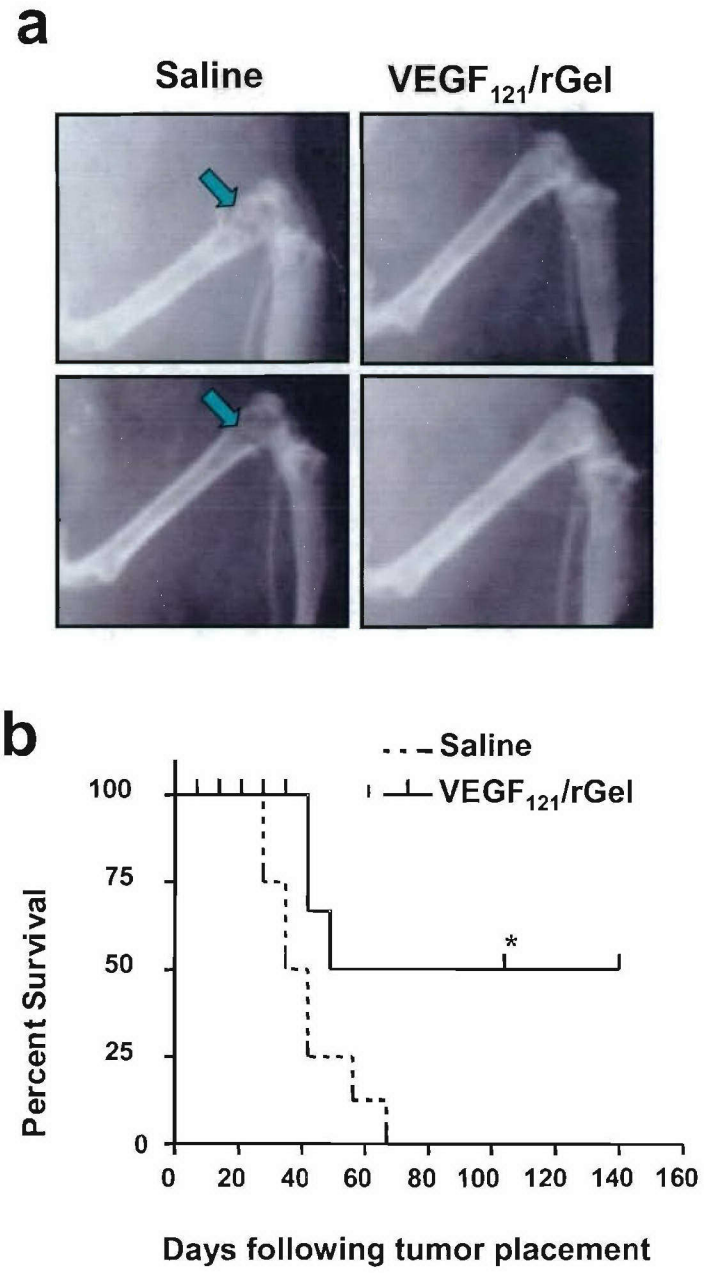
a
Saline
VEGF121/rGel
b
Saline
VEGF121/rGel
100
75
50
25
0
Percent Survival
*
0
20
40
60
80
100
120
140
160
Days following tumor placement
c

Figure 1

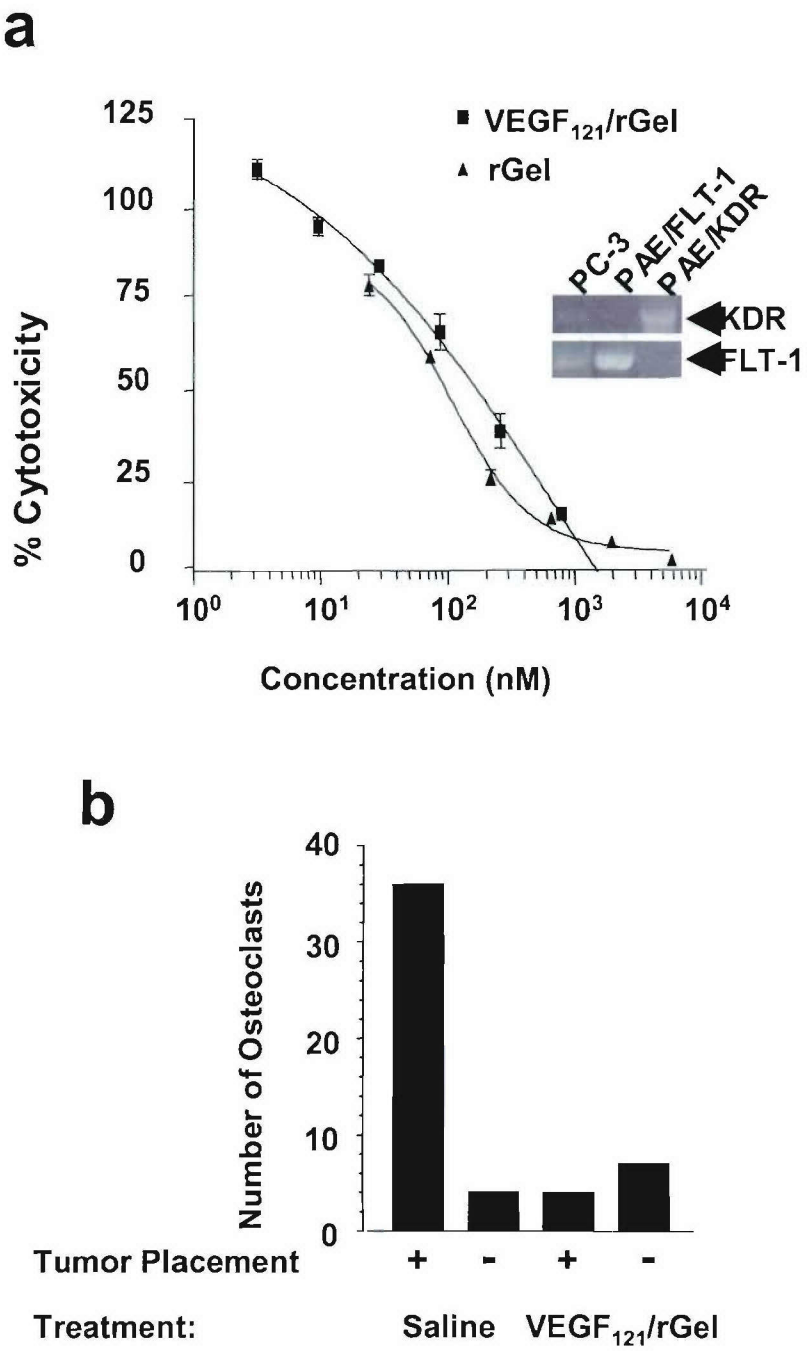
a
125
100
75
50
25
0
% Cytotoxicity
VEGF121/rGel
rGel
PC-3
PAE/FLT-1
PAE/KDR
KDR
FLT-1
10^0
10^1
10^2
10^3
10^4
Concentration (nM)
b
40
30
20
10
0
Number of Osteoclasts
Tumor Placement
+
-
+
-
Treatment:
Saline
VEGF121/rGel

Figure 2

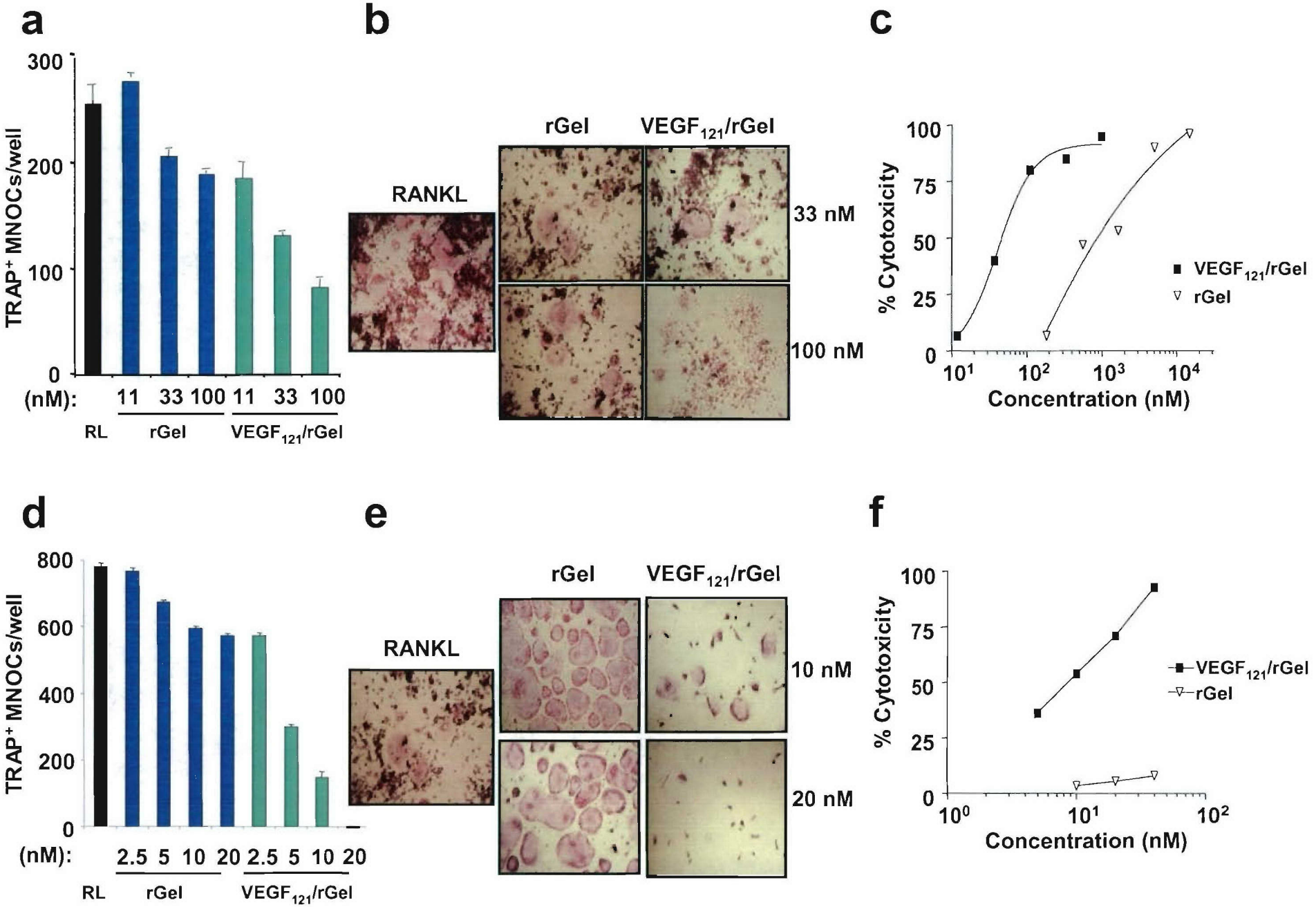
a
b
c
d
e
f
TRAP+ MNOCs/well
300
200
100
0
(nM):
11 33 100 11 33 100
RL
rGel
VEGF121/rGel
RANKL
rGel
VEGF121/rGel
33 nM
100 nM
% Cytotoxicity
100
75
50
25
0
10^1 10^2 10^3 10^4
Concentration (nM)
VEGF121/rGel
rGel
800
600
400
200
0
2.5 5 10 20 2.5 5 10 20
10 nM
20 nM
10^0 10^1 10^2

Figure 3

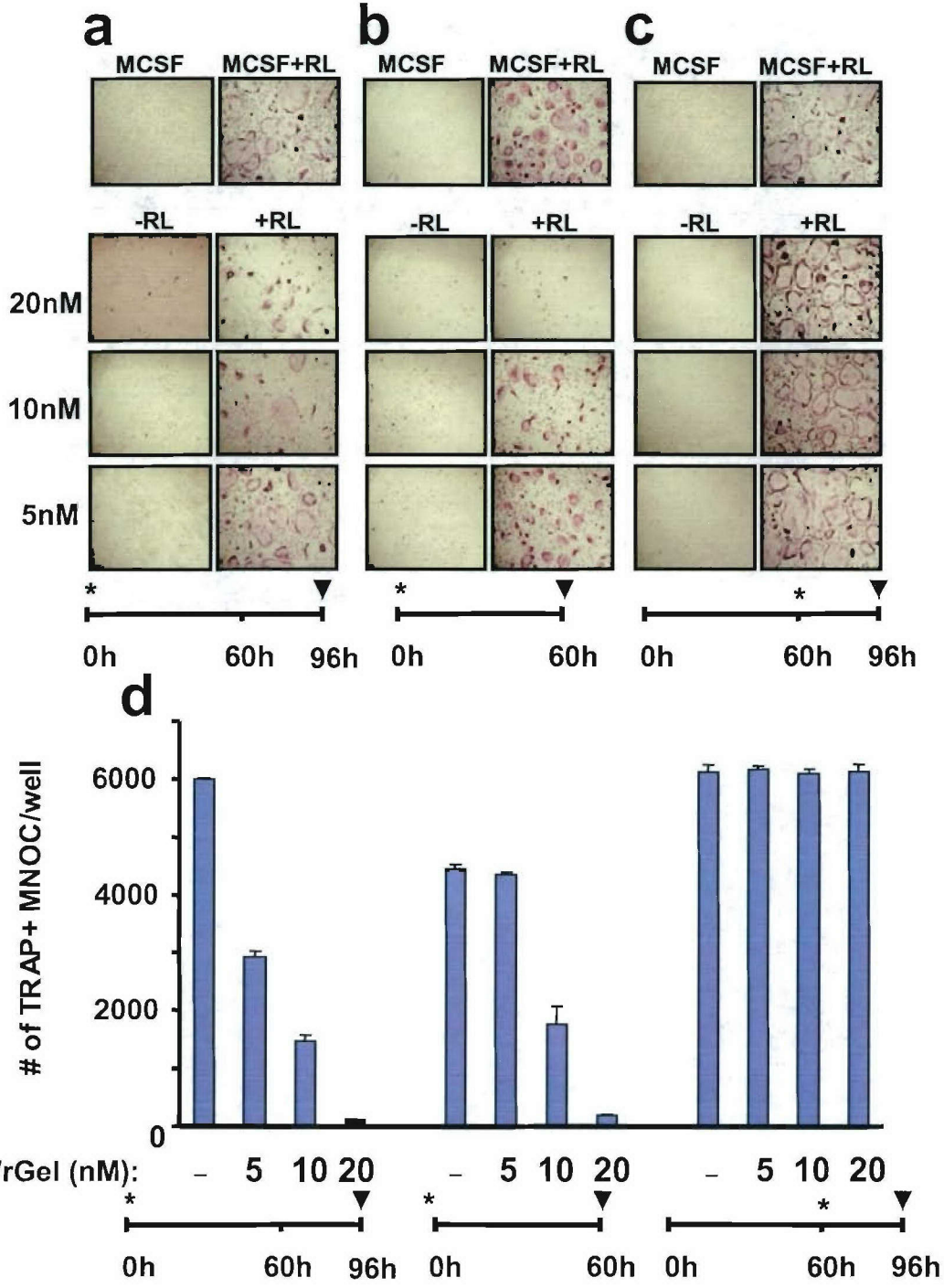

* : Addition of $VEGF_{121}$/rGel

▼ : TRAP staining

Figure 4

a

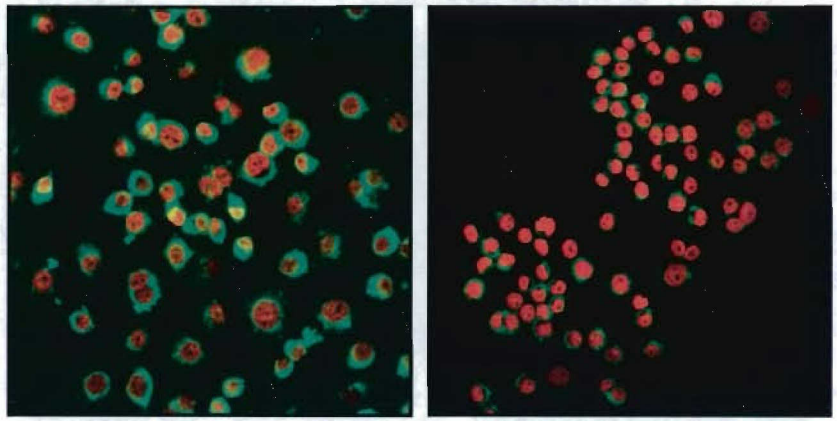

$VEGF_{121}$/rGel rGel

b

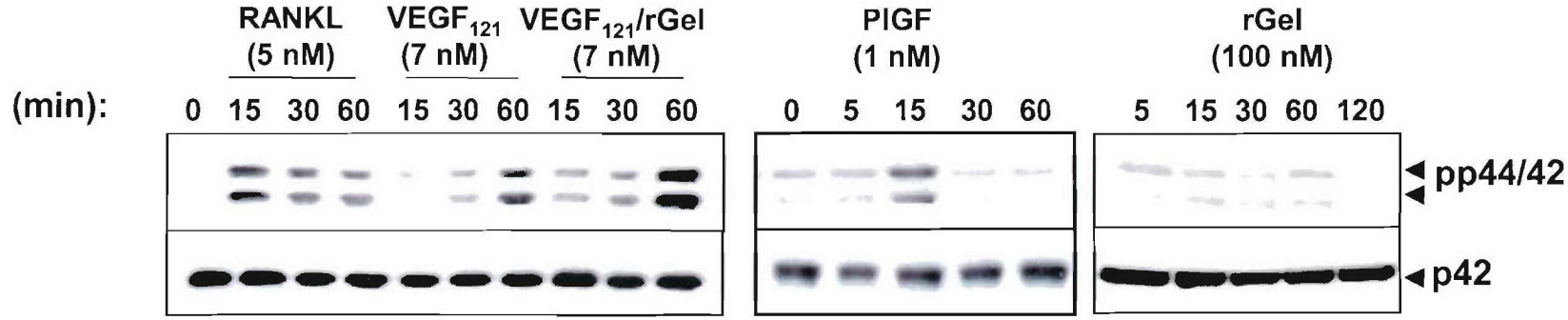

Figure 5

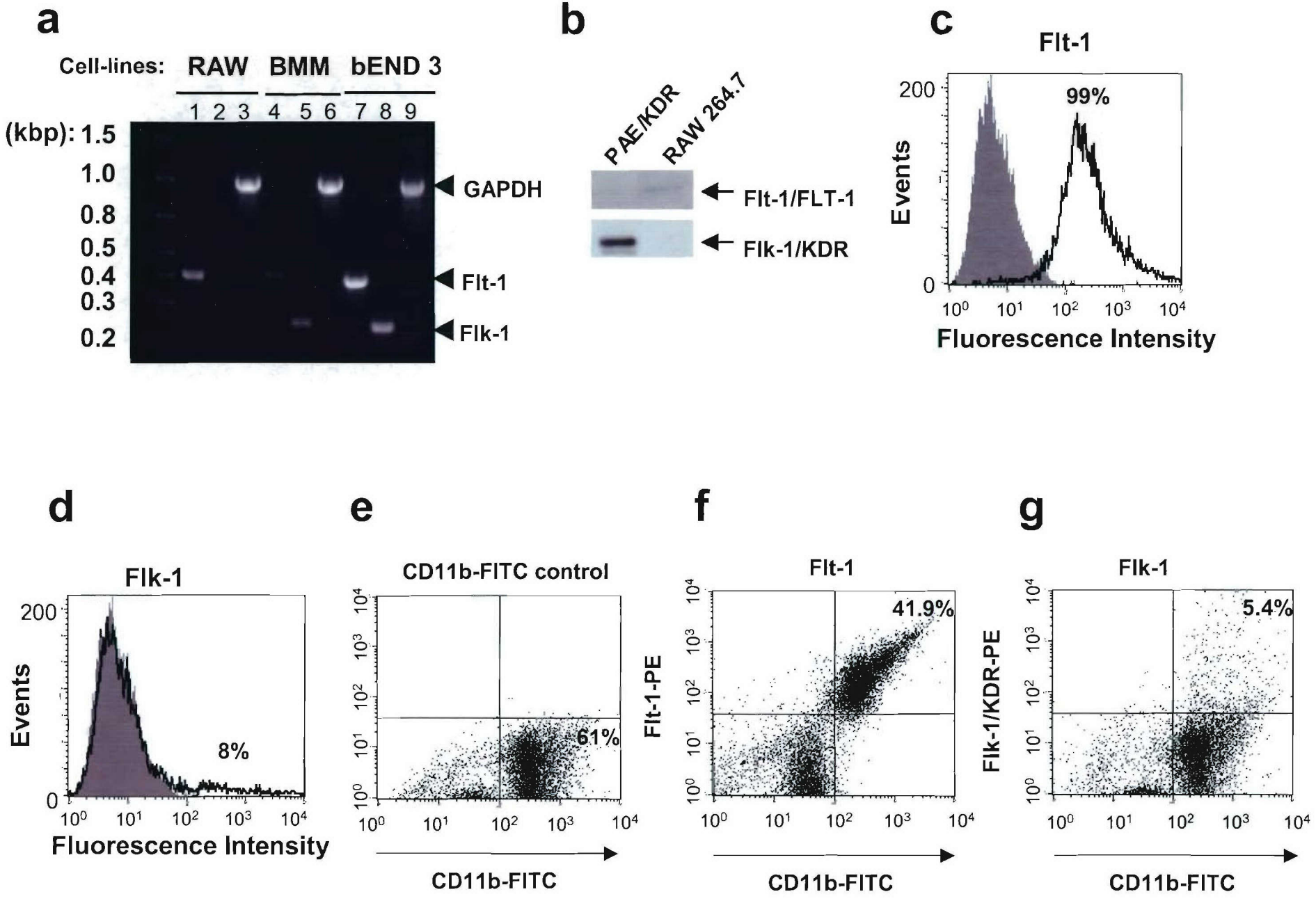
a
Cell-lines: RAW BMM bEND 3
1 2 3 4 5 6 7 8 9
(kbp): 1.5
1.0
0.8
0.5
0.4
0.3
0.2
GAPDH
Flt-1
Flk-1
b
PAE/KDR
RAW 264.7
Flt-1/FLT-1
Flk-1/KDR
c
Flt-1
99%
Events
Fluorescence Intensity
d
Flk-1
8%
Events
Fluorescence Intensity
e
CD11b-FITC control
61%
Flt-1-PE
CD11b-FITC
f
Flt-1
41.9%
CD11b-FITC
g
Flk-1
5.4%
Flk-1/KDR-PE
CD11b-FITC

Figure 6

h

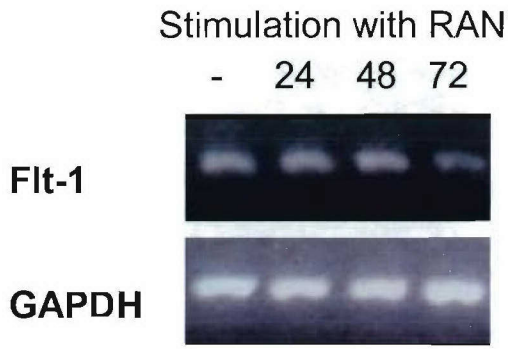
Stimulation with RANKL (h)
-
24
48
72
Flt-1
GAPDH

i

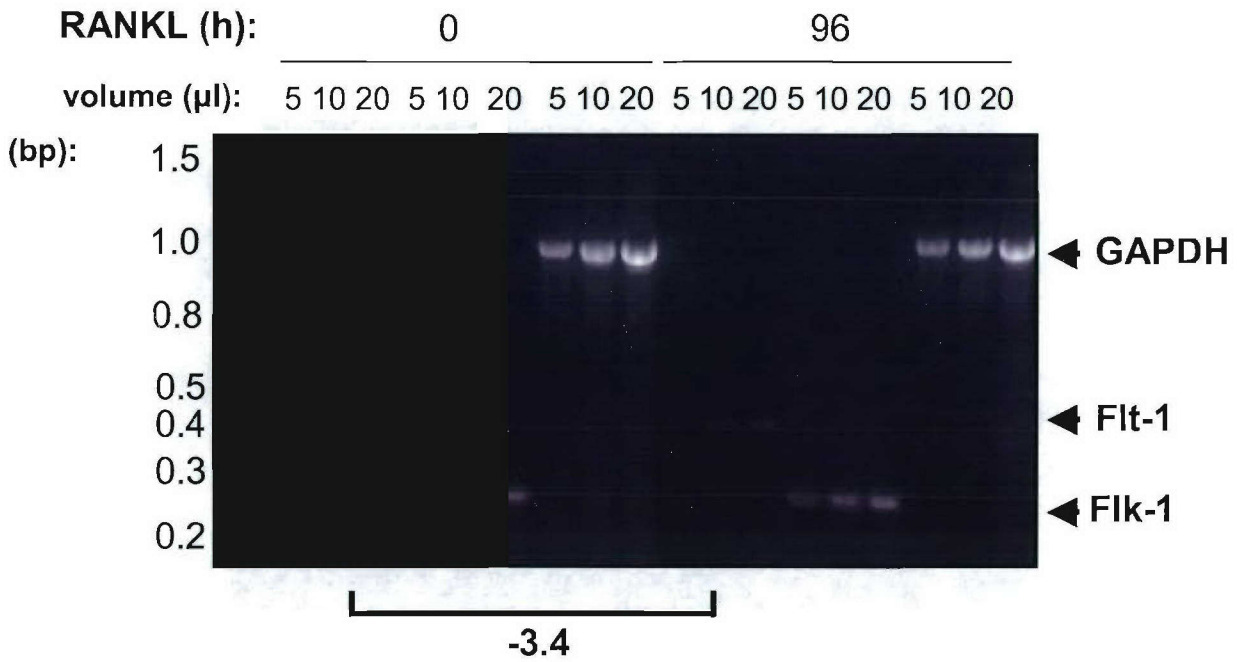
RANKL (h):
0
96
volume (µl):
5 10 20 5 10 20 5 10 20 5 10 20 5 10 20 5 10 20
(bp):
1.5
1.0
0.8
0.5
0.4
0.3
0.2
GAPDH
Flt-1
Flk-1
-3.4

Figure 6

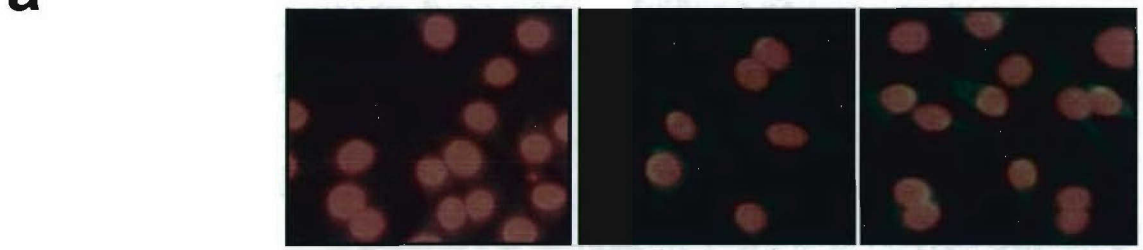
a
Anti-Flt-1 (10 μg/ml) + - -
Anti-Flk-1 (10 μg/ml) - + -
VEGF121/rGel (10 nM) + + +
b
Percent Survival
160
140
120
100
80
60
40
20
0
PIGF (25 nM) + - - +
VEGF121/rGel (40 nM) - - + +
MCSF (10 ng/ml) - - - -
c
Percent Survival
160
140
120
100
80
60
40
20
0
PIGF (25 nM) + - - +
VEGF121/rGel (40 nM) - - + +
MCSF (10 ng/ml) - - - -

Figure 7

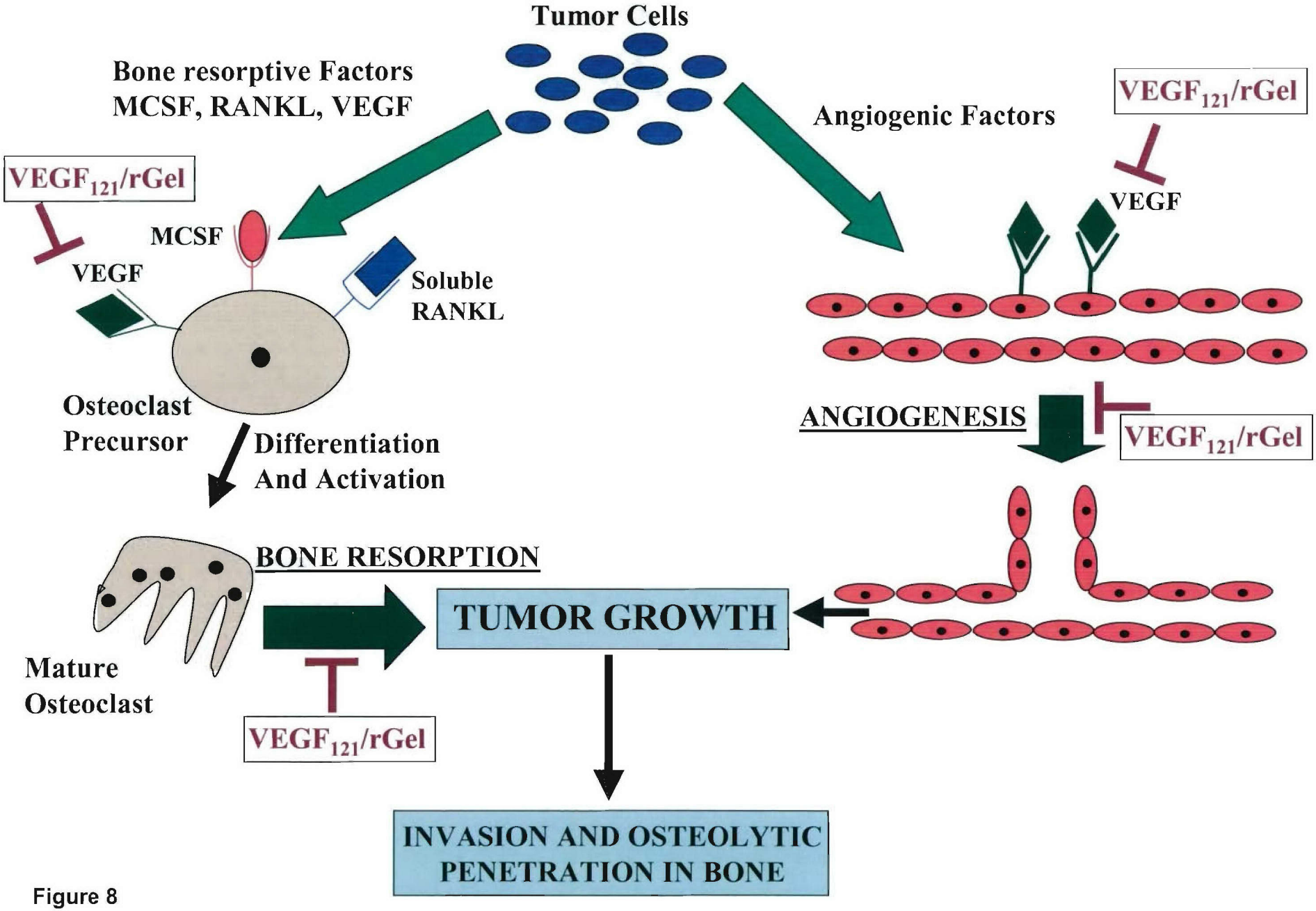
Tumor Cells
Bone resorptive Factors
MCSF, RANKL, VEGF
Angiogenic Factors
VEGF121/rGel
VEGF121/rGel
MCSF
VEGF
VEGF
Soluble
RANKL
Osteoclast
Precursor
Differentiation
And Activation
ANGIOGENESIS
VEGF121/rGel
BONE RESORPTION
TUMOR GROWTH
Mature
Osteoclast
VEGF121/rGel
INVASION AND OSTEOLYTIC
PENETRATION IN BONE

Figure 8

RESEARCH ARTICLE

Neoplasia • Vol. 7, No. 5, May 2005, pp. 486–496 486

www.neoplasia.com

The Vascular-Ablative Agent $VEGF_{121}$/rGel Inhibits Pulmonary Metastases of MDA-MB-231 Breast Tumors[1]

Sophia Ran[*,¶], *Khalid A. Mohamedali*[†], *Troy A. Luster*[*], *Philip E. Thorpe*[*] *and Michael G. Rosenblum*[†]

*Simmons Comprehensive Cancer Center and Department of Pharmacology, University of Texas Southwestern Medical Center, Dallas, TX, USA; †Department of Experimental Therapeutics, The University of Texas M. D. Anderson Cancer Center, Houston, TX; ¶Present Address: Department of Medical Microbiology, Immunology and Cell Biology, School of Medicine, Southern Illinois University, Springfield, IL 62794-9626

Abstract

$VEGF_{121}$/rGel, a fusion protein composed of the growth factor $VEGF_{121}$ and the recombinant toxin gelonin (rGel), targets the tumor neovasculature and exerts impressive cytotoxic effects by inhibiting protein synthesis. We evaluated the effect of $VEGF_{121}$/rGel on the growth of metastatic MDA-MB-231 tumor cells in SCID mice. $VEGF_{121}$/rGel treatment reduced surface lung tumor foci by 58% compared to controls (means were 22.4 and 53.3, respectively; $P < .05$) and the mean area of lung colonies by 50% (210 ± 37 m^2 *vs* 415 ± 10 m^2 for $VEGF_{121}$/rGel and control, respectively; $P < .01$). In addition, the vascularity of metastatic foci was significantly reduced (198 ± 37 *vs* 388 ± 21 vessels/mm^2 for treated and control, respectively). Approximately 62% of metastatic colonies from the $VEGF_{121}$/rGel–treated group had fewer than 10 vessels per colony compared to 23% in the control group. The VEGF receptor Flk-1 was intensely detected on the metastatic vessels in the control but not in the $VEGF_{121}$/rGel–treated group. Metastatic foci present in lungs had a three-fold lower Ki-67 labeling index compared to control tumors. Thus, the antitumor vascular-ablative effect of $VEGF_{121}$/rGel may be utilized not only for treating primary tumors but also for inhibiting metastatic spread and vascularization of metastases.

Neoplasia (2005) **7**, 486–496

Keywords: VEGF, gelonin, fusion toxin, vascular targeting, metastatic breast tumors.

Introduction

Biologic studies examining the development of vascular tree in normal development and in disease states have identified numerous cytokines and their receptors that are responsible for triggering and maintaining this process [1–7]. Tumor neovascularization is not only central to the growth and development of the primary lesion, but appears to be a critical factor in the development and maintenance of metastases [8–12]. Clinical studies in bladder cancer [9] have demonstrated a correlation between microvessel density (MVD) and metastases. In addition, studies of breast cancer metastases by Aranda and Laforga [11] and Fox et al. [12] have demonstrated that microvessel count in primary tumors appears to be related to the presence of metastases in lymph nodes and micrometastases in bone marrow.

The cytokine vascular endothelial growth factor-A (VEGF-A) and its receptors Flt-1/FLT-1 (VEGFR-1) and Flk-1/KDR (VEGFR-2) have been implicated as one of the central mediators of normal angiogenesis and tumor neovascularization [13–20]. Upregulation or overexpression of the KDR receptor or the VEGF-A ligand itself has been implicated as poor prognostic markers in various clinical studies of colon, breast, and pituitary cancers [21–23]. Recently, Padro et al. [24] have suggested that both VEGF-A and Flk-1/KDR may play a role in the neovascularization observed in bone marrow during acute myeloid leukemia tumor progression and may provide evidence that the VEGF/VEGFR-2 pathway is important in leukemic growth.

For these reasons, there have been several groups interested in developing therapeutic agents and approaches targeting the VEGF-A pathway. Agents that prevent VEGF-A binding to its receptors, antibodies that directly block the Flk-1/KDR receptor, and small molecules that block the kinase activity of Flk-1/KDR, and thereby block growth factor signaling, are all under development [25–37]. Recently, our laboratory reported the development of a growth factor fusion construct of $VEGF_{121}$ and the recombinant toxin gelonin (rGel) [38]. The rGel toxin is a single-chain *N*-glycosidase that is similar in its action to ricin-A chain [39]. Immunotoxins and fusion toxins containing rGel have been shown to

Abbreviations: SCID, severe combined immunodeficient; VEGF, VEGF-A, vascular endothelial growth factor-A; Flt-1, FLT-1, VEGFR-1, vascular endothelial growth factor receptor-1; Flk-1, KDR, VEGFR-2, vascular endothelial growth factor receptor-2; rGel, gelonin; i.v., intravenous

Address all correspondence to: Michael G. Rosenblum, PhD, Department of Experimental Therapeutics, The University of Texas M. D. Anderson Cancer Center, Unit 44, 1515 Holcombe Boulevard, Houston, TX 77030. E-mail: mrosenbl@mdanderson.org

[1]This research was supported, in part, by the following: Clayton Foundation for Research, Department of Defense (DAMD-17-02-1-0457), and the Gillson-Longenbaugh Foundation.

Received 27 September 2004; Revised 3 December 2004; Accepted 7 December 2004.

 1522-8002/05/$25.00

DOI 10.1593/neo.04631

specifically kill tumor cells *in vitro* and *in vivo* [40–43]. In currently ongoing clinical studies, gelonin does not appear to generate vascular leak syndrome (VLS) that limits the use of other toxins [44]. In addition, the development of hepatotoxicity commonly observed with toxin molecules has thus far not been observed for rGel-based agents. Our studies demonstrated that this agent was specifically cytotoxic only to cells expressing the KDR receptor and was not cytotoxic to cells overexpressing the FLT-1 receptor. In addition, this agent was shown to localize within the tumor vasculature and caused a significant damage to the vascular endothelium in both PC-3 prostate and A375 orthotopic xenograft tumor models.

There is now a significant body of evidence suggesting that breast tumor development, differentiation, and metastatic spread appear to be critically dependent on tumor neovascularization. Current studies suggest that the development of breast cancer primary tumors or metastatic sites > 2 mm are critically dependent on the growth of tumo neovasculature. We, therefore, evaluated the effect of $VEGF_{121}$/rGel fusion toxin treatment on the growth of metastatic MDA-MB-231 tumor cells in SCID mice. Our data strongly suggest that the vascular-ablative effect of $VEGF_{121}$/rGel may be used for inhibiting metastatic spread and the vascularization of metastases.

Materials and Methods

Materials

Bacterial strains, pET bacterial expression plasmids, and recombinant enterokinase were obtained from Novagen (Madison, WI). All other chemicals were from Sigma Chemical Co. (St. Louis, MO) or Fisher Scientific (Pittsburgh, PA). TALON metal affinity resin was obtained from Clontech Laboratories (Palo Alto, CA). Other chromatography resins and materials were from Amersham Pharmacia Biotech (Piscataway, NJ). Endothelial cell growth supplement (ECGS) from bovine neural tissue was obtained from Sigma. Murine brain endothelioma (bEnd.3) cells were provided by Professor Werner Risau (Max Plank Institute, Munich, Germany). Tissue culture reagents were from Gibco BRL (Gaithersburg, MD) or Mediatech Cellgro (Herndon, VA).

Antibodies

Rat antimouse CD31 antibody was from PharMingen (San Diego, CA). Rabbit antigelonin antibody was produced in the Veterinary Medicine Core Facility at MDACC. The hybridoma producing the mouse monoclonal w6/32 antibody directed against human HLA antigen was purchased from ATCC. The w6/32 antibody was purified from hybridoma supernatant using protein A resin. MECA 32, a pan mouse endothelial cell antibody, was kindly provided by Dr. E. Butcher (Stanford University, Stanford, CA) and served as a positive control for immunohistochemical studies. The Ki-67 antibody was from Abcam, Inc. (Cambridge, UK). Antibodies to KDR and FLT-1 were from Santa Cruz Biotechnology (Santa Cruz, CA). Goat antirat, antimouse, and antirabbit secondary antibodies conjugated to HRP were purchased from Dako (Carpinteria, CA). Protein A/G agarose resin was purchased from Pierce (Rockford, IL).

Cell Culture

Porcine aortic endothelial cells transfected with the KDR receptor (PAE/KDR) or the FLT-1 receptor (PAE/FLT-1) were a generous gift from Dr. J. Waltenberger. MDA-MB-231 cells were a generous gift from Dr. Janet Price. MDA-MB-231, MDA-MB-435, PAE/KDR, and PAE/FLT-1 cells were maintained as a monolayer in F12 Nutrient Media (HAM) supplemented with 100 U/ml penicillin, 100 U/ml streptomycin, and 10% fetal bovine serum. SK-BR3 cells were maintained in RPMI 1640 media supplemented with 100 U/ml penicillin, 100 U/ml streptomycin, and 10% fetal bovine serum. BT474 cells were maintained in SK-BR3 media supplemented with 5 μg/ml insulin. Cells were harvested by treatment with Versene (0.02% EDTA) or trypsin–EDTA. Tumor cells intended for injection into mice were washed once and resuspended in serum-free medium without supplements. Cell number and viability were determined by staining with 0.2% trypan blue dye diluted in saline. Only single-cell suspensions of greater than 90% viability were used for *in vivo* studies.

Expression and Purification of $VEGF_{121}$/rGel

The construction, expression, and purification of $VEGF_{121}$/rGel have been previously described [38]. The fusion toxin was stored in sterile PBS at −20°C.

Cytotoxicity of $VEGF_{121}$/rGel and rGel

The cytotoxicity of $VEGF_{121}$/rGel and rGel against log phase PAE/KDR and PAE/FLT-1 cells has been previously described [38]. Here, we assessed the cytotoxicity of $VEGF_{121}$/rGel and rGel against log phase human breast cancer cells and compared their cytotoxicity to PAE/KDR cells. Cells were grown in 96-well flat-bottom tissue culture plates. Purified $VEGF_{121}$/rGel and rGel were diluted in culture media and added to the wells in five-fold serial dilutions. Cells were incubated for 72 hours. The remaining adherent cells were stained with crystal violet (0.5% in 20% methanol) and solubilized with Sorenson's buffer (0.1 M sodium citrate, pH 4.2 in 50% ethanol). Absorbance was measured at 630 nm.

Western Blot Analysis

Whole cell extracts were obtained by lysing cells in cell lysis buffer (50 mM Tris, pH 8.0, 0.1 mM EDTA, 1 mM DTT, 12.5 mM $MgCl_2$, 0.1 M KCl, and 20% glycerol) supplemented with protease inhibitors [leupeptin (0.5%), aprotinin (0.5%), and PMSF (0.1%)]. Protein samples were separated by SDS-PAGE under reducing conditions and electrophoretically transferred to a PVDF membrane overnight at 4°C in transfer buffer (25 mM Tris–HCl, pH 7.6, 190 mM glycine, and 20% HPLC-grade methanol). The samples were analyzed for KDR with rabbit anti-KDR polyclonal antibody and FLT-1 using an anti–FLT-1 polyclonal antibody. The membranes were then incubated with goat antirabbit IgG

horseradish peroxidase (HRP), developed using the ECL detection system (Amersham Pharmacia Biotech) and exposed to X-ray film.

Immunoprecipitation

Cells were lysed as described above. Five hundred micrograms of whole cell lysates of MDA-MB-231, MDA-MB-435, BT474, and SK-BR3 cells was mixed with 2 μg of anti-KDR or anti–FLT-1 polyclonal antibodies in a final volume of 250 μl and incubated for 2 hours at 4°C. One hundred micrograms of PAE/KDR and PAE/FLT-1 cell lysates was immunoprecipitated as controls. The mixtures were then incubated for 2 hours with Protein A/G agarose beads that had been blocked with 5% BSA. The beads were washed four times in lysis buffer and the samples, along with 30 μg of PAE/KDR cell lysate, were run on a gel, transferred overnight onto a PVDF membrane, and probed using anti-KDR or anti–FLT-1 antibodies.

Isolation of RNA and Reverse Transcription Polymerase Chain Reaction (RT-PCR) Analysis

Total RNA was extracted using the RNeasy mini-kit (Qiagen, Valencia, CA) and its integrity was verified by electrophoresis on a denaturing formaldehyde agarose gel. RT-PCR analysis was performed using the following primers: KDR forward—5′ ATTACTTGCAGGGGACAG; KDR reverse—5′ GGAACAAATCTCTTTTCTGG; FLT-1 forward—5′ CAAATGCAACGTACAAAGA; FLT-1 reverse—5′ AGAGTGGCAGTGAGGTTTTT; GAPDH forward—5′GTCGTCTTCACCACCATGGAG; and GAPDH reverse—5′ CCACCCTGTTGCTGTAGC. Isolated RNA was subjected to first-strand cDNA synthesis as described by the manufacturer of the Superscript First Strand synthesis system (Invitrogen, Carlsbad, CA). RT-PCR was performed using a Minicycler PCR machine (MJ Research, Inc., San Francisco, CA).

Localization of $VEGF_{121}$/rGel to Blood Vessels of MDA-MB-231 Lung Metastatic Foci

All animal experiments were carried out in accordance with institutional guidelines and protocols. Tumor cells (5×10^5 per mouse) were injected intravenously (i.v.) and, 4 to 5 weeks later, the mice began to show signs of respiratory distress. At this time, the mice were injected i.v. with $VEGF_{121}$/rGel (50 μg/mouse) or free rGel (20 μg/mouse, molar equivalent to $VEGF_{121}$/rGel). One hour later, the mice were sacrificed and exsanguinated. All major organs and tumor were harvested and snap-frozen for the preparation of cryosections. Frozen sections were double-stained with anti–CD-31 (5 μg/ml) followed by detection of the localized fusion protein using rabbit antigelonin antibody (10 μg/ml). CD-31 rat IgG was visualized by goat antirat IgG conjugated to Cy-3 (red fluorescence). Rabbit antigelonin antibody was detected by goat antirabbit IgG conjugated to FITC (green fluorescence). Colocalization of both markers was indicated by the yellow color. Anti-rGel antibody had no reactivity with tissues sections derived from mice injected with saline or with $VEGF_{121}$.

Metastatic Model of MDA-MB-231 Tumors

A maximum tolerated dose of 45 mg/kg for $VEGF_{121}$/rGel under the conditions described below was established. For treatment purposes, 70% of the MTD was used. We currently demonstrate a comparison with a diluent (saline) control as previous studies have demonstrated no impact of free rGel on the growth of tumor xenografts [38]. Female SCID mice, aged 4 to 5 weeks, were injected in a tail vein with 0.1 ml of MDA-MB-231 cell suspension (5×10^5 cells). The mice were randomly separated into two groups (six mice per group) and were treated with either $VEGF_{121}$/rGel or rGel starting on the eighth day after the injection of cells. $VEGF_{121}$/rGel was delivered at 100 μg/dose intraperitoneally, for a total of six times, with the interval of 3 days. The molar equivalent of rGel (40 μg) was delivered at the same schedule. Intraperitoneal, rather than intravenous, injection was chosen solely to prevent necrosis of the tail vein due to repeated injections. Animal weight was monitored. Three weeks after termination of the treatment, the animals were sacrificed and their lungs were removed. One lobe was fixed in Bouin's fixative and the other lobe was snap-frozen. After fixation in Bouin's fixative, the tumor colonies on the lung surface appeared white, whereas the normal lung tissue appeared brown. The number of tumor colonies on the surface of each lung was counted and the weight of each lung was measured. The values obtained from individual mice in the $VEGF_{121}$/rGel and rGel groups were averaged per group.

Determination of the Number, Size, and Vascular Density of Lung Metastatic Foci

Frozen samples of lung tissue were cut to produce sections of 6 μm. Blood vessels were visualized by MECA 32 antibody and metastatic lesions were identified by morphology and w6/32 antibody, directed against human HLA antigens. Each section was also double-stained by MECA 32 and w6/32 antibodies to ensure that the analyzed blood vessels are located within a metastatic lesion. Slides were first viewed at low magnification (×2 objective) to determine the total number of foci per cross section. Six slides derived from individual mice in each group were analyzed and the number was averaged. Images of each colony were taken using a digital camera (CoolSnap) at magnifications of ×40 and ×100, and analyzed using Metaview software, which allows measurements of the smallest and largest diameter, perimeter (μm), and area (mm^2). The vascular endothelial structures identified within a lesion were counted and the number of vessels per each lesion was determined and normalized per square millimeter. The mean number of vessels per square millimeter was calculated per slide and averaged per $VEGF_{121}$/rGel and rGel groups (six slides per group). The results are expressed as ±SEM. The same method was applied to determine the mean number of vessels in nonmalignant tissues.

Immunohistochemical Analysis of Proliferation of Tumor Cells in Lung Colonies

Frozen sections of mouse normal organs and metastatic lungs were fixed with acetone for 5 minutes and rehydrated

with PBS-T for 10 minutes. All dilutions of antibodies were prepared in PBS-T containing 0.2% BSA. Primary antibodies were detected by appropriate antimouse, antirat, or antirabbit HRP conjugates. HRP activity was detected by developing with DAB substrate (Invitrogen, Carlsbad, CA). To determine number of cycling cells, sections were stained with the Ki-67 antibody followed by antimouse IgG HRP conjugate. Sections were analyzed at a magnification of ×100. The number of cells positive for Ki-67 was normalized per square millimeter. The mean ± SD per VEGF$_{121}$/rGel and control group is presented. The average numbers derived from analysis of each slide were combined per either VEGF$_{121}$/rGel or rGel group and analyzed for statistical differences.

Expression of Flk-1 in Metastatic Lung Tumors

The expression of Flk-1 on the vasculature of breast tumors metastatic to the lungs was also assessed using the RAFL-1 antibody as described by Ran et al. [45]. Frozen sections of lungs from mice treated with VEGF$_{121}$/rGel or free gelonin stained with monoclonal rat antimouse VEGFR-2 antibody RAFL-1 (10 μg/ml). RAFL-1 antibody was detected by goat antirat IgG HRP.

Statistical Analysis

Results are expressed as mean ± SEM, unless otherwise indicated. Statistical significance was determined by one-way analysis of variance followed by the Student's *t* test.

Results

Expression of KDR and FLT-1 RNA and Protein in Breast Cancer Cell Lines

Because VEGF$_{121}$ binds only to KDR and FLT-1, we first examined RNA and protein levels of these two receptors in several breast cancer cell lines: BT474, MDA-MB-231, MDA-MB-435, and SK-BR3. Total RNA was harvested from log phase cells, analyzed for integrity, and subjected to RT-PCR with primers KDR, FLT-1, and GAPDH (control). KDR and FLT-1 were immunoprecipitated from whole cell extracts and identified by Western blot analysis. PAE/KDR and PAE/FLT-1 cells were used as positive controls. None of the breast cancer cell lines expressed detectable levels of FLT-1 RNA or protein as determined by RT-PCR and Western blot analysis (data summarized in Table 1). RT-PCR analysis of MDA-MB-231 showed extremely low levels of KDR compared to PAE/KDR. However, MDA-MB-231 cells did not express detectable amounts of KDR protein. The other breast cell lines did not express detectable amounts of KDR RNA or protein.

Cytotoxicity of VEGF$_{121}$/rGel on MDA-MB-231 Cells

We have previously demonstrated that VEGF$_{121}$/rGel is cytotoxic to endothelial cells expressing KDR but not FLT-1 [38]. As assessed by Western blot, none of the breast cancer cell lines examined appears to express FLT-1 or KDR—the receptors that bind VEGF$_{121}$. We additionally examined the cytotoxicity of VEGF$_{121}$/rGel and rGel on these breast cancer cell lines. BT474, MDA-MB-435, and SK-BR3 all show a slightly lower IC$_{50}$ for VEGF$_{121}$/rGel compared to rGel alone. In contrast, MDA-MB-231 cells in culture showed an IC$_{50}$ slightly higher than that observed for recombinant gelonin (Table 1 and Figure 1), indicating that VEGF$_{121}$/rGel does not have a specific target on MBA-MB-231 cells. The IC$_{50}$ of untargeted rGel toward MDA-MB-231 cells is similar to its IC$_{50}$ toward PAE/KDR cells (Figure 1). Compared to the IC$_{50}$ of VEGF$_{121}$/rGel toward PAE/KDR cells (1 nM), the IC$_{50}$ of VEGF$_{121}$/rGel toward the breast cancer cell lines examined was much higher, ranging from 30 to 300 nM. Indeed, the IC$_{50}$ of VEGF$_{121}$/rGel toward these breast cancer cell lines was in the IC$_{50}$ range of untargeted rGel toward the PAE/KDR cells. Taken together, these *in vitro* data suggest that MDA-MB-231 tumor cells are not specifically targeted by VEGF$_{121}$/rGel, and that any *in vivo* effect on the growth of tumors would be due to VEGF$_{121}$/rGel targeting the tumor vasculature rather than the tumor cells themselves.

Localization of VEGF$_{121}$/rGel to the Vasculature of MDA-MB-231 Lung Metastatic Foci

Mice bearing metastatic MDA-MB-231 tumors were injected intravenously with either VEGF$_{121}$/rGel or free rGel and, 1 hour later, the mice were exsanguinated. Frozen sections were prepared from the lung tumor foci and normal organs, and examined immunohistochemically to determine the location of the free rGel and the gelonin fusion construct. VEGF$_{121}$/rGel was primarily detected on the endothelium of tumor (Figure 2). Vessels with bound VEGF$_{121}$/rGel were homogeneously distributed within the tumor vasculature. No VEGF$_{121}$/rGel staining was detected in any of the normal tissues examined (lung, liver, kidney, heart, spleen, pancreas, and brain; data not shown). Free rGel did not localize to tumor or normal vessels in any of the mice, indicating that only targeted rGel was able to bind to the tumor

Table 1. Correlation between the Presence of VEGF$_{121}$ Receptors and Sensitivity to VEGF$_{121}$/rGel.

Cell Type	RT-PCR		Immunoprecipitation		IC$_{50}$ (nM)		Targeting Index*
	KDR	FLT-1	KDR	FLT-1	VEGF$_{121}$/rGel	rGel	
BT474	–	–	–	–	300	2000	7
MDA-MB-231	+	–	–	–	150	40	0.3
MDA-MB-435	–	–	–	–	56	327	6
SK-BR3	–	–	–	–	200	500	2.5

*Targeting index is defined as (IC$_{50}$ rGel)/(IC$_{50}$ VEGF$_{121}$/rGel).

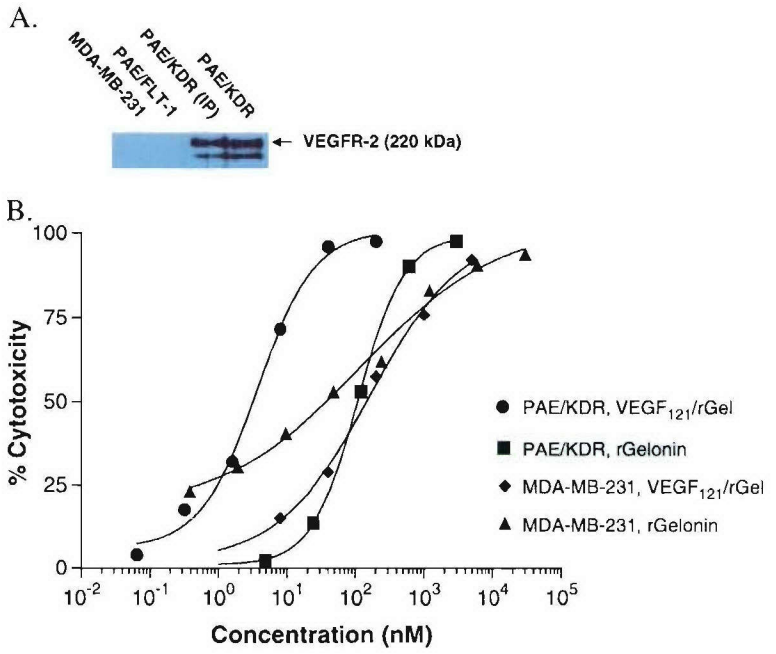

Figure 1. *MDA-MB-231 cells are not targeted by VEGF$_{121}$/rGel due to the lack of expression of VEGFR-2/KDR. (A) Western analysis demonstrating the presence of KDR on endothelial cells transfected with the KDR receptor (PAE/KDR) but not on cells expressing the FLT-1 receptor (PAE/FLT-1, negative control). As shown, the MDA-MB-231 cells did not express detectable amounts of KDR. (B) Log phase MDA-MB-231 and PAE/KDR cells were treated with various doses of VEGF$_{121}$/rGel or rGel for 72 hours. VEGF$_{121}$/rGel was far more toxic than rGel toward PAE/KDR cells (IC$_{50}$ of 1 vs 100 nM). In contrast, the cytotoxic effects of both agents were similar toward MDA-MB-231 cells (IC$_{50}$ of 150 nM with VEGF$_{121}$/rGel vs 40 nM with rGel), demonstrating no specific cytotoxicity of the fusion construct compared to free toxin on these cells.*

endothelium. These results indicate that VEGF$_{121}$/rGel specifically localizes to tumor vessels, which demonstrate a high density and a favorable distribution of the VEGF$_{121}$/rGel–binding sites.

MDA-MB-231 Model of Experimental Pulmonary Metastases and Rationale for Therapeutic Regimen

Human breast carcinoma MDA-MB-231 cells consistently lodge in lungs following intravenous injection into the tail vein

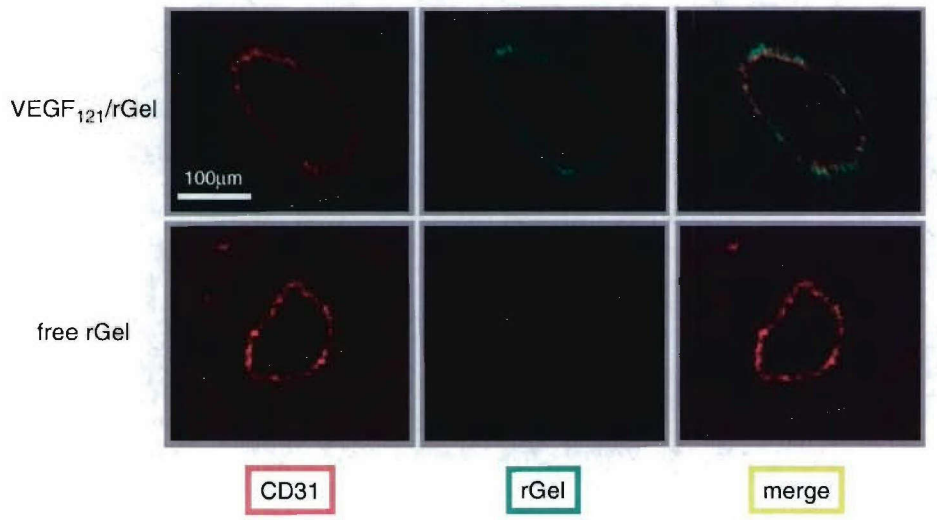

Figure 2. *VEGF$_{121}$/rGel localizes to the vasculature of breast tumor foci in the lungs of mice. Female SCID mice were injected i.v. with 0.1 ml of MDA-MB-231 cell suspension (5 × 10^5 cells) as described in the Materials and Methods section. Six weeks later, mice were administered one dose (i.v., tail vein) of 100 μg of VEGF$_{121}$/rGel. Four hours later, the mice were sacrificed and the tumor-bearing lungs were fixed. Tissue sections were stained for blood vessels using the anti–CD-31 antibody (red) and the section was counterstained using an antigelonin antibody (green). Colocalization of the stains (yellow) demonstrates the presence of the VEGF$_{121}$/rGel fusion construct specifically in blood vessels and not on tumor cells.*

of athymic or SCID mice. Micrometastases are first detected 3 to 7 days after injection of 5×10^5 cells, and macroscopic colonies develop in 100% of the injected mice within 4 to 7 weeks. Mortality occurs in all mice within 10 to 15 weeks. This model of experimental breast cancer metastasis examines the ability of tumor cells to survive in the blood circulation, extravasate through the pulmonary vasculature, and establish growing colonies in the lung parenchyma.

We evaluated the effect of VEGF$_{121}$/rGel on the growth and survival of the established micrometastases. We, therefore, started the treatment 8 days after injection of the tumor cells. By that time, based on our prior observations, tumor cells that were able to survive in the circulation and traverse the lung endothelial barrier are localized within the lung parenchyma and initiate tumor angiogenesis. Treatment with VEGF$_{121}$/rGel was given intraperitoneally for the following 3 weeks as described under the Materials and Methods section, with the mice receiving 70% of the maximum tolerated accumulative dose of the drug (900 μg/mouse). Prior studies established that the VEGF$_{121}$/rGel given at such dose did not cause histopathologic changes in normal organs. The accumulative dose of total VEGF$_{121}$/rGel fusion protein did not induce significant toxicity as judged by animal behavior morphologic evaluation of normal organs. Transient loss of weight (~10%) was observed 24 hours after most of the treatments with complete weight recovery thereafter. Colonies were allowed to expand in the absence of treatment for the following 3 weeks to evaluate the long-term effect of VEGF$_{121}$/rGel on the size of the colonies, proliferation index of tumor cells, and their ability to induce new blood vessel formation.

Effect of VEGF$_{121}$/rGel on the Number and Size of MDA-MB-231 Tumor Lesions in Lungs

An antibody directed against human HLA was used to identify metastatic lesions of MDA-MB-231 cells on samples of lung tissue. Treatment with VEGF$_{121}$/rGel, but not with free rGel, significantly reduced by between 42% and 58% both the number of colonies per lung and the size of the metastatic foci present in the lung, as shown in Figure 3 and Table 2.

Effect of VEGF$_{121}$/rGel on the Vascularity of MDA-MB-231 Pulmonary Metastatic Foci

Blood vessels were visualized by MECA 32 antibody. The overall mean vascular density of lung colonies was reduced by 51% compared to the rGel-treated controls (Table 3 and Figure 4); however, the observed effect was nonuniformly distributed by tumor colony size. The greatest impact on vascularization was observed on mid-sized and extremely small tumors (62% and 69% inhibition, respectively), whereas large tumors demonstrated the least effect (10% inhibition). The majority of lesions in the VEGF$_{121}$/rGel–treated mice (~70%) was avascular, whereas only 40% of lesions from the control group did not have vessels within the metastatic lung foci.

Effect of VEGF$_{121}$/rGel on the Number of Cycling Cells in the Metastatic Foci

The growth rate of MDA-MB-231 cells was determined by staining cells with Ki-67 antibody, as described. The number of cycling tumor cells in lesions from the VEGF$_{121}$/rGel group was also reduced by ~60% compared to controls (Figure 5). This finding suggests that the vascularity of metastases directly affects tumor cell proliferation.

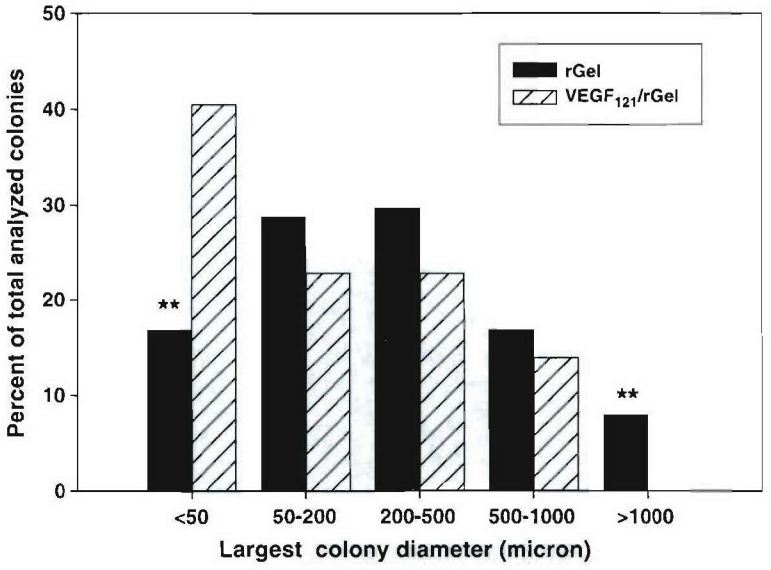

Figure 3. *VEGF$_{121}$/rGel reduces number of large colonies in the metastatic lungs. The size of tumor colonies was analyzed on slides stained with w6/32 antibody, which specifically recognizes human HLA antigens. The antibody delineates colonies of human tumor cells and defines borders between metastatic lesions and mouse lung parenchyma. The largest size differences between VEGF$_{121}$/rGel and control groups were found in groups of colonies having diameters either less than 50 μm or more than 1000 μm. In the VEGF$_{121}$/rGel–treated mice, more than 40% of total foci was extremely small (<50 μm) compared to 18% in the control group. The control mice had approximately 8% of the extremely large colonies (>1000 μm), whereas VEGF$_{121}$/rGel–treated mice did not have colonies of this size.*

Table 2. Effect of $VEGF_{121}$/rGel on the Number and Size of Pulmonary Metastases of MDA-MB-231 Human Breast Carcinoma Cells.

Parameter	Treatment*		% Inhibition *versus* rGel Treatment	*P* value†
	rGel	$VEGF_{121}$/rGel		
Number of surface colonies per lung (range)‡	53.3 ± 22 (33–80)	22.4 ± 9.2 (11–41)	58.0	0.03
Number of intraparenchymal colonies per cross section (range)§	22 ± 7.5 (18–28)	12.8 ± 5.5 (5–18)	42.0	0.02
Mean area of colonies (μm)¶	415 ± 10	201 ± 37	51.9	0.01
Mean % of colony-occupied area per lung section#	57.3 ± 19	25.6 ± 10.5	55.4	0.01

*Mice with MDA-MB-231 pulmonary micrometastases were treated intraperitoneally with $VEGF_{121}$/rGel or free gelonin as described under Materials and Methods and Results sections.

†*P* value was calculated using Student's *t* test.

‡Lungs were fixed with Bouin's fixative for 24 hours. The number of surface white colonies was determined for each sample and averaged among six mice from $VEGF_{121}$/rGel or rGel control group. Mean number per group ±SEM is shown. Numbers in parentheses represent the range of colonies in each group.

§Frozen sections were prepared from metastatic lungs. Sections were stained with 6w/32 antibody recognizing human tumor cells. The number of intraparenchymal colonies identified by brown color was determined for each cross section and averaged among six samples of individual mice from $VEGF_{121}$/rGel or rGel control group. The mean number per group ±SEM is shown. Numbers in parentheses represent the range of colonies in each group.

¶The area of foci identified by 6w/32 antibody was measured by using Metaview software. The total number of evaluated colonies was 101 and 79 for rGel and $VEGF_{121}$/rGel group, respectively. Six individual slides per group were analyzed. The mean area of colony in each group ±SEM is shown.

#The sum of all regions occupied by tumor cells and the total area of each lung cross section were determined and the percentage of metastatic regions from total was calculated. The values obtained from each slide were averaged among six samples from $VEGF_{121}$/rGel or rGel control group. The mean percent area occupied by metastases from the total area per group ±SEM is shown.

Effect of $VEGF_{121}$/rGel on Flk-1 Expression in Tumor Vessel Endothelium

The expression of Flk-1 on the remaining few vessels present in lung metastatic foci demonstrated a significant decline compared to that of lung foci present in control tumors (Figure 6). This suggests that the $VEGF_{121}$/rGel agent is able to significantly downregulate the receptor or prevent the outgrowth of highly receptor-positive endothelial cells.

Discussion

Neovascularization is a particularly important hallmark of breast tumor growth and metastatic spread [46–50]. The growth factor VEGF-A and the receptor KDR have both been implicated in highly metastatic breast cancers [51–53]. We have previously demonstrated that the $VEGF_{121}$/rGel growth factor fusion toxin specifically targets Flk-1/KDR–expressing tumor vascular endothelial cells and inhibits the growth of subcutaneously implanted human tumor xenografts [38]. The current study was designed to evaluate its effect on the development of breast cancer metastases in lungs following intravenous injection of MDA-MB-231 cells.

The salient finding of our study of the $VEGF_{121}$/rGel construct is that: this fusion toxin is specifically cytotoxic to cells overexpressing the KDR receptor for VEGF. However, the human breast MDA-MB-231 cells employed for these studies do not express this receptor and, therefore, were not directly affected by this agent (Figure 1). Although the antitumor effects of $VEGF_{121}$/rGel observed from our *in vivo* studies appear to be solely the result of targeting the Flk-1–expressing tumor vasculature and not the tumor cells themselves, one cannot rule out a direct effect on tumor cells or a combination of targeting both the tumor and the vasculature. Administration of the $VEGF_{121}$/rGel construct to mice previously injected (i.v.) with tumor cells dramatically reduced the number of tumor colonies found in the lung, their size, and their vascularity. In addition, the number of cycling breast tumor cells within lung metastatic foci was found to be reduced by an average of 60%. This reduction compares favorably to the effect of DT-VEGF on the growth of pancreatic cancer [54] and to other vascular targeting agents such as Avastin, which had an overall clinical response rate of 9.3% in a Phase I/II dose escalation trial in previously treated metastatic breast cancers [55]. In addition to the reduced number of blood vessels present in lung metastases of treated mice, we also found that the few vessels present

Table 3. Effect of $VEGF_{121}$/rGel on the Vascularity of Pulmonary Metastases of MDA-MB-231 Human Breast Carcinoma Cells.

Size of Colonies		Largest Diameter Range (μm)	Number of Vascularized Colonies from Total Inhibition Analyzed (%)*		% Inhibition *versus* Radiation Treatment
Group‡	Description		rGel	$VEGF_{121}$/rGel	
A	Extremely small	<50	7/24 (29%)	3/32 (9.3%)	69
B	Small	50–200	19/48 (39.5%)	6/24 (25%)	37
C	Mid-sized	200–500	25/30 (83.3%)	8/25 (32%)	62
D	Large	500–1000	17/17 (100%)	10/11 (90.0%)	10
E	Extremely large	>1000	8/8 (100%)	N/A	N/A
Number of vascular foci/total analyzed (%)†			76/127 (59.8%)	27/92 (29.3%)	51

*Frozen lung sections from $VEGF_{121}$/rGel and rGel-treated mice were stained with MECA 32 antibody. A colony was defined as vascularized if at least one blood vessel branched out from the periphery and reached a center of the lesion. Six slides per group derived from individual mice were analyzed and data were combined.

‡Colonies identified on each slide of a metastatic lung were subdivided into five groups (A–E) according to their largest diameter.

†The total number of the analyzed colonies was 127 and 92 for rGel- and $VEGF_{121}$/rGel–treated groups, respectively. Seventy percent of foci in the $VEGF_{121}$/rGel–treated group was a vascular, whereas only 40% of lesions from the control group did not have vessels within the metastatic foci.

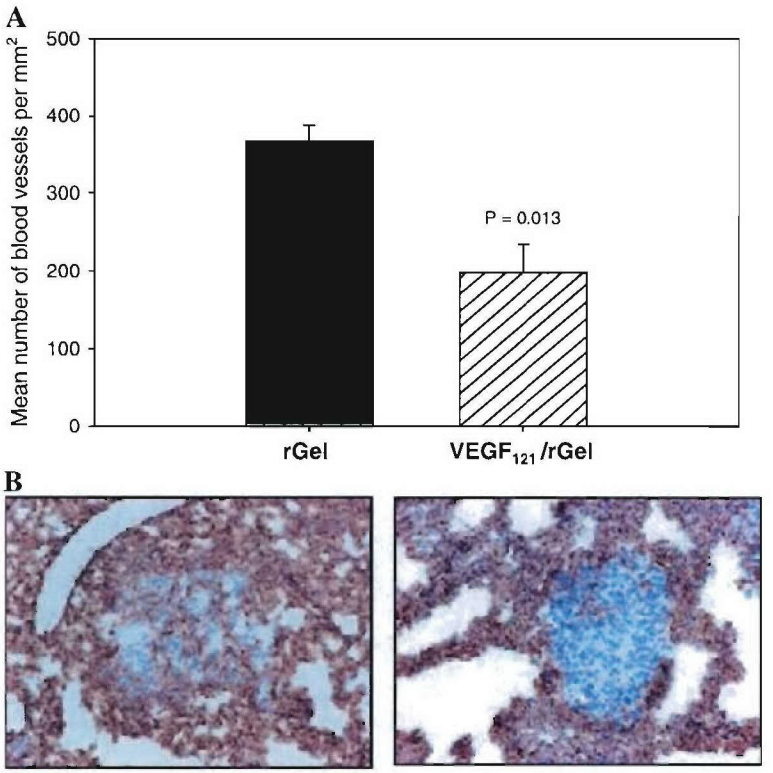

Figure 4. *$VEGF_{121}$/rGel inhibits the vascularization of MDA-MB-231 pulmonary metastases. (A) Lungs derived from $VEGF_{121}$/rGel and rGel-treated mice were stained with MECA 32 antibody and the vascular density within the metastatic foci was determined. The mean number of vessels per square millimeter in lung metastases of $VEGF_{121}$/rGel–treated mice was reduced by approximately 50% compared to those in rGel-treated mice. (B) Representative images demonstrating reduction of vascular density in foci of comparable size in mice treated with rGel (left) and $VEGF_{121}$/rGel fusion protein (right).*

had a greatly reduced expression of VEGFR-2. Therefore, this construct demonstrated an impressive long-term impact on the growth and development of breast tumor metastatic foci found in the lungs.

Targeting tumor vasculature with a variety of technologies has been shown to inhibit the growth and development of primary tumors as well as metastases. Recently, Shaheen et al. [56] demonstrated that small-molecule tyrosine kinase inhibitors active against the receptors for VEGF, fibroblast growth factor, and platelet-derived growth factors were also capable of inhibiting microvessel formation and metastases in tumor model systems. Previously, Seon et al. [57] demonstrated long-term antitumor effects of an antiendoglin antibody conjugated with ricin-A chain (RTA) in a human breast tumor xenograft model.

Surprisingly, one finding from our study was that administration of $VEGF_{121}$/rGel resulted in a three-fold decrease in the number of Ki-67–labeled (cycling) cells in the metastatic foci present in the lung (Figure 5). Clinical studies have suggested that tumor cell cycling may be an important prognostic marker for disease-free survival in metastatic breast cancer, but that Ki-67 labeling index, tumor MVD, and neovascularization appear to be independently regulated processes [58,59]. To our knowledge, this is the first report of a significant reduction in tumor labeling index produced by a vascular targeting agent.

Another critical finding from our studies is the observation that the vascular-ablative effects of the $VEGF_{121}$/rGel fusion construct alone were unable to completely eradicate lung metastases. Although the growth of larger pulmonary

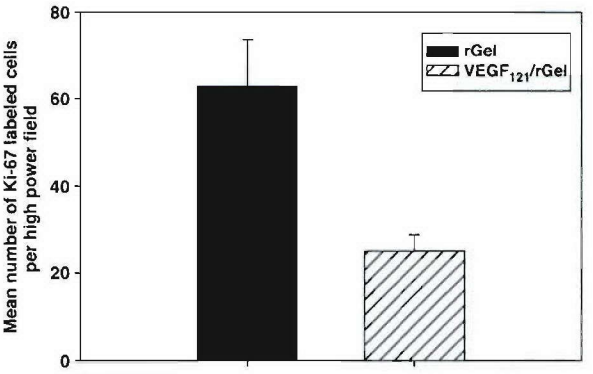

Figure 5. *$VEGF_{121}$/rGel inhibits the proliferation of metastatic MDA-MB-231 cells in the lungs. Frozen sections of lungs derived from $VEGF_{121}$/rGel and rGel-treated mice were stained with Ki-67 antibody. Stained sections were examined under ×40 objective to determine the number of tumor cells with positive nuclei (cycling cells). Positive cells were enumerated in 10 colonies per slide on six sections derived from individual mice per treatment group. The mean number per group ±SEM is presented. $VEGF_{121}$/rGel treatment reduced the average number of cycling cells within the metastatic foci by approximately 60%.*

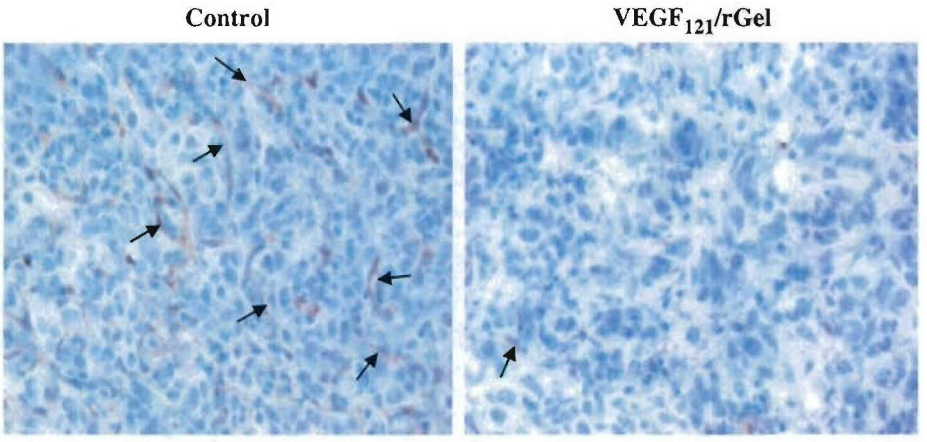

Figure 6. *Detection of Flk-1/VEGFR-2 on the vasculature of metastatic lesions by the anti–VEGFR-2 antibody, RAFL-1. Frozen sections of lungs from mice treated with $VEGF_{121}$/rGel or free gelonin stained with monoclonal rat antimouse VEGFR-2 antibody RAFL-1 (10 μg/ml). RAFL-1 antibody was detected by goat antirat IgG HRP, as described under the Materials and Methods section. Sections were developed with DAB and counterstained with hematoxylin. Representative images of lung metastases of comparable size (700–800 μm in the largest diameter) from each treatment group are shown. Images were taken with an objective of ×20. Note that the pulmonary metastases from the $VEGF_{121}$/rGel–treated group show both reduced vessel density and decreased intensity of anti–VEGFR-2 staining compared to control lesions.*

metastases was completely inhibited by this therapeutic approach, the development of small, avascular, metastatic foci within lung tissues was observed. Our findings indicate that vasculature in the small and mid-sized metastatic lesions (diameter < 500 μm) was much more susceptible to the action of $VEGF_{121}$/rGel than that in colonies with diameters larger than 500 μm. Several explanations might account for this observation. First, the number of VEGF receptors on endothelial cells within the small, exponentially expanding colonies might be higher than that in the well-established lesions. This would lead to an increase in binding sites for $VEGF_{121}$/rGel and, hence, an increased toxicity toward vessels specifically in small colonies. Second, vascular endothelial cells in small colonies might have a reduced capacity to survive after drug assault compared to vessels in established lesions. This could be due to insufficient recruitment of supporting cells (pericytes/smooth muscle cells) to the newly formed vessels, and/or derangements in the production of and interaction with components of basement membrane. Currently, the precise mechanism of the differential anti–vascular toxicity on different size colonies is not completely understood. However, these data strongly suggest that the combination of vascular targeting agents with chemotherapeutic agents or with radiotherapeutic agents, which directly damage tumor cells themselves, may provide for greater therapeutic effect. Studies of several vascular targeting agents in combination with chemotherapeutic agents have already demonstrated a distinct *in vivo* antitumor advantage of this combination modality against experimental tumors in mice [60]. Studies by Pedley et al. [61] have also suggested that the combination of vascular targeting and radioimmunotherapy may also present a potent antitumor combination. Finally, studies combining hyperthermia and radiotherapy with vascular targeting agents have demonstrated an enhanced activity against mammary carcinoma tumors in mice [62]. Studies in our laboratory combining $VEGF_{121}$/rGel and various chemotherapeutic agents, biologic agents, or therapeutic agents targeting tumor cells are currently ongoing.

The rGel toxin is a single-chain *N*-glycosidase that is similar in its action to ricin-A chain [39]. However, unlike ricin-A chain, the use of rGel does not appear to result in VLS [44]. Side effects have been observed with clinical administration of RTA-based, diphtheria toxin–based, and *Pseudomonas* exotoxin–based fusion proteins. These side effects include liver toxicity, development of neutralizing antibodies, and development of VLS. The development of neutralizing antibodies was found in 69% of patients treated with RTA immunotoxins [63], 37% of patients treated with PE-based constructs [64], and 92% of patients treated with DT constructs [65]. In contrast, our ongoing clinical trial with an rGel-based conjugate currently demonstrates a relatively low antigenicity of the rGel component, with only 2 of 22 patients developing antibodies to the rGel portion of the drug [44]. In addition, the development of hepatoxicity and VLS is commonly observed, with toxin molecules thus far not having been observed for rGel-based agents. These findings support continuing development in a clinical setting of targeted therapy using rGel. In addition, our laboratory continues to develop designer toxins with reduced antigenicity and size [66].

The presented findings demonstrate that $VEGF_{121}$/rGel can clearly and specifically target Flk-1/KDR–expressing tumor vasculature both *in vitro* and *in vivo* and that this agent can have an impressive inhibitory effect on tumor metastases. Studies are continuing in our laboratory to examine the activity of this agent alone and in combination against a variety of orthotopic and metastatic tumor models.

References

[1] Birnbaum D (1995). VEGF–FLT1 receptor system: a new ligand–receptor system involved in normal and tumor angiogenesis. *Jpn J Cancer Res* **86** (inside cover).

[2] Kerbel RS (2000). Tumor angiogenesis: past, present and the near future. *Carcinogenesis* **21,** 505–515.
[3] Bando H and Toi M (2000). Tumor angiogenesis, macrophages, and cytokines. *Adv Exp Med Biol* **476,** 267–284.
[4] Falterman KW, Ausprunk H, and Klein MD (1976). Role of tumor angiogenesis factor in maintenance of tumor-induced vessels. *Surg Forum* **27,** 157–159.
[5] Patt LM and Houck JC (1983). Role of polypeptide growth factors in normal and abnormal growth. *Kidney Int* **23,** 603–610.
[6] Ravi R, Mookerjee B, Bhujwalla ZM, Sutter CH, Artemov D, Zeng Q, Dillehay LE, Madan A, Semenza GL, and Bedi L (2000). Regulation of tumor angiogenesis by p53-induced degradation of hypoxia-inducible factor 1 alpha. *Genes Dev* **14,** 34–44.
[7] Folkman J (1974). Proceedings: tumor angiogenesis factor. *Cancer Res* **34,** 2109–2113.
[8] Strugar J, Rothbart D, Harrington W, and Criscuolo GR (1994). Vascular permeability factor in brain metastases: correlation with vasogenic brain edema and tumor angiogenesis. *J Neurosurg* **81,** 560–566.
[9] Jaeger TM, Weidner N, Chew K, Moore DH, Kerschmann RL, Waldman FM, and Carroll PR (1995). Tumor angiogenesis correlates with lymph node metastases in invasive bladder cancer. *J Urol* **154,** 69–71.
[10] Melnyk O, Zimmerman M, Kim KJ, and Shuman M (1999). Neutralizing anti-vascular endothelial growth factor antibody inhibits further growth of established prostate cancer and metastases in a pre-clinical model. *J Urol* **161,** 960–963.
[11] Aranda FI and Laforga JB (1996). Microvessel quantitation in breast ductal invasive carcinoma. Correlation with proliferative activity, hormonal receptors and lymph node metastases. *Pathol Res Pract* **192,** 124–129.
[12] Fox SB, Leek RD, Bliss J, Mansi JL, Gusterson B, Gatter KC, and Harris AL (1997). Association of tumor angiogenesis with bone marrow micrometastases in breast cancer patients. *J Natl Cancer Inst* **89,** 1044–1049.
[13] Senger DR, Van de Water L, Brown LF, Nagy JA, Yeo KT, Yeo TK, Berse B, Jackman RW, Dvorak AM, and Dvorak HF (1993). Vascular permeability factor (VPF, VEGF) in tumor biology. *Cancer Metastasis Rev* **12,** 303–324.
[14] McMahon G (2000). VEGF receptor signaling in tumor angiogenesis. *Oncologist* **5** (Suppl 1), 3–10.
[15] Obermair A, Kucera E, Mayerhofer K, Speiser P, Seifert M, Czerwenka K, Kaider A, Leodolter S, Kainz C, Zeillinger R (199). Vascular endothelial growth factor (VEGF) in human breast cancer: correlation with disease-free survival. *Int J Cancer* **74,** 455–458.
[16] Miyoshi C and Ohshima N (2001). Vascular endothelial growth factor (VEGF) expression regulates angiogenesis accompanying tumor growth in a peritoneal disseminated tumor model. *In Vivo* **15,** 233–238.
[17] Neufeld G, Cohen T, Gengrinovitch S, and Poltorak Z (1999). Vascular endothelial growth factor (VEGF) and its receptors. *FASEB J* **13,** 9–22.
[18] Shibuya M (1995). Role of VEGF–flt receptor system in normal and tumor angiogenesis. *Adv Cancer Res* **67,** 281–316.
[19] Detmar M (2000). The role of VEGF and thrombospondins in skin angiogenesis. *J Dermatol Sci* **24** (Suppl 1), S78–S84.
[20] Verheul HM and Pinedo HM (2000). The role of vascular endothelial growth factor (VEGF) in tumor angiogenesis and early clinical development of VEGF-receptor kinase inhibitors. *Clin Breast Cancer* **1** (Suppl 1), S80–S84.
[21] McCabe CJ, Boelaert K, Tannahill LA, Heaney AP, Stratford AL, Khaira JS, Hussain S, Sheppard MC, Franklyn JA, and Gittoes NJ (2002). Vascular endothelial growth factor, its receptor KDR/Flk-1, and pituitary tumor transforming gene in pituitary tumors. *J Clin Endocrinol Metab* **87,** 4238–4244.
[22] Kranz A, Mattfeldt T, and Waltenberger J (1999). Molecular mediators of tumor angiogenesis: enhanced expression and activation of vascular endothelial growth factor receptor KDR in primary breast cancer. *Int J Cancer* **84,** 293–298.
[23] Harada Y, Ogata Y, and Shirouzu K (2001). Expression of vascular endothelial growth factor and its receptor KDR (kinase domain–containing receptor)/Flk-1 (fetal liver kinase-1) as prognostic factors in human colorectal cancer. *Int J Clin Oncol* **6,** 221–228.
[24] Padro T, Bieker R, Ruiz S, Steins M, Retzlaff S, Burger H, Buchner T, Kessler T, Herrera F, Kienast J, et al. (2002). Overexpression of vascular endothelial growth factor (VEGF) and its cellular receptor KDR (VEGFR-2) in the bone marrow of patients with acute myeloid leukemia. *Leukemia* **16,** 1302–1310.
[25] Wedge SR, Ogilvie DJ, Dukes M, Kendrew J, Curwen JO, Hennequin LF, Thomas AP, Stokes ES, Curry B, Richmond GH, et al. (2000). ZD4190: an orally active inhibitor of vascular endothelial growth factor signaling with broad-spectrum antitumor efficacy. *Cancer Res* **60,** 970–975.
[26] Laird AD, Vajkoczy P, Shawver LK, Thurnher A, Liang C, Mohammadi M, Schlessinger M, Ullrich A, Hubbard SR, Blake RA, et al. (2000). SU6668 is a potent antiangiogenic and antitumor agent that induces regression of established tumors. *Cancer Res* **60,** 4152–4160.
[27] Haluska P and Adjei AA (2001). Receptor tyrosine kinase inhibitors. *Curr Opin Invest Drugs* **2,** 280–286.
[28] Fabbro D, Ruetz S, Bodis S, Pruschy M, Csermak K, Man A, Campochiaro P, Wood J, O'Reilly T, and Meyer T (2000). PKC412—a protein kinase inhibitor with a broad therapeutic potential. *Anticancer Drug Des* **15,** 17–28.
[29] Fabbro D, Buchdunger E, Wood J, Mestan J, Hofmann F, Ferrari S, Mett H, O'Reilly T, and Meyer T (1999). Inhibitors of protein kinases: CGP 41251, a protein kinase inhibitor with potential as an anticancer agent. *Pharmacol Ther* **82,** 293–301.
[30] Sun L and McMahon G (2000). Inhibition of tumor angiogenesis by synthetic receptor tyrosine kinase inhibitors. *Drug Discov Today* **5,** 344–353.
[31] Solorzano CC, Baker CH, Bruns CJ, Killion JJ, Ellis LM, Wood J, and Fidler IJ (2001). Inhibition of growth and metastasis of human pancreatic cancer growing in nude mice by PTK 787/ZK222584, an inhibitor of the vascular endothelial growth factor receptor tyrosine kinases. *Cancer Biother Radiopharm* **16,** 359–370.
[32] Drevs J, Hofmann I, Hugenschmidt H, Wittig C, Madjar H, Muller M, Wood J, Martiny-Baron G, Unger C, and Marme D (2000). Effects of PTK787/ZK 222584, a specific inhibitor of vascular endothelial growth factor receptor tyrosine kinases, on primary tumor, metastasis, vessel density, and blood flow in a murine renal cell carcinoma model. *Cancer Res* **60,** 4819–4824.
[33] Dimitroff CJ, Klohs W, Sharma A, Pera P, Driscoll D, Veith J, Steinkampf R, Schroeder M, Klutchko S, Sumlin A, et al. (1999). Anti-angiogenic activity of selected receptor tyrosine kinase inhibitors, PD166285 and PD173074: implications for combination treatment with photodynamic therapy. *Invest New Drugs* **17,** 121–135.
[34] Mendel DB, Schreck RE, West DC, Li G, Strawn LM, Tanciongco SS, Vasile S, Shawver LK, and Cherrington JM (2000). The angiogenesis inhibitor SU5416 has long-lasting effects on vascular endothelial growth factor receptor phosphorylation and function. *Clin Cancer Res* **6,** 4848–4858.
[35] Prewett M, Huber J, Li Y, Santiago A, O'Connor W, King K, Overholser J, Hooper A, Pytowski B, Witte L, et al. (1999). Antivascular endothelial growth factor receptor (fetal liver kinase 1) monoclonal antibody inhibits tumor angiogenesis and growth of several mouse and human tumors. *Cancer Res* **59,** 5209–5218.
[36] Chen Y, Wiesmann C, Fuh G, Li B, Christinger HW, McKay P, de Vos AM, and Lowman HB (1999). Selection and analysis of an optimized anti-VEGF antibody: crystal structure of an affinity-matured Fab in complex with antigen. *J Mol Biol* **293,** 865–881.
[37] Ryan AM, Eppler DB, Hagler KE, Bruner RH, Thomford PJ, Hall RL, Shopp GM, and O'Neill CA (1999). Preclinical safety evaluation of rhuMAbVEGF, an antiangiogenic humanized monoclonal antibody. *Toxicol Pathol* **27,** 78–86.
[38] Veenendaal LM, Jin H, Ran S, Cheung L, Navone N, Marks JW, Waltenberger J, Thorpe P, and Rosenblum MG (2002). *In vitro* and *in vivo* studies of a VEGF121/rGelonin chimeric fusion toxin targeting the neovasculature of solid tumors. *Proc Natl Acad Sci USA* **99,** 7866–7871.
[39] Stirpe F, Olsnes S, and Pihl A (1980). Gelonin, a new inhibitor of protein synthesis, nontoxic to intact cells. Isolation, characterization, and preparation of cytotoxic complexes with concanavalin A. *J Biol Chem* **255,** 6947–6953.
[40] Rosenblum MG, Cheung L, Kim SK, Mujoo K, Donato NJ, and Murray JL (1996). Cellular resistance to the antimelanoma immunotoxin ZME-gelonin and strategies to target resistant cells. *Cancer Immunol Immunother* **42,** 115–121.
[41] Rosenblum MG, Zuckerman JE, Marks JW, Rotbein J, and Allen WR (1992). A gelonin-containing immunotoxin directed against human breast carcinoma. *Mol Biother* **4,** 122–129.
[42] Rosenblum MG, Murray JL, Cheung L, Rifkin R, Salmon S, and Bartholomew R (1991). A specific and potent immunotoxin composed of antibody ZME-018 and the plant toxin gelonin. *Mol Biother* **3,** 6–13.
[43] Xu Y, Xu Q, Rosenblum MG, and Scheinberg DA (1996). Antileukemic activity of recombinant humanized M195-gelonin immunotoxin in nude mice. *Leukemia* **10,** 321–326.

[44] Talpaz M, Kantarjian H, Freireich E, Lopez V, Zhang W, Cortes-Franco J, Scheinberg D, and Rosenblum MG (2003). Phase I clinical trial of the anti-CD-33 immunotoxin HuM195/rGel. *Abstract R5362, 94th Annual Meeting, American Association for Cancer Research* **44,** 1066.

[45] Ran S, Huang X, Downes A, and Thorpe PE (2003). Evaluation of novel antimouse VEGFR2 antibodies as potential antiangiogenic or vascular targeting agents for tumor therapy. *Neoplasia* **5,** 297–307.

[46] Axelsson K, Ljung BM, Moore II DH, Thor AD, Chew KL, Edgerton SM, Smith HS, and Mayall BH (1995). Tumor angiogenesis as a prognostic assay for invasive ductal breast carcinoma. *J Natl Cancer Inst* **87,** 997–1008.

[47] Balsari A, Maier JA, Colnaghi MI, and Menard S (1999). Correlation between tumor vascularity, vascular endothelial growth factor production by tumor cells, serum vascular endothelial growth factor levels, and serum angiogenic activity in patients with breast carcinoma. *Lab Invest* **79,** 897–902.

[48] Bosari S, Leek AK, DeLellis RA, Wiley BD, Heatley GJ, Silverman ML (1992). Microvessel quantitation and prognosis in invasive breast carcinoma. *Hum Pathol* **23,** 755–761.

[49] Bottini A, Berruti A, Bersiga A, Brizzi MP, Allevi G, Bolsi G, Aguggini S, Brunelli A, Betri E, Generali D, et al. (2002). Changes in microvessel density as assessed by CD34 antibodies after primary chemotherapy in human breast cancer. *Clin Cancer Res* **8,** 1816–1821.

[50] Chu JS, Lee WJ, Chang TC, Chang KJ, and Hsu HC (1995). Correlation between tumor angiogenesis and metastasis in breast cancer. *J Formos Med Assoc* **94,** 373–378.

[51] Nakopoulou L, Stefanaki K, Panayotopoulou E, Giannopoulou I, Athanassiadou P, Gakiopoulou-Givalou H, and Louvrou A (2002). Expression of the vascular endothelial growth factor receptor-2/Flk-1 in breast carcinomas: correlation with proliferation. *Hum Pathol* **33,** 863–870.

[52] Brown LF, Guidi AJ, Schnitt SJ, Van De Water L, Iruela-Arispe ML, Yeo TK, Tognazzi K, and Dvorak HF (1999). Vascular stroma formation in carcinoma *in situ*, invasive carcinoma, and metastatic carcinoma of the breast. *Clin Cancer Res* **5,** 1041–1056.

[53] Brown LF, Berse B, Jackman RW, Tognazzi K, Guidi AJ, Dvorak HF, Senger DR, Connolly JL, and Schnitt SJ (1995). Expression of vascular permeability factor (vascular endothelial growth factor) and its receptors in breast cancer. *Hum Pathol* **26,** 86–91.

[54] Hotz HG, Gill PS, Masood R, Hotz B, Buhr HJ, Foitzik T, Hines OJ, and Reber HA (2002). Specific targeting of tumor vasculature by diphtheria toxin—vascular endothelial growth factor fusion protein reduces angiogenesis and growth of pancreatic cancer. *J Gastrointest Surg* **6,** 159–166.

[55] Cobleigh MA, Langmuir VK, Sledge GW, Miller KD, Haney L, Novotny WF, Reimann JD, and Vassel D (2003). A phase I/II dose-escalation trial of bevacizumab in previously treated metastatic breast cancer. *Semin Oncol* **30** (5 Suppl 16), 117–124.

[56] Shaheen RM, Davis DW, Liu W, Zebrowski BK, Wilson MR, Bucana CD, McConkey DJ, McMahon G, and Ellis LM (1999). Antiangiogenic therapy targeting the tyrosine kinase receptor for vascular endothelial growth factor receptor inhibits the growth of colon cancer liver metastasis and induces tumor and endothelial cell apoptosis. *Cancer Res* **59,** 5412–5416.

[57] Seon BK, Matsuno F, Haruta Y, Kondo M, and Barcos M (1997). Long-lasting complete inhibition of human solid tumors in SCID mice by targeting endothelial cells of tumor vasculature with antihuman endoglin immunotoxin. *Clin Cancer Res* **3,** 1031–1044.

[58] Honkoop AH, van Diest PJ, de Jong JS, Linn SC, Giaccone G, Hoekman K, Wagstaff J, and Pinedo HM (1998). Prognostic role of clinical, pathological and biological characteristics in patients with locally advanced breast cancer. *Br J Cancer* **77,** 621–626.

[59] Vartanian RK and Weidner N (1994). Correlation of intratumoral endothelial cell proliferation with microvessel density (tumor angiogenesis) and tumor cell proliferation in breast carcinoma. *Am J Pathol* **144,** 1188–1194.

[60] Siemann DW, Mercer E, Lepler S, and Rojiani AM (2002). Vascular targeting agents enhance chemotherapeutic agent activities in solid tumor therapy. *Int J Cancer* **99,** 1–6.

[61] Pedley RB, El Emir E, Flynn AA, Boxer GM, Dearling J, Raleigh JA, Hill SA, Stuart S, Motha R, and Begent RH (2002). Synergy between vascular targeting agents and antibody-directed therapy. *Int J Radiat Oncol Biol Phys* **54,** 1524–1531.

[62] Murata R, Overgaard J, and Horsman MR (2001). Combretastatin A-4 disodium phosphate: a vascular targeting agent that improves that improves the anti-tumor effects of hyperthermia, radiation, and mild thermoradiotherapy. *Int J Radiat Oncol Biol Phys* **51,** 1018–1024.

[63] Schnell R, Vitetta E, Schindler J, Borchmann P, Barth S, Ghetie V, Hell K,Drillich S, Diehl V, and Engert A (2000). Treatment of refractory Hodgkin's lymphoma patients with an anti-CD25 ricin-A chain immunotoxin. *Leukemia* **14,** 129–135.

[64] Kreitman RJ, Wilson WH, White JD, Stetler-Stevenson M, Jaffe ES, Giardina S, Waldmann TA, and Pastan I (2000). Phase I trial of recombinant immunotoxin anti-Tac(Fv)-PE38 (LMB-2) in patients with hematologic malignancies. *J Clin Oncol* **18,** 1622–1636.

[65] LeMaistre CF, Saleh MN, Kuzel TM, Foss F, Platanias LC, Schwartz G, Ratain M, Rook A, Freytes CO, Craig F, et al. (1998). Phase I trial of a ligand fusion-protein (DAB389IL-2) in lymphomas expressing the receptor for interleukin-2. *Blood* **91,** 399–405.

[66] Cheung LH, Marks JW, and Rosenblum MG (2004). Development of "designer toxins" with reduced antigenicity and size. *Abstract 3790, 95th Annual Meeting, American Association for Cancer Research* **45,** 874.

Manuscript Submitted to Molecular Cancer Therapeutics

Targeting Human Pancreatic Tumor Cells with The anti-HER-2/neu Immunocytokine scFv23/TNF

Mi-Ae Lyu, Razelle Kurzrock, and Michael G. Rosenblum*

Running Title: scFv23/TNF targeting HER-2/neu

Department of Experimental Therapeutics, The University of Texas M.D. Anderson Cancer Center, Houston, Texas, USA

**Correspondence to*: Michael G. Rosenblum, Department of Experimental Therapeutics, The University of Texas M.D. Anderson Cancer Center, 1515 Holcombe Boulevard, Unit 44, Houston, TX 77030. Tel: 713-792-3554; Fax: 713-794-4261. E-mail: mrosenbl@mdanderson.org

Research conducted, in part, by The Clayton Foundation for Research and supported, in part by DOD Grant DAMD17-02-1-0457.

Key Words: Immunocytokine, HER-2/neu, Pancreatic cancer, scFv23/TNF, Combination therapy

Abbreviations List: scFv23/TNF, anti-HER-2/neu single chain antibody fused to TNF; TNF, tumor necrosis factor; HER-2/neu, epidermal growth factor receptor-2; HER-1, epidermal growth factor receptor-1; TNF-R1, TNF receptor-1; TNF-R2, TNF receptor-2; p-Akt, phospho-Akt; 5-FU, 5-fluorouracil; PARP, poly ADP-ribose polymerase; TUNEL, terminal deoxynucleotidyl transferase-mediated nick end labeling

Abstract

Human pancreatic tumor cells are highly resistant to both TNF and to chemotherapeutic agents. HER-2/neu expression has been proposed as a negative prognostic marker in pancreatic intraepithelial neoplasia. Our approach was to utilize HER-2/neu expression on the surface of tumor cells as a therapeutic target employing the immunocytokine scFv23/TNF to deliver TNF directly to tumor cells. Using a panel of human pancreatic cell lines, we evaluated the in vitro response of cells to scFv23/TNF in combination with various chemotherapeutic agents. We found a correlation between the expression levels of HER-2/neu, TNF-R1 and cellular response to the tested agents. L3.6pl cells expressing the highest levels of HER-2/neu and TNF-R1 were the most sensitive to the conventional chemotherapeutic agents, whereas Capan-2 cells expressing comparatively lower levels of HER-2/neu and TNF-R1 were the most resistant to the tested drugs. Doxorubicin, gemcitabine and scFv23/TNF were the most active cytotoxic agents whereas all cell lines were relatively resistant to 5-fluorouracil (5-FU), cisplatin, etoposide, and TNF. Combination studies demonstrated a uniform synergistic effect of scFv23/TNF with 5-FU in all pancreatic cell lines. Mechanistic studies demonstrated that combination 5-FU plus scFv23/TNF specifically resulted in a down-regulation of both the survival protein phospho-Akt and the anti-apoptotic protein Bcl-2. In addition, the combination 5-FU plus scFv23/TNF induced apoptosis and this synergistic effect was dependent on activation of caspase-8 and caspase-3. Delivery of the cytokine TNF to HER-2/neu expressing tumor cells using the immunocytokine scFv23/TNF may be an effective therapy for pancreatic cancer especially when utilized in combination with 5-FU.

Introduction

Pancreatic cancer remains one of the leading causes of cancer-related deaths in the United States and Europe (1-3). This is a highly aggressive and metastatic tumor type virtually resistant to all chemotherapeutic and radiotherapeutic intervention (4, 5). Recent studies have demonstrated some clinical benefit to treatment with gemcitabine and gemcitabine-containing regimens (6-8).

There are numerous oncogenes such as HER-2/neu, HER-1 (9-13) which are over-expressed in pancreatic tumor biopsy specimens as well as mutations in various genes such as p53, Ki-ras, and p-21 (14-16). Many of these genetic abnormalities play a major role in the development of the aggressive, metastatic and therapy-resistant phenotype presented clinically. Experimental therapeutic approaches to use vaccines (17-20) or antibodies to target oncogene protein products (21-23) are underway or have been completed to provide more focused control of tumor growth.

Imunocytokines are a novel class of recombinant agents composed of cytokines fused to antibodies and theses fusion constructs are capable of re-directing their biological effects to target specific cells and to prevent non-target toxicity. We initially described a novel chemical conjugate of a tumor-targeting antibody and the cytokine tumor necrosis factor-alpha (TNF-α) (24, 25). Against antigen-positive cells, this chemical conjugate was more cytotoxic to target cells than TNF-α itself. More recently, we developed novel immunocytokine scFv23/TNF composed of single-chain antibodies targeting HER-2/neu antigen on the cell surface of breast cancer tumor fused to the gene for TNF-α. This immunocytokine was also shown to be highly cytotoxic and specifically active against target cells resistant to TNF-α.

Because many human pancreatic tumor cell lines express HER-2/neu and tend to be generally resistant to TNF and chemotherapeutic agents, the purpose of the current study was to examine the effects on pancreatic tumor cells of an immunocytokine scFv23/TNF composed of TNF tethered to the single chain antibody scFv23 recognizes the cell-surface domain of HER-2/neu in vitro. We evaluated the cytotoxic response of the scFv23/TNF against a panel of four pancreatic lines (AsPc-1, Capan-1, Capan-2 and L3.6pl) and characterized the HER-2/neu, TNF receptor-1 (TNF-R1), and TNF receptor-2 (TNF-R2) expression of each cell line. Additionally, we examined the cytotoxic effects of conventionally used chemotherapeutic agents alone and in combination with scFv23/TNF and we investigated the possible mechanisms which may account for the observed synergistic cytotoxic effects of scFv23/TNF in combination with 5-fluorouracil.

Materials and Methods

Cell Lines and Culture

L3.6pl and Capan-1 human pancreatic cancer cell lines were kindly provided by Dr. Killian and Dr. Chiao (M.D. Anderson Cancer Center, Houston), respectively. AsPc-1 and Capan-2 human pancreatic cancer cell lines were kindly provided by Dr. Dr. Xie (M.D. Anderson Cancer Center, Houston). Four human pancreatic cancer cell lines (AsPc-1, Capan-1, Capan-2, and L3.6pl) were grown in Dulbecco's modified Eagle's medium (DMEM, Life Technologies Inc., Rockville, MD) supplemented with 10% heat-inactivated fetal bovine serum (FBS), 100 units/ml penicillin and 100 μg/ml streptomycin.

Chemotherapeutic agents and immunocytokine scFv23/TNF

5-fluorouracil (5-FU) was from Roche Laboratories (Nutley, NJ). Cisplatin and Etoposide (VP-16) were from Bristol Laboratories (Princeton, NJ). Doxorubicin was from Cetus Corporation (Emeryville, CA). Gemcitabine was from Eli Lilly Co. (Indianapolis, IN). The immunocytokine scFv23/TNF was produced in a bacterial expression host, purified to homogeniety and assessed for biological activity as previously described (26).

Antibodies and Chemicals

Monoclonal anti-HER-2/neu antibody (Ab), rabbit polyclonal anti-TNF-R1 Ab, rabbit polyclonal anti-TNF-R2 Ab, rabbit polyclonal anti-phospho Akt Ab, rabbit polyclonal anti-Akt, mouse anti-Bcl-2 Ab, rabbit polyclonal anti-caspase-8 Ab, monoclonal anti-caspase-3 Ab, and monoclonal anti-PARP Ab were obtained from Santa Cruz Biotechnology, Santa Cruz, CA. General caspase inhibitor (Z-VAD-FMK), caspase-8 inhibitor (Z-IETD-FMK), and caspase-3 inhibitor (Z-DEVD-FMK) were purchased from R&D Systems, Minneapolis, MN.

In Vitro Cytotoxicity Assays and Combination Studies

All human pancreatic cancer cells were seeded ($1x10^4$/well) in flat-bottom 96-well microtiter plates (Becton Dickinson Labware, Franklin Lakes, NJ) and 24 hr later, scFv23/TNF, TNF or five chemotherapeutic agents (5-fluorouracil, cisplatin, etoposide, doxorubicin, and gemcitabine,) were added in triplicate wells. For combination studies, scFV23/TNF and each of five chemotherapeutic agents were combined at their individual IC_{25} concentrations. To examine the effect of caspase inhibitor on the cytotoxicity of combination, L3.6pl cells were pretreated with or without 200 μM general caspase inhibitor (Z-VAD-FMK), caspase-8 inhibitor (Z-IETD-FMK), or caspase-3 inhibitor (Z-DEVD-FMK) (R&D) for 2 hr and then treated with their

individual IC_{25} concentrations. After incubation for an additional 72 hr, remaining adherent cells were stained by adding 50 µl of crystal violet solution (0.5% w/v in 20% MeOH/H_2O). Dye-stained cells were solubilized by addition of 100 µl of Sorenson's buffer [100 mM sodium citrate (pH 4.2) in 50% ethanol], and absorbance was measured at 630 nm using an ELISA plate reader (Bio-Tek Instruments, Inc., Winooski, VT).

The synergistic, additive or antagonistic effects of drug combinations were assessed according to the median effect principle as described by Chou and Talalay (27): fa/fu = (D/Dm)m. Where D is the dose of the drug, Dm is the IC_{50}, fa is the fraction affected by the dose, fu is the fraction unaffected and m is a coefficient that determines the sigmoidicity of the curve.

Western Blot Analysis

To check the status of HER-2/neu, TNF receptor-1, and TNF receptor-2, four human pancreatic cancer cell lines (AsPc-1, Capan-1, Capn-2, and L3.6pl) were washed two times with phosphate buffered saline (PBS) and lysed on ice for 20 min in 0.3 ml of lysis buffer (10 mM Tris-HCl, pH 8, 60 mM KCl, 1 mM EDTA, 1 mM DTT, 0.2% NP-40). L3.6pl cell lines were seeded at 5 x 10^5 cells/60 mm petri-dish, allowed to grow overnight, and then treated with IC_{25} concentrations of 5-FU, scFv23/TNF or combination. After treatment, cells were washed twice with phosphate buffered saline (PBS) and lysed on ice for 20 min in 0.3 ml of lysis buffer (10 mM Tris-HCl, pH 8, 60 mM KCl, 1 mM EDTA, 1 mM DTT, 0.2% NP-40). Cell lysates (50 µg) were fractionated by 8-15% SDS-PAGE and transferred on Immobilon-P nitrocellulose membranes (Schleicher & Schuell Inc., Keene, NH). Membranes were blocked for 2 hours in Tris-buffered saline (TBS) containing 3% bovine serum and then probed with various antibodies. Goat anti-mouse/goat anti-rabbit or swain anti-goat antibodies conjugated with horseradish

peroxidase (Bio-Rad Laboratories, Hercules, CA) were used to visualize immunoreactive proteins at a 1:4000 dilution using ECL detection reagent (Amersham Pharmacia Biotech Inc., Piscataway, NJ). Data are presented as the relative density of protein bands normalized to β-actin. The intensity of the bands was quantified using Histogram.

Detection of Apoptosis

The development of apoptotic cell death was detected by TUNEL assay. To assess apoptosis, L3.6pl cells were plated on glass cover slips, allowed to adhere overnight and then treated with IC_{25} concentrations of 5-FU, scFv23/TNF, or combination for 48 hr. The cells were washed with PBS, permeabilized (0.1% Triton X-100, 0.1% sodium citrate), and then fixed in 4% paraformaldehyde. Fixed cells were stained with an *in situ* cell death detection kit (Roche). Cells undergoing apoptosis were identified by fluorescence microscopy (Nikon, Japan).

Results

Status of HER-2/neu, TNF-R1, and TNF-R2 in Four Human Pancreatic Cancer Cell Lines

HER-2/neu has previously been found to be over-expressed in pancreatic tumor biopsy specimens and HER-2/neu expression has been proposed as a negative prognostic marker in pancreatic intraepithelial neoplasia (9). We therefore determined HER-2/neu expression in four pancreatic cancer cell lines. All four pancreatic cancer cell lines (AsPc-1, Capan-1, Capan-2, and L3.6pl) expressed HER-2/neu, TNF-R1, and TNF-R2. We compared the expression levels of HER-2/neu, TNF-R1, and TNF-R2 in each cell line with levels in AcPc-1 cells. Compared with AsPc-1 cells, Capan-1 and L3.6pl cells expressed higher levels of HER-2/neu and TNFR-1 (3.3 –

3.8 fold vs. 2.3-3.0 fold, respectively) whereas Capan-2 cells expressed similar levels of HER-2/neu, TNF-R1, and TNF-R2 (Fig. 1).

Dose-Response Curves of Various Agents on Four Pancreatic Cancer Cell Lines

The ability of various agents to inhibit cell proliferation *in vitro* was markedly different among the four cell lines tested. All pancreatic cancer cell lines were highly resistant to the cytotoxic effects of TNF (IC_{50}> 1600 nM). 5-fluorouracil, cisplatin, and etoposide showed IC_{50} values between 1 μM and 300 μM whereas doxorubicin, gemcitabine and scFv23/TNF were comparatively more active with IC_{50} values ranging between 6 nM and 700 nM. Interestingly, L3.6pl cells expressing the highest levels of HER-2/neu, TNF-R1, and TNF-R2 were the most sensitive to the tested drugs, whereas Capan-2 cells expressing comparatively lower levels of HER-2/neu, TNF-R1, and TNF-R2 were the most resistant to the tested drugs. AsPc-1 cells expressing similar levels of HER-2/neu and TNF-R1 as Capan-2 showed the moderate resistant to the tested drugs (Fig. 2a-d and Table 1).

Cytotoxic Effect of scFv23/TNF in Combination with Various Chemotherapeutic Agents

Studies combining scFv23/TNF and various chemotherapeutic agents demonstrated a synergistic cytotoxic effect of scFv23/TNF with 5-fluorouracil and an antagonistic effect of scFv23/TNF with doxorubicin in all pancreatic cancer cell lines. However, the addition of cisplatin or gemcitabine to scFv23/TNF resulted in antagonistic cytotoxic effects in 3/4 cell lines tested whereas the addition of etoposide to scFv23/TNF resulted in synergistic effect in 3/4 pancreatic cancer cell lines (Table 2). These results suggest that targeting HER-2/neu and TNF-

R1 expressing tumor cells using the immunocytokine scFv23/TNF may be an effective therapy for pancreatic cancer especially when utilized in combination with specific chemotherapeutic agents such as 5-FU.

Inhibition of Akt Phosphorylation by Combination Treatment

HER-2/neu over-expression results in activation of different downstream pathways such as the Akt kinase pathway, which leads to cell proliferation and cell survival. To determine whether combination treatment affects this survival pathway, L3.6pl cells were treated with IC_{25} doses of 5-fluorouracil, scFv23/TNF, or 5-FU + scFv23/TNF. The activation of Akt kinase was then assessed by Western blot analysis using antibodies to Akt and to phospho-Akt. As shown in Fig. 3, treatment of cells with 5-FU, scFv23/TNF as single agents or combination had no impact on the total levels of Akt while the combination treatment of scFv23/TNF plus 5-FU inhibited phosphorylation of the Akt protein by 50%. These results suggest that 5-FU + scFv23/TNF-induced cytotoxicity may be mediated, at least in part, by an inhibitory effect on Akt phosphorylation events.

Effect of Combination Treatment on Bcl-2 Expression

Increased levels of the anti-apoptotic protein Bcl-2 contribute to cellular resistance of tumor cells to a variety of chemotherapeutic agents including cyclophosphamide, methotrexate, anthracycline, cytarabine, paclitaxel, and corticosteroids (28). To determine whether the cytotoxic effects of combination treatment are mediated through changes in cellular levels of Bcl-2, L3.6pl cells were treated with IC_{25} doses of 5-fluorouracil, scFv23/TNF, or 5-FU + scFv23/TNF. As shown in Fig. 4, treatment of cells with 5-FU had no impact on cellular levels

of Bcl-2 while scFv23/TNF and 5-FU + scFv23/TNF inhibited Bcl-2 expression levels 43% and 71%, respectively. These results suggest that 5-FU + scFv23/TNF-induced cytotoxicity may be mediated, at least in part, by inhibition of Bcl-2 expression.

Induction of Apoptosis and Caspases Cleavage by Combination Treatment

To determine whether the cytotoxic effect of combination treatment was associated with apoptosis, L3.6pl cells were assayed for apoptosis by TUNEL staining. L3.6pl cells were treated with IC_{25} doses of 5-fluorouracil, scFv23, TNF, or 5-FU + scFv23/TNF. As shown in Figure 5, 5-FU + scFv23/TNF-treated cells demonstrated a marked induction of apoptotic cell death within 48 hrs after treatment. The caspase series of proteins is known to be a central mediator of the apoptotic effects of TNF and other cytokines. To determine whether caspase-8 and caspase-3 were activated in L3.6pl cells during 5-FU + scFv23/TNF-induced cell death, we investigated the cleavage of caspase-8, caspase-3, and its substrate poly (ADP)-ribose polymerase (PARP). Treatment with IC_{25} dose of 5-FU had no effect on caspase-8, caspase-3, and PARP cleavage whereas exposure of the cells to the scFv23/TNF or scFv23/TNF plus 5-FU combination resulted in cleavage of caspase-8, and caspase-3. In addition, combination treatment induced PARP cleavage at 48 hr (Fig. 6). To determine whether 5-FU + scFv23/TNF-induced apoptosis was dependent on activation of the caspases pathway, we examined the effect of caspase inhibitors on the cytotoxicity of 5-FU + scFv23/TNF against L3.6pl cells. As shown in Fig 7, pre-treatment with the caspase inhibitors followed by combination treatment (5-FU + scFv23/TNF) was able to inhibit the synergistic cytotoxic effects observed. This suggests that the synergistic cytotoxic effects of the combination may depend, at least in part, on a caspase-driven pathway.

Discussion

Human epidermal growth factor receptor-2 (HER-2/erbB-2) belongs to a family of four transmembrane receptors (HER-1, HER-3, and HER-4) and it plays a key role in the HER family signaling events, cooperating with other HER receptors via a complex signaling network to regulate cell growth, differentiation, and survival (29-31). Over-expression of HER-2/neu has been observed in several cancers where it is associated with multiple drug resistance, higher metastatic potential, and decreased patient survival times (9, 32-36). To evaluate the influence of HER-2/neu expression in pancreatic cancer as it relates to clinical response to therapeutic agents, a variety of groups have used several HER-2/neu targeting strategies including using HER-2/neu targeted ribozymes (37-39), humanized anti-HER-2/neu antibody (Herceptin), and combination chemotherapeutic treatment regimens with Herceptin (40-43).

Our approach was to utilize HER-2/neu expression on the surface of tumor cells as a therapeutic target employing the HER-2/neu single chain antibody to deliver TNF directly to tumor cells. Previous studies in our laboratory demonstrated that immunocytokine containing TNF were highly cytotoxic even to tumor cells resistant to TNF itself (26). We examined in depth the mechanistic effects of the immunocytokine scFv23/TNF in combination with chemotherapeutic agents on a panel of four pancreatic cancer cell lines, which were characterized for various levels of oncogene expression and comparative response to chemotherapeutic agents.

The chemotherapeutic agents utilized in this study were selected to present a spectrum of different cellular targets and are representative of the major classes of agents with therapeutic value. The potential combinations of tumor-targeted delivery of TNF in combination with chemotherapeutic agents have not been previously examined. Our studies combining

scFv23/TNF and various chemotherapeutic agents clearly demonstrated a uniform synergistic effect of scFv23/TNF and 5-FU in all pancreatic tumor cell lines. L3.6pl cells expressing the highest levels of HER-2/neu, TNF-R1, and TNF-R2 were the most sensitive to the tested drugs. Pegram *et al* reported that 5-FU has an antagonistic effect *in vitro* in combination with anti-HER-2/neu monoclonal antibodies whereas cisplatin, etoposide, and doxorubicin, previously showed a synergistic or an additive effect in combination with Herceptin (43). However, we found a uniform synergistic effect of scFv23/TNF in combination with 5-FU and an antagonistic effect of scFv23/TNF in combination with doxorubicin in against all four pancreatic cancer cell lines (Table 2).

Over-expression of HER-2/neu is known to activate the Akt pathway and to confer resistance to apoptosis induced by many therapeutic drugs (44). Treatment of L3.6pl cells with combination 5-FU + scFv23/TNF resulted in significant reduction in Akt phosphorylation. Our result suggests that 5-FU + scFv23/TNF-induced cytotoxicity may be mediated, at least in part, by the inhibition of Akt survival signaling pathway.

Over-expression of Bcl-2 has also been shown to contribute to the cellular resistance of a variety of chemotherapeutic drugs, including cyclophosphamide, methotrexate, anthracycline, cytarabine, paclitaxel, and corticosteroids (28). Sasaki *et al* reported that the level of Bcl-2 in cancer cells was an indicator of 5-FU efficacy (45). We found that scFv23/TNF and 5-FU + scFv23/TNF inhibited 43% and 71%, respectively. However, treatment of cells with IC_{25} dose of 5-FU had no impact on the levels of Bcl-2. Down-regulation of Bcl-2 by scFv23/TNF may be induced the sensitization of L3.6pl cells to be more sensitive to 5-FU. Therefore, scFv23/TNF in combination with 5-FU accelerates the inhibition of Bcl-2 expression.

We also found that another critical factor in the mediation of 5-FU + scFv23/TNF synergy is the caspase activation cascade. Binding of TNF to TNFR-1 can induce the formation of signaling complexes, TNF-R1-TRADD-FADD-pro-caspase-8, resulting in the activation of caspase-8 (46). The activation of caspase-8 is though to result in proteolytic activation of the other caspases (47). The activation of caspase-3 contributes to paclitaxel-induced apoptosis in HER-2/neu-overexpressing SKOV3.ip1 (48) and immunotoxin-induced apoptosis (49). We observed that treatment with scFv23/TNF alone and combination 5-FU + scFv23/TNF resulted in activation of caspase-8, caspase-3 and PARP cleavage.

Our results suggest that delivery of the cytokine TNF to HER-2/neu expressing tumor cells using the immunocytokine scFv23/TNF may be an effective therapy for pancreatic cancer especially when utilized in combination with specific chemotherapeutic agents. These observations provide a rationale for further developmental therapeutic studies of the immunocytokine scFv23/TNF against HER-2/neu expressing pancreatic xenograft models alone and in combination with selected chemotherapeutic agents.

References

1. Haycox A, Lombard M, Neoptolemos J, Walley T. Review article: current treatment and optimal patient management in pancreatic cancer. Aliment Pharmacol Ther 1998;12:949-64.

2. Ward S, Morris E, Bansback N, et al. A rapid and systematic review of the clinical effectiveness and cost-effectiveness of gemcitabine for the treatment of pancreatic cancer. Health Technol Assess 2001;5:1-70.

3. Kulke MH. Metastatic pancreatic cancer. Curr Treat Options Oncol 2002;3:449-57.

4. Permert J, Hafstrom L, Nygren P, Glimelius B. A systematic overview of chemotherapy effects in pancreatic cancer. Acta Oncol 2001;40:361-70.

5. Matsuno S, Egawa S, Arai K. Trends in treatment for pancreatic cancer. J Hepatobiliary Pancreat Surg 2001;8:544-48.

6. van Moorsel CJ, Peters G J, Pinedo HM. Gemcitabine: Future Prospects of Single-Agent and Combination Studies. Oncologist 1997;2:127-34.

7. Carmichael J. Clinical response benefit in patients with advanced pancreatic cancer. Role of gemcitabine. Digestion 1997;58:503-7.

8. Michael M, Moore M. Clinical experience with gemcitabine in pancreatic carcinoma. Oncology (Huntingt) 1997;11:1615-22.

9. Tomaszewska R, Okon K, Nowak K, Stachura J. HER-2/Neu expression as a progression marker in pancreatic intraepithelial neoplasia. Pol J Pathol1998;49:83-92.

10. Sakorafas GH, Lazaris A, Tsiotou AG, Koullias G, Glinatsis MT, Golematis BC. Oncogenes in cancer of the pancreas. Eur J Surg Oncol 1995;21:251-53.

11. Williams TM, Weiner DB, Greene MI, Maguire HC, Jr. Expression of c-erbB-2 in human pancreatic adenocarcinomas. Pathobiology 1991;59:46-52.

12. Lemoine NR, Hughes CM, Barton CM, et al. The epidermal growth factor receptor in human pancreatic cancer. J Pathol 1992;166:7-12.

13. Ozawa S, Ueda M, Ando N, Abe O, Shimizu N. Epidermal growth factor receptors in cancer tissues of esophagus, lung, pancreas, colorectum, breast and stomach. Jpn J Cancer Res 1988;79:1201-07.

14. Yokoyama M, Yamanaka Y, Friess H, Buchler M, Korc M. p53 expression in human pancreatic cancer correlates with enhanced biological aggressiveness. Anticancer Res 1994;14:2477-83.

15. Hahn SA, Kern SE. Molecular genetics of exocrine pancreatic neoplasms. Surg Clin North Am 1995;75:857-69.

16. Dergham ST, Dugan MC, Joshi US, et al. The clinical significance of p21 (WAF1/CIP-1) and p53 expression in pancreatic adenocarcinoma. Cancer 1997;80:372-81.

17. Gjertsen MK, Gaudernack G. Mutated Ras peptides as vaccines in immunotherapy of cancer. Vox Sang 1998;74(2):489-95.

18. Gunzburg WH, Salmons B. Novel clinical strategies for the treatment of pancreatic carcinoma. Trends Mol Med 2001;7:30-7.

19. Jaffee EM, Hruban RH, Biedrzycki B, et al. Novel allogeneic granulocyte-macrophage colony-stimulating factor-secreting tumor vaccine for pancreatic cancer: a phase I trial of safety and immune activation. J Clin Oncol 2001;19: 145-56.

20. Kaufman HL, Di VJ, Jr, Horig H. Immunotherapy for pancreatic cancer: current concepts. Hematol Oncol Clin North Am 2002;16:159-97.

21. Buchler P, Reber HA, Buchler MC, et al. Therapy for pancreatic cancer with a recombinant humanized anti-HER2 antibody (herceptin). J Gastrointest Surg 2001;5:139-46.

22. Xiong HQ, Abbruzzese JL. Epidermal growth factor receptor-targeted therapy for pancreatic cancer. Semin Oncol 2002;29:31-7.

23. Buchsbaum DJ, Bonner JA, Grizzle WE, et al. Treatment of pancreatic cancer xenografts with Erbitux (IMC-C225) anti-EGFR antibody, gemcitabine, and radiation. Int J Radiat Oncol Biol Phys 2002;54:1180-93.

24. Rosenblum MG, Cheung L, Mujoo K, Murray JL. An antimelanoma immunotoxin containing recombinant human tumor necrosis factor: tissue disposition, pharmacokinetic, and therapeutic studies in xenograft models. Cancer Immunol Immunother 1995;40:322-28.

25. Rosenblum MG, Cheung L, Murray JL, Bartholomew R. Antibody-mediated delivery of tumor necrosis factor (TNF-alpha): improvement of cytotoxicity and reduction of cellular resistance. Cancer Commun 1991;3:21-7.

26. Rosenblum MG, Horn SA, Cheung LH. A novel recombinant fusion toxin targeting HER-2/NEU-over-expressing cells and containing human tumor necrosis factor. Int J Cancer 2000;88:267-73.

27. Chou TC, Talalay P. Quantitative analysis of dose-effect relationships: the combined effects of multiple drugs or enzyme inhibitors. Adv Enyme Regul 1984;22:27-55.

28. Wuchter C, Karawajew L, Ruppert V, et al. Clinical significance of CD95, Bcl-2 and Bax expression and CD95 function in adult de novo acute myeloid leukemia in context of P-glycoprotein function, maturation stage, and cytogenetics. Leukemia 1999:13:1943-1953.

29. Lohrisch C, Piccart M. An overview of HER2. Semin Oncol 2001;28:3-11.

30. Yarden Y. Biology of HER2 and its importance in breast cancer. Oncology 2001;61(2):1-13.

31. Rubin I, Yarden Y. The basic biology of HER2. Ann Oncol 2001;12(1 1):S3-S8.

32. Hynes NE, Stern DF. The biology of erbB-2/neu/HER-2 and its role in cancer. Biochim Biophys Acta 1994;1198:165-184.

33. Singleton TP, Strickler JG. Clinical and pathologic significance of the c-erbB-2 (HER-2/neu) oncogene. Pathol Annu 1992;27:165-90.

34. Stancovski I, Sela M, Yarden Y. Molecular and clinical aspects of the Neu/ErbB-2 receptor tyrosine kinase. Cancer Treat Res 1994;71:161-91.

35. Torre EA, Salimbeni V, Fulco RA. The erbB 2 oncogene and chemotherapy: a mini-review. J Chemother 1997;9:51-5.

36. Safran H, Steinhoff M, Mangray S, et al. Overexpression of the HER-2/neu oncogene in pancreatic adenocarcinoma. Am J Clin Oncol 2001;24:496-99.

37. Thybusch-Bernhardt A, Aigner A, Beckmann S, Czubayko F, Juhl H. Ribozyme targeting of HER-2 inhibits pancreatic cancer cell growth in vivo. Eur J Cancer 2001;37:1688-94.

38. Aigner A, Hsieh SS, Malerczyk C, Czubayko F. Reversal of HER-2 over-expression renders human ovarian cancer cells highly resistant to taxol. Toxicology 2000;144:221-28.

39. Suzuki T, Anderegg B, Ohkawa T, et al. Adenovirus-mediated ribozyme targeting of HER-2/neu inhibits in vivo growth of breast cancer cells. Gene Ther 2000;7: 241-48.

40. Waldmann TA, Levy R, Coller BS. Emerging Therapies: Spectrum of Applications of Monoclonal Antibody Therapy. Hematology (Am Soc Hematol Educ Program) 2000;394-408.

41. Buchler P, Reber HA, Buchler MC, et al. Therapy for pancreatic cancer with a recombinant humanized anti-HER2 antibody (herceptin). J Gastrointest Surg 2001;5:139-46.

42. Butera J, Malachovsky M, Rathore R, Safran H. Novel approaches in development for the treatment of pancreatic cancer. Front Biosci 1998;3:E226-E229.

43. Pegram MD, Lopez A, Konecny G, Slamon DJ. Trastuzumab and chemotherapeutics: drug interactions and synergies. Semin Oncol 2000;27: 21-5.

44. Knuefermann C, Lu Y, Liu B, et al. HER2/PI-3K/Akt activation leads to a multidrug resistance in human breast adenocarcinoma cells. Oncogene 2003;22:3205-12.

45. Sasaki M, Kumazaki T, Tanimoto K, Nishiyama M. Bcl-2 in cancer and normal tissue cells as a predication marker of response to 5-fluorouracil. 2003;22:181-86.

46. Nagata S. Apoptosis by death factor. Cell 1997;88:355-65.

47. Medema JP, Scaffidi C, Kischkel FC, et al. FLICE is activated by association with the CD95 death-inducing signaling complex (DISC). EMBO J 1997;16:2794-804.

48. Ueno NT, Bartholomeusz C, Herrmann JL, et al. E1A-mediated paclitaxel sensitization in HER-2/neu-overexpressing ovarian cancer SKOV3.ip1 through apoptosis involving the caspase-3 pathway. Clin Cancer Res 2000;6:250-59.

49. Keppler-Hafkemeyer A, Brinkmann U, Pastan I. Role of caspases in immunotoxin-induced apoptosis of cancer cells. Biochemistry 1998;37:16934-942.

TABLE 1. IC_{50} OF VARIOUS AGENTS AGAINST FOUR HUMAN PANCREATIC CANCER CELL LINES

	IC_{50} (μM)			
Drug	AsPc-1	Capan-1	Capan-2	L3.6pl
5-Fluorouracil (5-FU)	7.5	6	300	1
Cisplatin (CIS)	14	4.5	50	3.6
Etoposide (ETO)	28	2	40	2
Doxorubicin (DOX)	0.32	0.06	0.5	0.03
Gemcitabine (GEM)	0.2	0.02	0.15	0.006
scFv23/TNF	0.5	0.7	0.4	0.15
TNF	>1.6*	>1.6*	>1.6*	>1.6*

* Highest concentration achieved.

The IC_{50} values were determined after 72 hr of exposure to the drugs and were defined as the concentration causing 50% growth inhibition in treated cells compared to control cells.

TABLE 2. ANALYSIS OF CYTOTOXICITY INDUCED BY scFV23/TNF IN COMBINATION WITH OTHER CHEMOTHERAPEUTIC AGENTS

Treatment	Combination Index (CI)			
	AsPc-1	Capan-1	Capan-2	L3.6pl
5-FU + scFv23/TNF	0.632 ± 0.015	0.611 ± 0.027	0.548 ± 0.026	0.366 ± 0.016
CIS + scFv23/TNF	2.250 ± 0.095	0.566 ± 0.028	1.532 ± 0.118	4.667 ± 0.247
ETO + scFv23/TNF	0.498 ± 0.023	0.869 ± 0.017	0.664 ± 0.019	1.640 ± 0.067
DOX + scFv23/TNF	1.805 ± 0.061	1.203 ± 0.000	2.084 ± 0.140	3.578 ± 0.172
GEM + scFv23/TNF	2.375 ± 0.114	1.250 ± 0.054	0.703 ± 0.027	2.833 ± 0.252

To analyze the cellular interaction between the 2 agents, for tested combination of the 2 agents combination index (CI) values were calculated as proposed by Chou[27]: $CI = (D)_1/(Dx)_1 + (D)_2/(Dx)_2+\alpha D_1D_2/(Dx)_1(Dx)_2$. Where $(D)_1$ and $(D)_2$ in combination kill X% of cells, and $(Dx)_1$ and $(Dx)_2$ are the estimated dose of the drug alone capable of producing the same effect of the combined drugs. α=1 or 0 depending on whether the drugs are assumed to be mutually nonexclusive or mutually exclusive, respectively, in their action. If CI near to 1 indicates additive effect, CI>1 indicates antagonism, CI<1 indicates synergism.

Figure Legends

FIGURE 1. Expression Pattern of HER-2/neu, TNF-R1, and TNF-R2 in Four Human Pancreatic Cell Lines. Four pancreatic cancer cell lines (AsPc-1, Capan-1, Capan-2, and L3.6pl) were seeded at 5 x 10^5 cells/ϕ60 mm petri-dish and incubated for 24 hr after which cell lysates were collected. Whole cell lysates (50 μg) were analyzed by SDS-PAGE and immunoblotting with anti-HER-2/neu, TNF receptor-1, and TNF receptor-2 antibodies, followed by incubation with an anti-mouse or anti-rabbit horseradish peroxidase-labeled antibody and chemiluminescent detection. Actin was used as a loading control for protein loading. Data are presented as the relative density of protein bands normalized to β-actin. The intensity of the bands was quantified using Histogram.

FIGURE 2. Dose-Response Curves of various agents. AsPc-1 (*a*), Capan-1 (*b*), Capan-2 (*c*), and L3.6pl (*d*). Cells were treated with different drugs for 72 hr and then assessed growth inhibition by crystal violet staining. Values are means ± SD from at least four independent exposures.

FIGURE 3. Effects of combination treatment on the expression of phospho-Akt. L3.6pl cells were treated with IC_{25} of 5-FU, scFv23 or scFv23/TNF plus 5-FU combination for 48 hr. For combination studies, scFv23/TNF and 5-FU were combined at their individual IC_{25} concentrations. After treatment, cell lysates (50 μg) were analyzed by SDS-PAGE and immunoblotting with anti-Akt and phospho-Akt antibodies, followed by incubation with an anti-rabbit horseradish peroxidase-labeled antibody and chemiluminescent detection. Actin was used as a loading control. Data are presented as the relative density of protein bands normalized to β-actin. The intensity of the bands was quantified using Histogram.

FIGURE 4. Effects of combination treatment on the expression of Bcl-2. L3.6pl cells were treated with IC_{25} of 5-FU, scFv23, and 5-FU plus scFv23/TNF combination for 48 hr. For combination studies, scFv23/TNF and 5-FU were combined at their individual IC_{25} concentrations. After treatment, cell lysates (50 μg) were analyzed by SDS-PAGE and immunoblotting with anti-Bcl-2 antibody, followed by incubation with an anti-rabbit horseradish peroxidase-labeled antibody and chemiluminescent detection. Actin was used as a loading control. Data are presented as the relative density of protein bands normalized to β-actin. The intensity of the bands was quantified using Histogram.

FIGURE 5. Effects of combination treatment on the apoptosis in L3.6pl cells. L3.6pl exposed to IC_{25} of 5-FU, scFv23/TNF, or combination for 48 hr. After treatment, the cells were washed with PBS, permeabilized in permeabilization solution (0.1% Triton X-100, 0.1% sodium citrate), and then fixed in 4% paraformaldehyde. Fixed cells were stained with *in situ* cell death detection kit (Roche). Cells undergoing apoptosis were determined by fluorescence microscope (x 400).

FIGURE 6. Effects of combination treatment on the activation of caspase-8, caspase-3, and PARP cleavage. L3.6pl cells were treated with IC_{25} of 5-FU, scFv23/TNF or combination for 48 hr. For combination studies, scFv23/TNF and 5-FU were combined at their individual IC_{25} concentrations. After treatment, cell lysates (50 μg) were analyzed by SDS-PAGE and immunoblotting with anti-caspase-8, caspase-3, and PARP antibodies, followed by incubation with an anti-mouse horseradish peroxidase-labeled antibody and chemiluminescent detection. Actin was used as a loading control.

FIGURE 7. Influence of caspase inhibitors on the viability of 5-FU+ scFv23/TNF-treated L3.6pl cells. L3.6pl cells pre-treated with or without 200 μM general caspase inhibitor (Z-VAD-FMK), caspase-8 inhibitor (Z-IETD-FMK), or caspase-3 inhibitor (Z-DEVD-FMK) (R&D) for 2 hr and then treated with their individual IC_{25} concentrations. After 72 hr of exposure, viability was determined using an XTT assay.

Figure 1 Mi-Ae Lyu

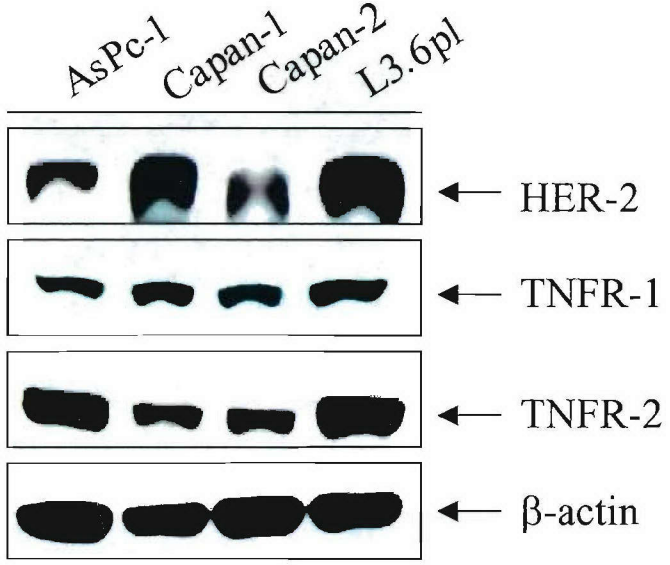

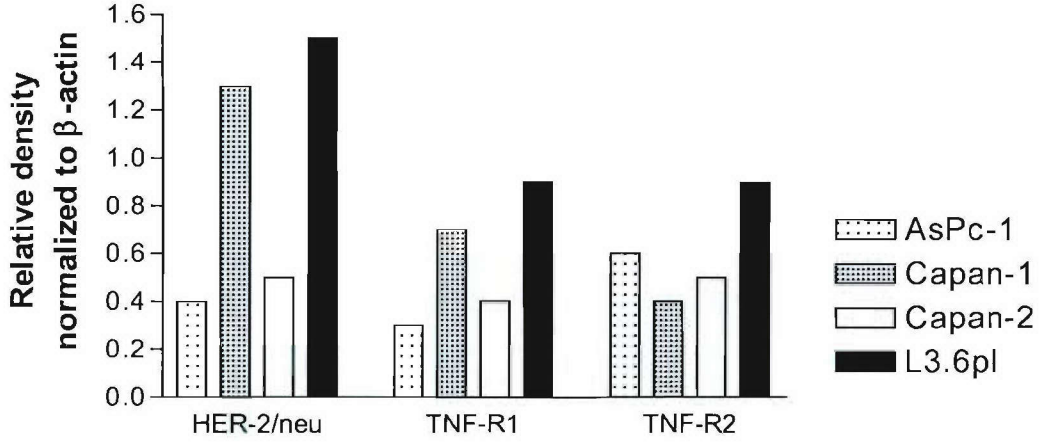

Figure 2A and 2B Mi-Ae Lyu

A

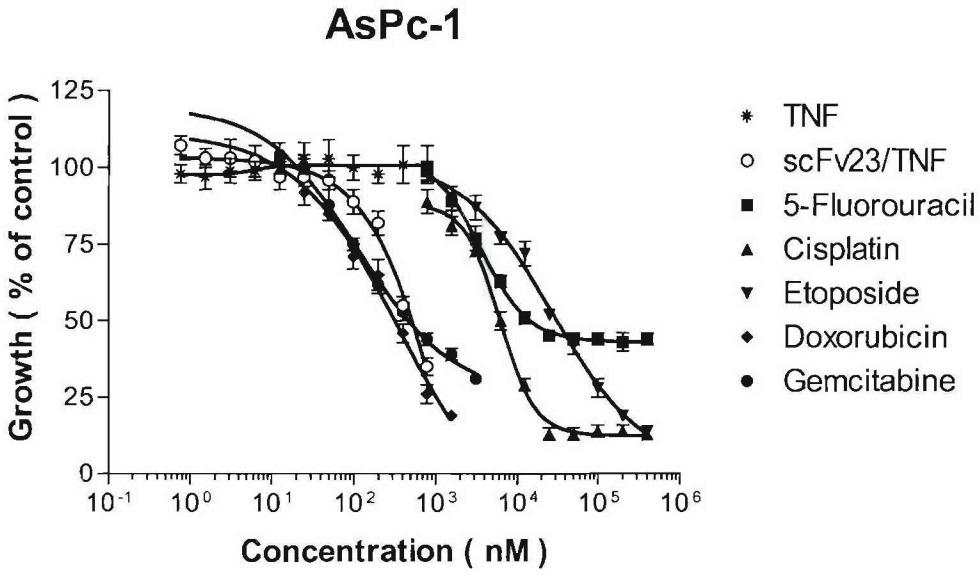

B

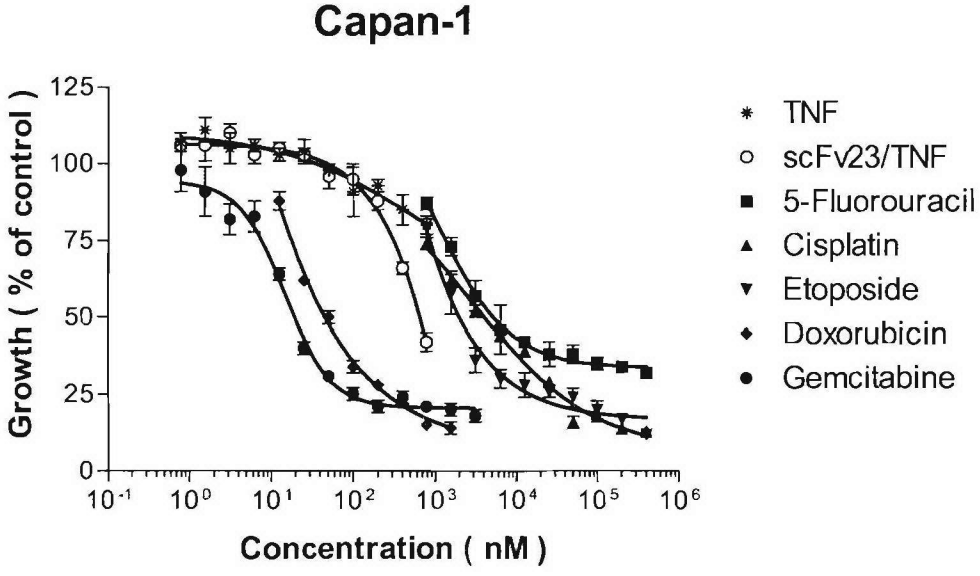

Figure 2C and 2D Mi-Ae Lyu

C

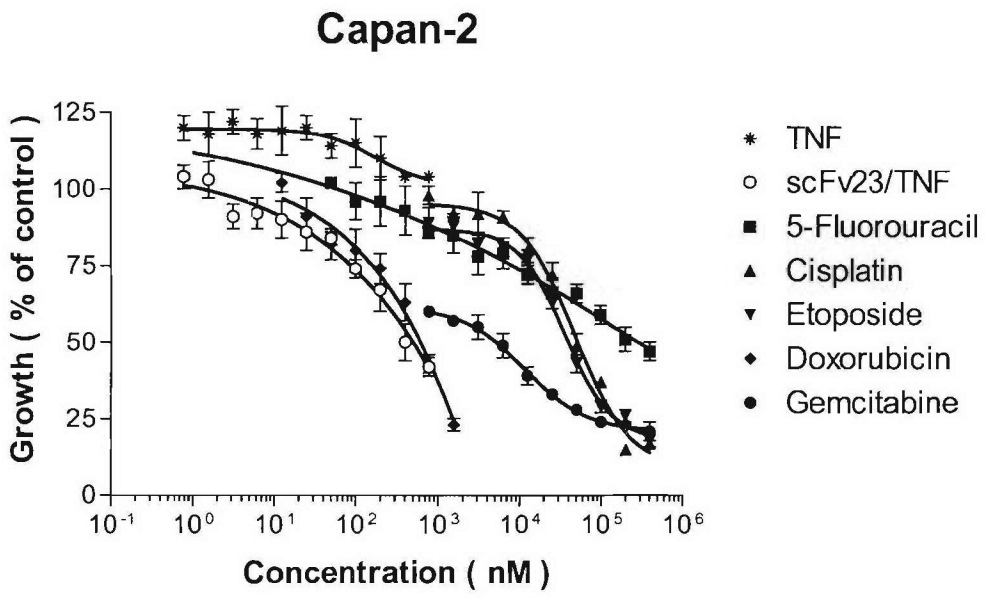

D

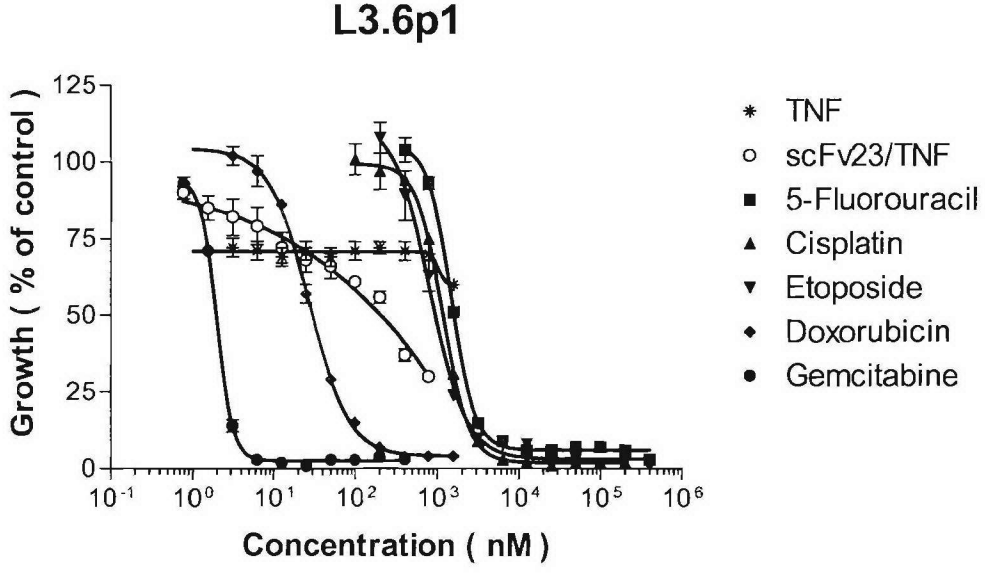

Figure 3 Mi-Ae Lyu

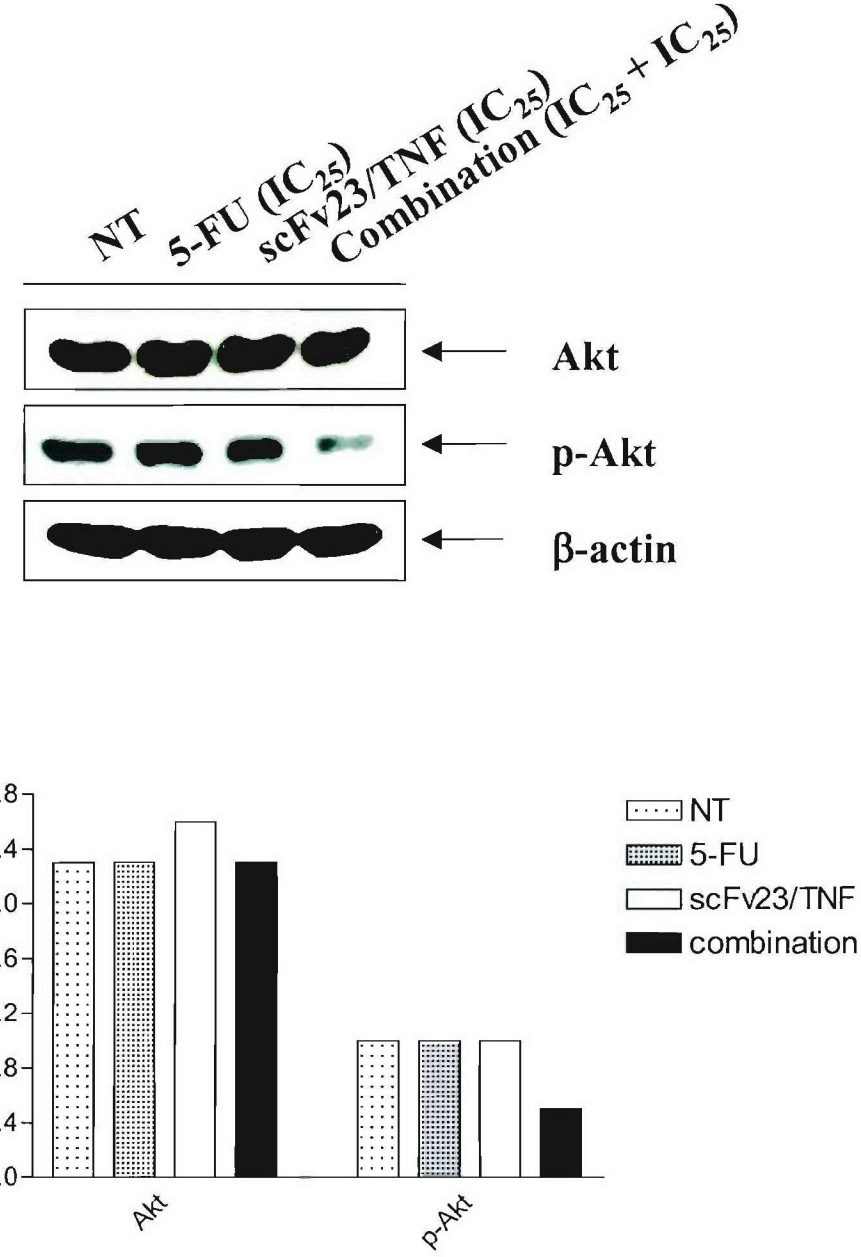

Figure 4 Mi-Ae Lyu

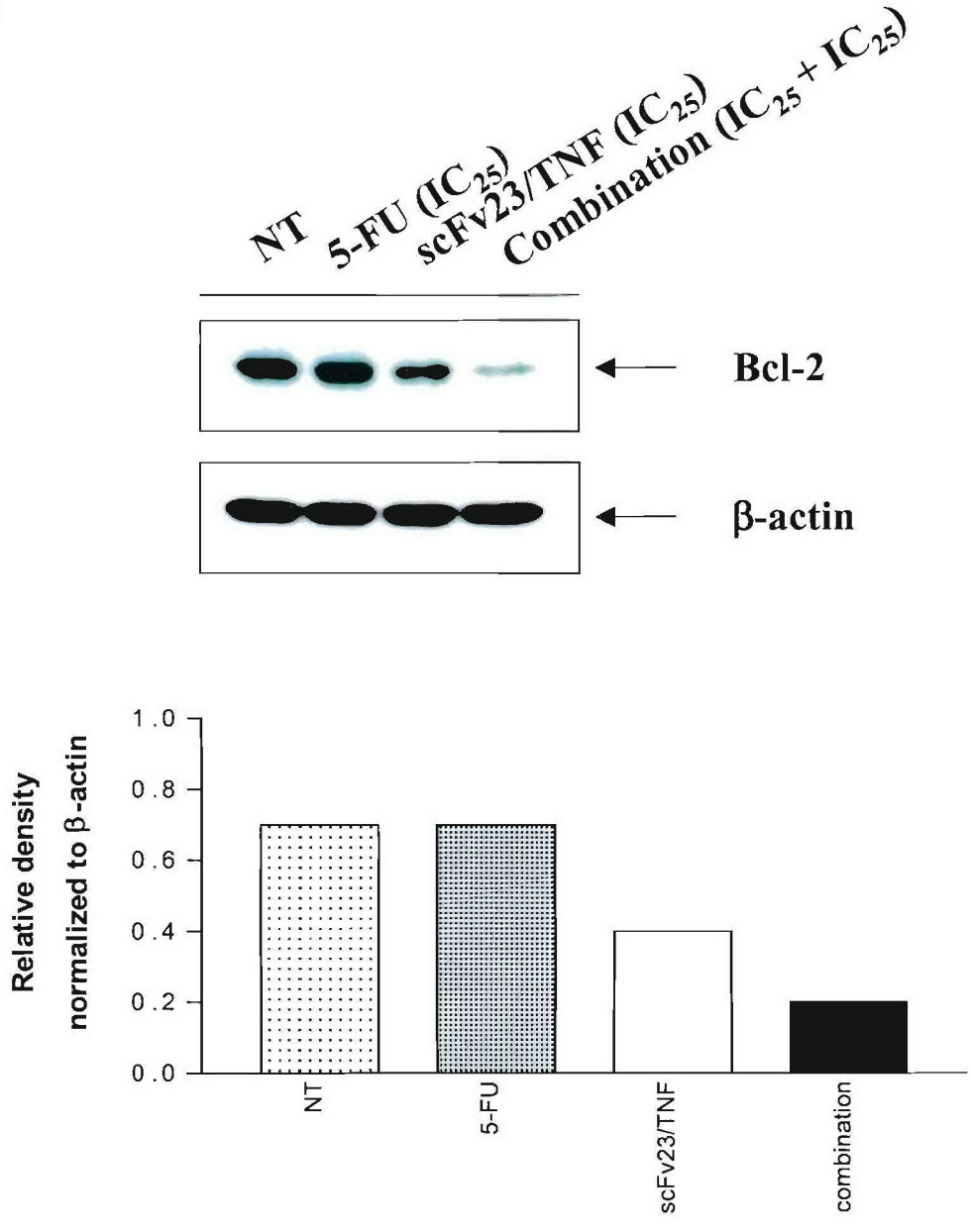

Figure 5 Mi-Ae Lyu

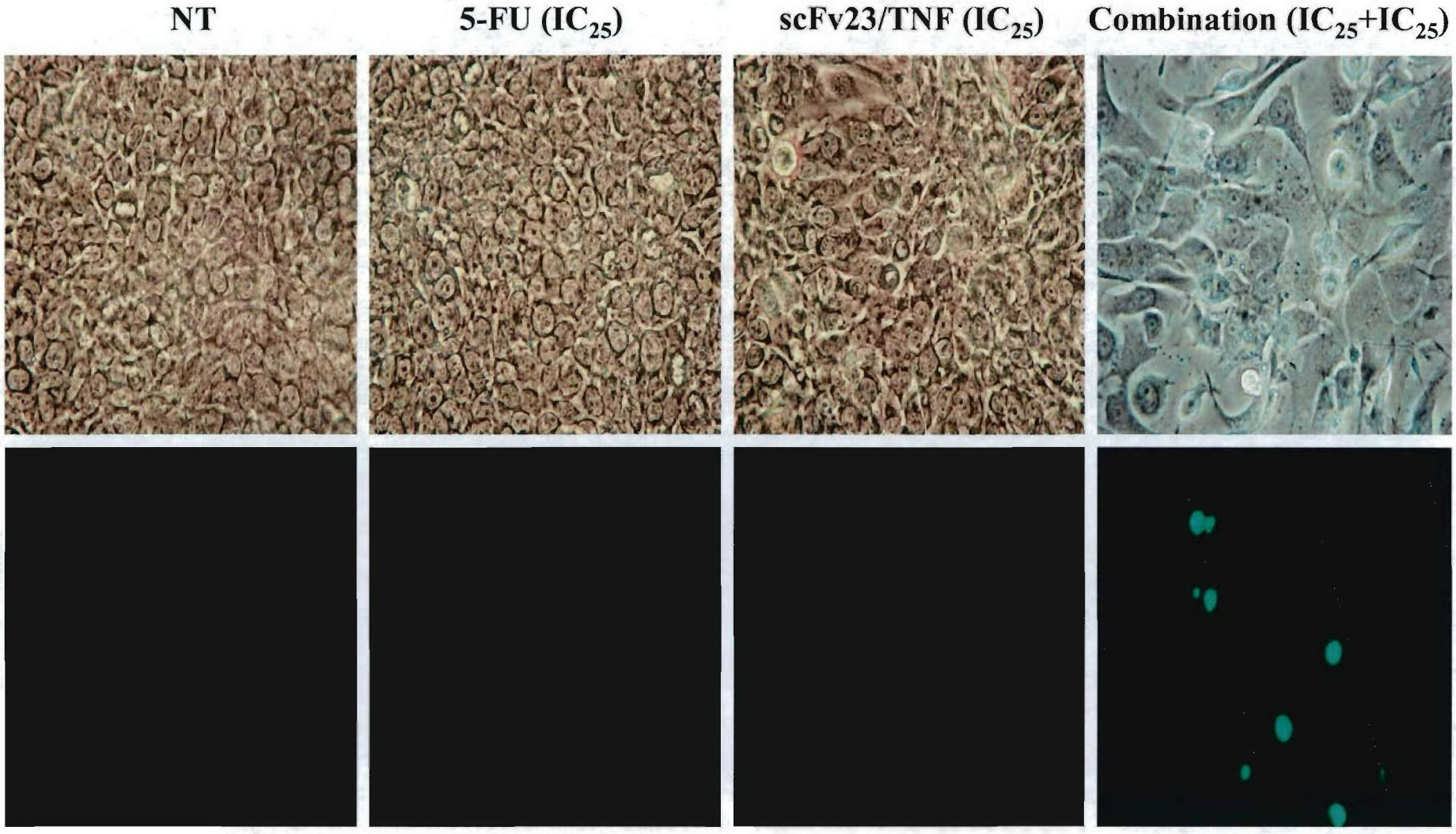

(x 400)

Figure 6 Mi-Ae Lyu

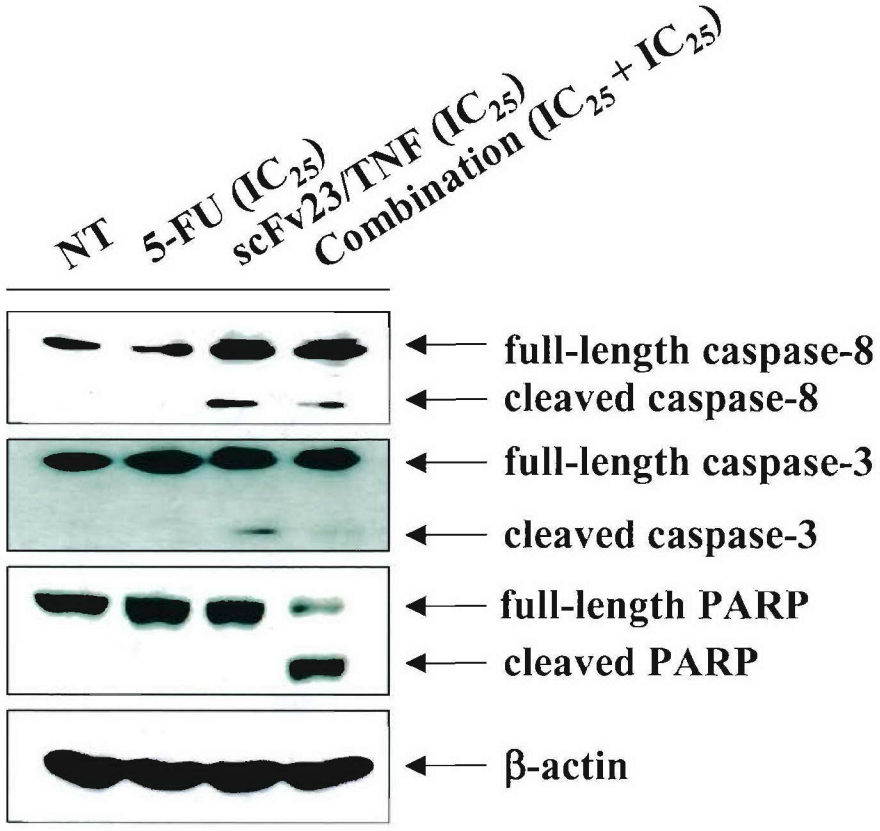

Figure 7 Mi-Ae Lyu

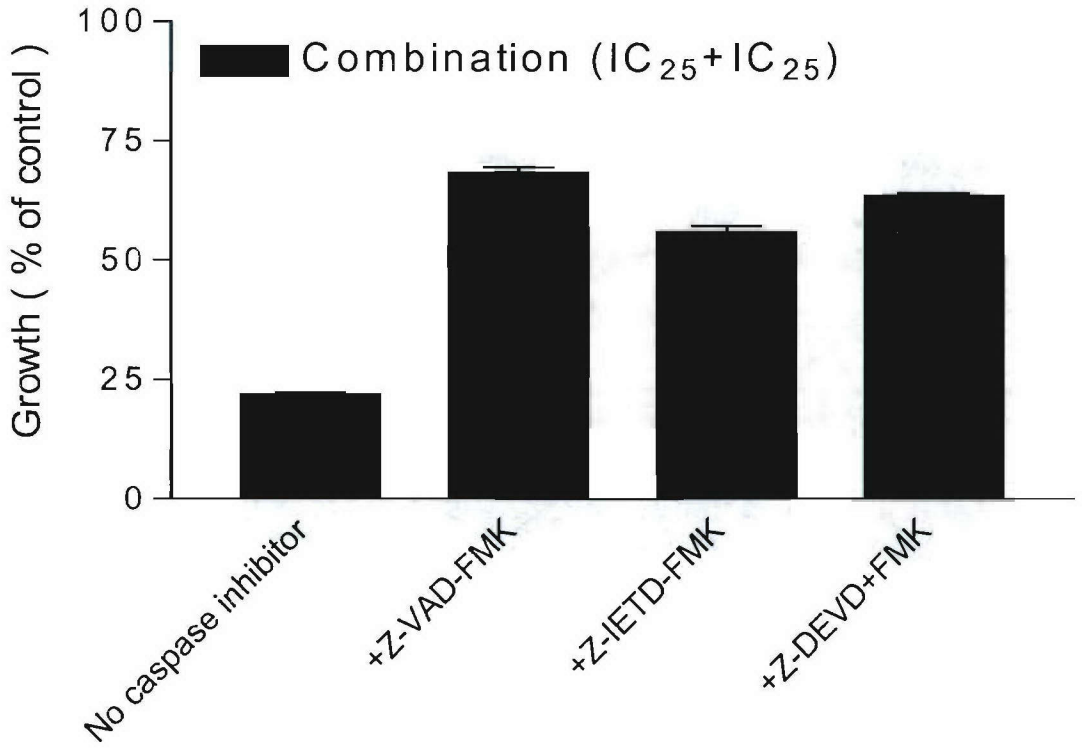

Manuscript Submitted to JOurnal of Biological Chemistry

$VEGF_{121}$/rGel Fusion Toxin Targets the KDR Receptor to Inhibit Vascular Endothelial Growth *In Vitro* and *In Vivo*: Specific Effects Assessed Using Microarray Analysis*

Khalid A. Mohamedali[‡], Candelaria Gomez-Manzano[§], Latha Ramdas[¶], Jing Xu[§], Lawrence Cheung[‡], Wei Zhang[#], Philip Thorpe[‖] and Michael G. Rosenblum[‡]**

Running Title: Inhibition of Angiogenesis by $VEGF_{121}$/rGel

** To whom correspondence should be addressed: Department of Bioimmunotherapy, Unit 44, The University of Texas M. D. Anderson Cancer Center, 1515 Holcombe Blvd., Houston, Texas 77030. Tel: 713-792-3554; Fax: 713-794-4261 or 713-745-3916; E-mail: mrosenbl@mdanderson.org.

From the Departments of [‡]Bioimmunotherapy, [§]Neuro-Oncology, ¶Experimental Radiation Oncology, and [#]Pathology, The University of Texas M. D. Anderson Cancer Center, Houston, Texas 77030, and [‖]Department of Pharmacology, Simmons Comprehensive Cancer Center, The University of Texas Southwestern Medical Center, Dallas, Texas 75390

Key Words: Fusion toxin, VEGF, gelonin, vascular targeting, angiogenesis, microarray

* This research was conducted, in part, by the Clayton Foundation for Research and supported by DAMD grant 17-02-1-0457. Work done at the Cancer Genomics Core Lab was supported by the Tobacco Settlement Funds appropriated by the Texas State Legislature, by a generous donation from the Michael and Betty Kadoorie Foundation, by a grant from the Goodwin Fund, and by Cancer Center Core Grant P30 CA016672 28 from the National Cancer Institute.

SUMMARY

$VEGF_{121}$/rGel, a fusion protein composed of the growth factor $VEGF_{121}$ and the recombinant toxin gelonin targets the tumor neovasculature and exerts impressive cytotoxic effects on cells by inhibiting cellular protein synthesis. We assessed the effects of $VEGF_{121}$/rGel on angiogenesis in vitro and in vivo. 1 nM $VEGF_{121}$/rGel was sufficient to inhibit tube formation by over 50% of endothelial cells overexpressing VEGFR-2 on Matrigel-coated plates. In contrast, endothelial cells overexpressing VEGFR-1 were relatively insensitive to $VEGF_{121}$/rGel, requiring 100 nM to inhibit tube formation by over 50%. In vascularization studies using chicken chorioallantoic membranes, 1 nM $VEGF_{121}$/rGel completely inhibited bFGF-stimulated neovascular growth. Treatment with $VEGF_{121}$/rGel decreased the number of newly-sprouting vessels but did not affect mature vessels. Treatment with gelonin alone at equivalent concentrations had no effect. Examination by microarray analysis of $VEGF_{121}$/rGel-induced cytotoxicity against HUVECs revealed that 22 genes were upregulated by $VEGF_{121}$/rGel treatment, including genes involved in the control of cell adhesion, apoptosis, transcription regulation, chemotaxis, and inflammatory response. RT-PCR of selected genes, including E-selectin, cytokine A2, NF-κB inhibitor alpha and tumor necrosis factor alpha-induced protein 3, confirmed their upregulation. Our data suggest that $VEGF_{121}$/rGel induces the expression of a unique "fingerprint" profile of genes that mediate the cytotoxic effects of this construct on tumor vascular endothelial cells. The cytotoxic effects of $VEGF_{121}$/rGel appear to be necrotic rather than apoptotic since no TUNEL staining or alterations in the protein levels of the apoptotic markers Bax, Bcl-XL, or caspase-3 were observed. Together, these data represent the first analysis of genes governing intoxication of mammalian cells by a toxin-based targeted therapeutic agent. These data also confirm the selectivity of the fusion construct for KDR-

overexpressing endothelial cells and support the use of this molecule in understanding the role of VEGFR-2 expression in the development of toxic effects of VEGF-containing fusion toxin constructs.

INTRODUCTION

Angiogenesis has emerged as a critical process in numerous diseases and intervention in neovascularization may have therapeutic value in diabetic retinopathy (1-4), arthritis (5-8) and in tumor maturation and metastatic spread (9-12). Indeed, because tumor neovascularization provides an available target for therapeutic intervention, numerous groups have focused drug development strategies on the elements of this process. Inhibitors of various growth factor receptor tyrosine kinases (13-15), blocking antibodies that interfere with receptor signal transduction (16-19) and strategies that trap growth factor ligands (20-22) have all been used with varying degrees of success in preclinical and clinical studies.

Although tumor neovascularization is increasingly being revealed as highly complex as factors that can play a role in driving critical events continue to be identified, vascular endothelial growth factor-A (VEGF-A)[1] and its receptors, Flt-1 and KDR, are exceptionally important in many aspects of neovascularization (15;23-25) . Therefore, numerous laboratories have developed recombinant growth factor fusion constructs of VEGF-A and various toxins (26-30) to target cells bearing receptors of VEGF-A. We described a novel fusion toxin composed of the 121-amino-acid splice variant of VEGF-A (designated $VEGF_{121}$) and containing the highly potent recombinant toxin gelonin (rGel) (31). Recent studies in our laboratory have demonstrated that this construct is highly cytotoxic at nanomolar concentrations to both log-phase and confluent endothelial cells that overexpress the KDR receptor and not specifically cytotoxic to cells that overexpress the Flt-1 receptor (31). In addition, tumor xenograft studies demonstrate impressive tumor growth-inhibitory effects of the fusion construct when administered systemically against established melanoma and prostate tumors. In ongoing studies in our

laboratory, we are examining the effects of $VEGF_{121}$/rGel on numerous other orthotopic and metastatic models.

Although toxin-based therapeutic agents have been studied for many years, the exact molecular mechanisms within the target cell that occur as part of the cytotoxic effect have never been clearly identified. Therefore, we sought to quantify the ability of $VEGF_{121}$/rGel to inhibit tube formation in vitro and basic fibroblast growth factor (bFGF)-mediated angiogenesis in vivo and intracellular effects of this agent on cells in culture using microarray technology to delineate molecular mechanisms that uniquely define the effects of this agent at the genetic level.

EXPERIMENTAL PROCEDURES

Materials-- Bacterial strains, pET bacterial expression plasmids and recombinant enterokinase were obtained from Novagen (Madison, WI). All other chemicals were obtained from Sigma Chemical Company (St. Louis, MO) or Fisher Scientific (Pittsburgh, PA). bFGF was purchased from R&D Systems (Minneapolis, MN). TALON metal affinity resin was obtained from Clontech Laboratories (Palo Alto, CA). Other chromatography resin and materials were from Pharmacia Biotech (Piscataway, NJ). Tissue culture reagents were from Invitrogen (Carlsbad, CA) or Mediatech Cellgro (Herndon, VA). Rabbit anti-gelonin antiserum was obtained from the Veterinary Medicine Core Facility at The University of Texas M. D. Anderson Cancer Center. Antibodies against the following proteins were purchased from Santa Cruz Biotechnology, Inc. (Santa Cruz, CA) (catalog numbers are given in parentheses): KDR (sc-504), phosphorylated KDR (p-KDR) (sc-16628-R), Bcl-2 (sc-7382), Bcl-XL (sc-7195), Bax (sc-493), cytochrome C (sc-8385), caspase-3 (sc-7148), caspase-6 (sc-1230), E-selectin (14011), actin (sc-1616), MKP-1 (sc-1199), and ERK2 (sc-1647).

Cell Culture-- Porcine aortic endothelial (PAE) cells transfected with the KDR receptor (PAE/KDR) or the Flt-1 receptor (PAE/Flt-1) were a generous gift from Dr. Johannes Waltenberger. The KDR and Flt-1 receptor sites in these cell lines were previously determined (27;32). Both cell lines have been used as in vitro models of the tumor neovasculature (33-35). Cells were maintained as a monolayer in F12 nutrient medium (HAM) supplemented with 100 units/ml penicillin, 100 units/ml streptomycin, and 10% fetal bovine serum (FBS). Human umbilical vein endothelial cells (HUVECs) were maintained in EBM medium (Cambrex, East Rutherford, NJ). Cells were harvested by treatment with Versene (0.02% EDTA/PBS).

Purification of $VEGF_{121}$/rGel-- Construction and purification of $VEGF_{121}$/rGel was essentially as described (31). $VEGF_{121}$/rGel was concentrated and stored in sterile PBS at –20°C.

Cytoxicity of $VEGF_{121}$/rGel and rGel-- The quantification of the cytotoxicity of $VEGF_{121}$/rGel and rGel against log-phase PAE/KDR, PAE/Flt-1, and HUVECs was performed as follows. Log-phase cells (1×10^4 HUVECs, 1×10^3 PAE/KDR or PAE/Flt-1 cells) were plated in 96-well flat-bottom tissue culture plates and allowed to attach overnight. Purified $VEGF_{121}$/rGel and rGel were diluted in culture media and added to the wells in 5-fold serial dilutions. Cells were incubated for 72 h. The remaining adherent cells were stained with crystal violet (0.5% in 20% methanol) and solubilized with Sorenson's buffer (0.1 M sodium citrate, pH 4.2, in 50% ethanol). Absorbance was measured at 630 nm.

Effect of $VEGF_{121}$/rGel on Phosphorylation of KDR-- Whole cell extracts of HUVECs and PAE/KDR cells, either untreated or treated with $VEGF_{121}$/rGel for up to 48 h at their respective IC_{50} doses, were prepared. Cells were lysed in 50 mM Tris (pH 8.0), 0.1 mM EDTA, 1 mM DTT, 12.5 mM $MgCl_2$, 0.1 M KCl, 20% glycerol, 1% Triton-X100, 2 μg/ml leupeptin, 1.5 μg/ml aprotinin, and 1 mM PMSF. Twenty micrograms of cell lysate was run on a sodium dodecyl sulfate polyacrylamide gel electrophoresis (SDS-PAGE) gel and the protein transferred to a PVDF/Imobilon membrane (Millipore, Billerica, MA). The membrane was blocked with 5% bovine serum albumin SA followed by incubation for 1 h with the following primary antibodies: anti-KDR, anti-p-KDR, and actin. Appropriate secondary antibodies were used at a 1:2000 dilution for 1 h and detected using an ECL detection kit (Amersham Biosciences, Buckinghamshire, England).

Effect of $VEGF_{121}$/rGel on E-Selectin Protein Levels-- Whole cell extracts of HUVECs and PAE/KDR cells treated for up to 48 h with $VEGF_{121}$/rGel at their respective IC_{50} doses were analyzed for changes in levels of E-selectin. Whole cell extracts and western blots were prepared as detailed above.

Endothelial Cell Tube Formation Assay-- PAE/KDR and PAE/Flt-1 cells were grown to 80% confluence, detached using Versene, and plated at a concentration of 2×10^4 cells per well in a 96-well Matrigel-coated plate under reduced serum (2% FBS) conditions. Cells were treated with 100 nM, 10 nM, 1 nM, 0.1 nM, or 0.01 nM $VEGF_{121}$/rGel or rGel, in triplicate, for 24 h. Inhibition of tube formation was assessed by counting the number of tubes formed per well under bright field microscopy. The ability of $VEGF_{121}$/rGel to inhibit tube formation as a function of incubation time before plating on Matrigel was studied by incubating PAE/KDR cells at the IC_{50} dose (1 nM) for different periods up to 24 h. Cells were detached and plated in 96-well Matrigel-coated plates under the conditions described above and the tubes in each well were counted.

Angiogenesis Assessment in Chicken Chorioallantoic Membranes (CAMs)-- Fertilized chicken eggs (SPAFAS; Charles River Laboratories, Wilmington, MA) were incubated at 37°C at 55% humidity for 9 days. An artificial air sac was created over a region containing small blood vessels in the CAM as described (36). A small "window" was cut in the shell after removal of 3 ml of albumen. Filter disks measuring 6 mm in diameter were coated with cortisone acetate in absolute ethanol (3 mg/ml). Each CAM was locally treated with filter disks saturated with a

solution containing bFGF (50 ng/disk) and $VEGF_{121}$/rGel (1 or 10 nM), rGel (1 or 10 nM), or buffer (PBS). The filter was placed on the CAM in a region with the lowest density of blood vessels and, as a reference, in the vicinity of a large vessel. Angiogenesis was documented photographically 3 days after treatment; images were captured using an Olympus stereomicroscope (SZ x12) and Spot Basic software (Diagnostic Instruments, Inc.). The relative vascular density was determined by measuring the area occupiedby blood vessels (37). This analysis was performed on a Macintosh computer using the public domain NIH Image program (developed at the U.S. National Institutes of Health and available on the Internet at http://rsb.info.nih.gov/nih-image/). The numbers of blood vessel branch points were quantified by two researchers (C.G-M. and J.X) and compared with the numbers in the treatment controls (36).

RNA extraction-- HUVECs and PAE/KDR cells were treated with their respective IC_{50} $VEGF_{121}$/rGel doses for various periods up to 48 h. Control cells were treated with PBS. Total RNA was extracted using the RNeasy mini-kit (Qiagen, Valencia, CA) and its integrity verified by electrophoresis on a denaturing formaldehyde-agarose gel and on a 2100 Bioanalyzer (Agilent, Foster City, CA).

Gene expression analysis-- HUVEC RNA was amplified using protocol previously described (38). The test and control samples (HUVECs treated with $VEGF_{121}$/rGel or saline, respectively, for 24 h) were labeled using Cy3- and Cy5-dCTP in the reverse transcription reaction. Duplicate experiments were conducted by dye swapping. The labeled samples were hybridized to a cDNA array of 2304 sequence-verified clones in duplicate printed by the Cancer Genomics Core

Laboratory of the Department of Pathology at M. D. Anderson Cancer Center. The array included 4800 genes involved in signal transduction, stress response, cell cycle control, hypoxia, and metastatic spread. Hybridization was performed overnight at 60°C in a humid incubator. After washing, the hybridized slides were scanned using a GeneTAC LS IV laser scanner (Genomic Solutions, Ann Arbor, MI) and the signal intensities were quantified with ArrayVision (Imaging Research Inc., St. Catherines, Ontario, Canada). The local background-subtracted spot intensities were used for further analysis, which was performed by the M. D. Anderson in-house program for microarray analysis (39). Differentially expressed genes were identified on the basis of a cutoff value of the *T* value. Generally, a cutoff value of |3| is considered statistically significant.

The dye swapping experiments were designed to limit dye bias, which raises concern in microarray experiments. The two factors addressed by this design are the differences in dye incorporation and the gene-specific effects of the dye. Normalization of the data typically corrects for differences in incorporation of the dye that affects all the genes. Dye-specific effects can be insignificant compared with other sources of variation in the experiment (40). Hence, the dye swapping experiments were treated as duplicates. The signal-to-noise ratio of the images was evaluated to determine the quality of the array. Only those spots with a signal-to-noise ratio of $\geq$2 were evaluated (80%). Genes that showed values greater than |2| in at least 3 of 4 arrays were identified, and the average fold change was determined.

RT-PCR Correlative Analysis-- Microarray data were verified by performing RT-PCR analysis on the genes that showed the highest level of induction, namely E-selectin (SELE), cytokine A2 (SCYA2, MCP-1), tumor necrosis factor alpha induced protein 3 (TNFAIP3) and NF-κB

inhibitor alpha (NF-κBIα). Primers were designed on the basis of the accession numbers from the microarray and confirmation of homology using BLAST (NCBI). Induction of E-selectin in PAE/KDR cells was also verified by RT-PCR. GAPDH primers were used as controls. The primers were as follows: SELE forward - 5'GGTTTGGTGAGGTGTGCTC; SELE reverse - 5' TGATCTTTCCCGGAACTGC; SCYA2 forward - 5' TCTGTGCCTGCTGCTCATAG; SCYA2 reverse - 5' TGGAATCCTGAACCCACTTC; TNFAIP3 forward - 5' ATGCACCGATACACACTGGA; TNFAIP3 reverse - 5' CGCCTTCCTCAGTACCAAGT; NF-κBIα forward - 5' AACCTGCAGCAGACTCCACT; NF-κBIα reverse - 5' GACACGTGTGGCCATTGTAG; porcine E-selectin (PORESEL) forward - 5' GCCAACGTGTAAAGCTGTGA; PORESEL reverse - 5' TCCTCACAGCTGAAGGCACA; GAPDH forward - 5' GTCTTCACCACCATGGAG; and GAPDH reverse - 5' CCACCCTGTTGCTGTAGC. Isolated RNA was subjected to first-strand cDNA synthesis as described by the manufacturer of the Superscript First Strand synthesis system (Invitrogen, Carlsbad, CA). RT-PCR was performed using a Minicycler PCR machine (MJ Research, Inc., San Francisco, CA).

Effect of $VEGF_{121}$/rGel on Apoptotic Markers-- Whole cell extracts of HUVEs and PAE/KDR cells treated for 24 h with $VEGF_{121}$/rGel at their respective IC_{50} doses were analyzed for changes in levels of the apoptotic markers caspase-3, caspase-6, cytochrome C, Bcl-XL, Bcl-2, and Bax. Whole cell extracts and western blots were prepared as detailed above.

TUNEL Assay—Log-phase PAE/KDR and PAE/Flt-1 cells were diluted to 2000 cells/100 μl. Aliquots (100 μl) were added in 16-well chamber slides (Nalge Nunc International, Rochester,

NY) and incubated overnight at 37°C with 5% CO_2. Purified $VEGF_{121}$/rGel was diluted in culture medium and added at 72-, 48-, and 24-h time points at a final concentration of 1 nM, which is twice the IC_{50} dose. The cells were then processed and analyzed for TUNEL as described by the manufacturer of the reagent. Positive control cells were incubated with 1 mg/ml DNAse for 10 min at 37°C.

RESULTS

$VEGF_{121}$/rGel Is Specifically Cytotoxic to Endothelial Cells that Overexpress KDR-- The cytotoxic effect of $VEGF_{121}$/rGel and rGel *in vitro* was examined employing both HUVECs and PAE cells transfected with either the human Flt-1 receptor (PAE/Flt-1) or the human KDR receptor (PAE/KDR). Each cell type expressed the KDR receptor at varying levels (27;32;41). Treatment of log-phase cells with $VEGF_{121}$/rGel for 72 h showed the greatest cytotoxic effect against PAE/KDR cells, with an IC_{50} of 1 nM (Fig. 1). In contrast, the IC_{50} of $VEGF_{121}$/rGel on HUVECs and PAE/Flt-1 cells was approximately 300 nM. The cytotoxic effects of the untargeted rGel were similar in all three cell lines ($IC_{50} \sim$ 150 nM).

$VEGF_{121}$/rGel Treatment Activates the KDR Receptor-- We previously showed that the cytotoxicity of $VEGF_{121}$/rGel is mediated via VEGFR-2 (KDR) and not VEGFR-1 (Flt-1) (31). However, we hypothesized that the VEGF component of $VEGF_{121}$/rGel could also stimulate cell growth through interaction with the receptors for VEGF. In the present study, we investigated this hypothesis by evaluating endogenous levels of p-KDR in endothelial cells that had been treated with $VEGF_{121}$/rGel. PAE/KDR cells expressed levels of p-KDR that increased within 2 h after $VEGF_{121}$/rGel treatment. The levels of p-KDR peaked at 4 h and gradually decreased to endogenous levels by 24 h posttreatment (Fig. 2). Endogenous levels of total KDR were also increased by 4 h and were reduced to pretreatment levels by 24 h (Fig. 2A). In contrast, endogenous levels of total KDR in HUVECs were decreased slightly at 24 h after treatment with $VEGF_{121}$/rGel, whereas p-KDR levels after 24 h were markedly upregulated compared with the

levels of untreated cells (Fig. 2B). Thus, the cytotoxic effect of the rGel component of $VEGF_{121}$/rGel does not interfere with the stimulatory effect of the VEGF component.

Cytotoxic Effects of $VEGF_{121}$/rGel on Endothelial Cells Are Not Mediated via Apoptotic Mechanisms-- To investigate the mechanisms of the cytotoxic effects of $VEGF_{121}$/rGel on endothelial cells, we performed a TUNEL assay on cells treated with the construct for 24, 48, and 72 h. As shown in Fig. 3, we found no TUNEL staining in PAE/KDR cells exposed to $VEGF_{121}$/rGel for periods of up to 72 h. In contrast, the nuclei of positive control cells showed intense staining. These findings clearly indicate that the mechanism of cytotoxicity of $VEGF_{121}$/rGel is necrotic rather than apoptotic. To confirm and validate these observations, we examined various key apoptotic signaling events using western blot analysis (Fig. 4). After HUVECs and PAE/KDR cells were treated with $VEGF_{121}$/rGel or saline for 24 h, their whole cell extracts were harvested and analyzed. Levels of the pro-apoptotic proteins cytochrome C and caspase-6, as well as the anti-apoptotic protein Bcl-2 were undetectable before or after treatment (data not shown). Levels of caspase-3 (full length pre-cursor), Bax (a pro-apoptotic protein), and Bcl-XL (an apoptosis inhibitor) were not affected by $VEGF_{121}$/rGel treatment. In addition, the p11 and p20 subunits of activated/cleaved caspase-3 were not detected after treatment with the fusion construct.

Microarray Analysis of HUVECs Treated with $VEGF_{121}$/rGel-- To further elucidate the biochemical mechanisms that govern the effects of $VEGF_{121}$/rGel on endothelial cells, we treated HUVECs with saline or the IC_{50} dose of $VEGF_{121}$/rGel for 24 h. RNA was isolated, evaluated for integrity, and subjected to microarray analysis and a dye-swap comparison was performed for

reproducibility. Only those differentially expressed genes whose levels were elevated to at least 2 times the baseline value in repeated experiments were selected. On this basis, 22 genes (out of the 4800 in the microarray) were upregulated by $VEGF_{121}$/rGel at 24 h (Table I). In addition to upregulating select genes known to be induced by VEGF alone, treatment with $VEGF_{121}$/rGel upregulated genes involved in inflammation, chemotaxis and transcription regulation. The genes with the highest levels of expression from four gene classifications were validated by RT-PCR analysis. When normalized for GAPDH, all four of the other PCR products were increased after treatment with $VEGF_{121}$/rGel, thus validating the results observed in the original microarray (Fig. 5A). However, the induction of E-selectin protein levels did not match the induction of mRNA (Fig. 5B).

Because PAE/KDR cells have been used as *in vitro* models for endothelial cells in the tumor neovasculature, we investigated the effect of $VEGF_{121}$/rGel on gene induction and protein expression in these cells. PAE/KDR cells were treated with saline or the IC_{50} dose of $VEGF_{121}$/rGel for up to 48 h. As shown in Fig. 6A, PCR analysis for E-selectin confirmed the increase in message within 2 h after treatment of cells with $VEGF_{121}$/rGel. In addition, western blot analysis demonstrated a slight increase in E-selectin protein expression, although the increase in cellular protein levels was slight compared with the observed increase in message (Fig. 6B). Western blots using anti-MKP-1 and anti-ERK2 antibodies also showed no change in protein expression (data not shown).

$VEGF_{121}$/rGel Inhibits Tube Formation in KDR-Expressing Endothelial Cells—We investigated the anti-angiogenic effect of $VEGF_{121}$/rGel *in vitro* by examining the inhibition of tube formation in receptor-transfected PAE cells. PAE/KDR and PAE/Flt-1 cells were placed on

Matrigel-coated plates, to which either $VEGF_{121}$/rGel or rGel at various concentrations was added, and tube formation was assessed 24 h later. As shown in Fig. 7A, the addition of 1 nM $VEGF_{121}$/rGel significantly inhibited tube formation in KDR-transfected cells, whereas rGel alone had little effect at this dose level. Doses of rGel alone caused ~42% inhibition at only the highest concentration tested (100 nM). Endothelial cells expressing VEGFR-1 (PAE/Flt-1) were not as sensitive to $VEGF_{121}$/rGel as were the PAE/KDR cells, requiring 100 nM $VEGF_{121}$/rGel or rGel to inhibit tube formation by 50% (Fig. 7B). To determine whether pre-treatment of PAE/KDR cells with $VEGF_{121}$/rGel affects tube formation, cells were treated with the IC_{50} dose of $VEGF_{121}$/rGel for 4, 16, and 24 h, washed with PBS, detached, added to Matrigel-coated plates in $VEGF_{121}$/rGel-free medium, and incubated for an additional 24 h. This prior incubation of cells with $VEGF_{121}$/rGel for 16 or 24 h virtually abolished tube formation (Fig. 8).

$VEGF_{121}$/rGel Inhibits Angiogenesis in the CAM of Chicken Embryos-- We investigated the antiangiogenic effects of $VEGF_{121}$/rGel *in vivo* using a chicken CAM model. Angiogenesis in the CAMs of 9-day-old chicken embryos were stimulated by treatment with filter disks containing either bFGF alone, bFGF plus $VEGF_{121}$/rGel (at 1 or 10 nM), rGel (at 1 or 10 nM), or buffer (PBS) alone (45). CAMs were treated for 72 h and the effect of each treatment was quantified by determining the relative vascularized area: the area taken up by blood vessels in treated CAMs, normalized to that in CAMs treated with PBS (equal to 100%). The vascularized area was about 35% higher in the CAMs treated with bFGF than in those treated with PBS, and the difference was significant ($P < 0.001$; *t*-test, double-sided; Figs. 9A and 10A). This observation was consistent with the finding of more than a 60% increase in the number of newly sprouted vessels in the bFGF-treated CAMs compared with the PBS-treated CAMs ($P < 0.001$; *t*-test,

double-sided; Fig. 10B). Incubation of CAMs with bFGF without or with 10 nM rGel resulted in angiogenic activity and the formation of an ordered neovasculature (Figs. 9A and 9B). In contrast, treatment with 1 or 10 nM $VEGF_{121}$/rGel resulted in considerable destruction of the neovasculature (Fig. 9C). Treatment with $VEGF_{121}$/rGel also completely inhibited bFGF-stimulated angiogenesis ($P < 0.001$; *t*-test, double sided; Fig. 10). Many of the treated CAMs also appeared to be devoid of vessel infiltration. Interestingly, the number of branching points in the $VEGF_{121}$/rGel-treated CAMs was similar to that in the PBS-treated CAMs ($P > 0.5$; *t*-test, double-sided; Fig. 10B), suggesting that $VEGF_{121}$/rGel mainly inhibits bFGF-mediated formation of newly sprouting branches from preexisiting vessels. As expected, the disks treated with bFGF in combination with rGel (at 1 or 10 nM) consistently showed extensive vascularization that was comparable to that found in those treated with bFGF alone ($P > 0.5$; *t*-test, double-sided).

DISCUSSION

Our study clearly demonstrates that the $VEGF_{121}$/rGel fusion construct is specifically cytotoxic to KDR-overexpressing endothelial cells and that the cytotoxic effect of the treatment is due to necrosis rather than to apoptosis. Previous studies of gelonin-based immunotoxins targeting tumor cells showed that intoxicated cells did not appear to display apoptotic characteristics (42). The toxin gelonin appears to be distinct from toxins such as engineered diphtheria toxin (DT) (43;44) and pseudomonas exotoxin (PE) (45;46), both of which have been demonstrated to cause apoptotic damage to target cells. A closely related toxin, ricin-A chain (RTA), also causes apoptotic damage to target cells (47;48); however, Baluna et al (47) suggest that different portions of the RTA molecule are responsible for generating apoptotic and necrotic effects.

VEGF-A was shown to play a role in tube formation of endothelial cells *in vitro* (49;50) and in angiogenesis (51-53). In the present study, the effect of $VEGF_{121}$/rGel on tube formation of endothelial cells on Matrigel-coated plates was striking in that cells overexpressing the KDR receptor, but not cells overexpressing the Flt-1 receptor, were affected. This result is consistent with our findings that $VEGF_{121}$/rGel is cytotoxic only to KDR-expressing endothelial cells(31) and that $VEGF_{121}$/rGel is internalized only into endothelial cells that express KDR but not Flt-1 (manuscript submitted). The fact that the IC_{50} dose for cytotoxicity is identical to the IC_{50} dose for preventing tube formation in PAE/KDR cells suggests that $VEGF_{121}$/rGel action *in vitro* immediately disrupts angiogenic tube formation as a temporal prelude to its eventual cytotoxicity to rapidly dividing endothelial cells. Our preliminary results examining *in vivo* endothelialization of Matrigel plugs appear to support the observation that the $VEGF_{121}$/rGel construct can ablate neovascularization at several steps in this complex process.

CAM membrane assays are frequently used to assess the antiangiogenic potential of agents (54-57). The inhibition by $VEGF_{121}$/rGel of tube formation *in vitro* translates well to inhibition of both vascular endothelial growth and neovasculature *in vivo*. Treatment with $VEGF_{121}$/rGel at doses as low as 1 nM resulted in complete ablation of bFGF-induced neovasculature. Not surprisingly, the CAM assay also demonstrated that treatment with the construct did not affect mature vessels. This critical finding suggests that $VEGF_{121}$/rGel does not affect mature vessels in either normal tissues or tumors. Therefore, small, newly vascularizing tumors and metastases may be the lesions most responsive to therapy with this agent.

To better understand the cytotoxic effects of $VEGF_{121}$/rGel at the molecular level, we treated HUVECs with $VEGF_{121}$/rGel for 24 h, and harvested the RNA for microarray analysis. The results suggest that treatment of HUVECs with $VEGF_{121}$/rGel increases the RNA levels of several genes that are involved in inflammation, chemotaxis, intermediary metabolism, and apoptotic pathways (Table I). A previous report showed that only two of these genes, MKP-1 and CXCR4, were also upregulated after treatment with $VEGF_{165}$ for 24 h (58). Therefore, for most of the genes found to be upregulated in our present study, the upregulation appears to be attributable to the $VEGF_{121}$/rGel construct and not the VEGF component itself. To our knowledge, this microarray analysis was the first to be performed on cells treated with a plant-derived protein toxin such as gelonin.

Of all the molecules we studied, the highest level of mRNA induced was that of the cell adhesion molecule E-selectin. In previous studies, treatment with VEGF induced adhesion molecules (E-selectin, VCAM-1, and ICAM-1) in HUVECs (59-61) via an NFκB-mediated process. E-selectin has been shown to be upregulated after VEGF treatment (50) or in response to inflammation (60;62) and plays an important role in both tube formation and angiogenesis.

Previous studies have shown that E-selectin also plays a major role in the adhesion of epithelial cancer cells to the endothelium (63) and that the ability of cancer cell clones to bind E-selectin on endothelial cells is directly proportional to their metastatic potential (62;64). Moreover, drugs that inhibit the expression of E-selectin, such as cimetidine, block the adhesion of tumor cells to the endothelium and prevent metastasis (65). However, E-selectin does not necessarily have a role in the adhesion of all cancer cells (66;67), nor do all cancer cells require expression of the same endothelial adhesive molecule (68;69). Our present study shows that $VEGF_{121}$/rGel is a member of the class of molecules that can prevent E-selectin-mediated metastasis because protein levels barely doubled in both PAE/KDR and HUVECs after treatment with $VEGF_{121}$/rGel. We observed a similar pattern of induction of RNA but not protein levels with other genes as well. For example, although MKP-1 RNA levels were induced in HUVECs after treatment with $VEGF_{121}$/rGel, western blots of PAE/KDR and HUVEC whole cell extract did not show a corresponding increase in protein levels (data not shown). In addition, levels of ERK2, which was previously shown to be upregulated by MKP-1 in HUVECs after endothelial cell injury (59), did not show a change up to 48 h after $VEGF_{121}$/rGel treatment. Taken together, we conclude $VEGF_{121}$/rGel induces an increase in mRNA levels of genes that are important in cell adhesion, migration, and spread but generally does not induce a concomitant increase in protein expression. Since the rGel component of the fusion construct operates by inhibiting protein synthesis, $VEGF_{121}$/rGel could inhibit synthesis of critical proteins that are important for suppression of these specific genes. Our data also suggest that in addition to exerting a cytotoxic effect, $VEGF_{121}$/rGel may act through cellular mechanisms involved in inflammation and stress.

Previous studies have showed that several genes HUVECs are induced as a result of cellular inflammation. For example, Early growth response factor 1 (EGR1), SCYA2, E-selectin

and VCAM-1 are all up-regulated in HUVECs (60;70), and all of these genes are induced by treatment with $VEGF_{121}$/rGel. In addition, several members of the small inducible cytokine (SCYA) family of proteins are overexpressed after $VEGF_{121}$/rGel treatment. All of these SCYA proteins respond to inflammation stimuli and play a role in chemotaxis: SCYA2 plays a role in inflammation and wound healing (71-73); SCYA4 (MIP-1β) is involved in directional migration of cells during normal and inflammatory processes (74;75); and SCYA7 (MCP-3) and SCYA11 (eotaxin) share 65% amino acid sequence identity and play major roles in the recruitment and activation of eosinophils in allergic disorders (71;73) while binding to different receptors and having different modes of action (76). Another molecule that plays a role in chemotaxis is CXCR4. Although treatment with $VEGF_{121}$/rGel increases the CXCR4 level to less than twice the level without treatment, array spot intensities and reproducibility data indicate that the increase is significant.

Transcription factors represent one of the larger classes of genes to be upregulated by treatment with $VEGF_{121}$/rGel. Interestingly, two of them, NF-κBIα (IκB-α) and NF-κB (p105 subunit), are from the NF-κB family. Since NF-κB and IκB-α interact in an autoregulatory mechanism, the upregulation of IκB-α is most likely due to NF-κB's mediating activation of the IκB-α gene, resulting in replenishment of the cytoplasmic pool of its own inhibitor (77-80). NF-κB may play a role in the upregulation of several genes, including SCYA2, SCYA7, SCYA11, and JunB (81;82). Another transcription factor, Kruppel-like factor (KLF4), has not been shown to be expressed in endothelial cells. However, this molecule is an important nuclear factor in the up-regulation of histidine decarboxylase, an enzyme that catalyzes the conversion of histidine to histamine, a bioamine that plays an important role in allergic responses, inflammation, neurotransmission, and gastric acid secretion (83).

Among the molecules governing apoptosis, TNFAIP3, a putative DNA binding protein in the NF-κB signal transduction pathway, functions by inhibiting NF-κB activation and TNF-mediated apoptosis (84). BIRC3, another gene that is upregulated by treatment with $VEGF_{121}$/rGel, forms a heterodimer with a caspase-9 monomer *in vitro* and prevents the activation of caspase-9 in apoptosis (85). Surprisingly, we found in this study that several genes involved in the control of the apoptotic pathway were modulated in response to the fusion toxin even though the overall cytotoxic effect on target cells did not include an observable impact on the apoptotic pathway.

A critical finding of this study is the identification of several genes that are regulated in response to treatment with the $VEGF_{121}$/rGel fusion construct. Since many of these genes regulate cell adhesion, chemotaxis, and inflammatory responses, the construct may influence tumor development in addition to exerting direct cycotoxic effects on the tumor neovasculature. Therefore, important considerations for future study are the effects of $VEGF_{121}$/rGel cytotoxicity on tumor endothelial cells and the potential bystander effects of the construct on adjacent tumor cells. In our laboratory, current studies are under way in breast and prostate orthotopic and metastatic (i.e., lung and bone) tumor cells to further characterize the effects of this drug *in vitro* and *in vivo*.

FIGURE LEGENDS

Fig. 1. **Cytotoxic effects of $VEGF_{121}$/rGel on endothelial cells.** Log-phase HUVECs, PAE/KDRcells, and PAE/Flt-1 cells were plated in 96-well plates and incubated with serial dilutions of $VEGF_{121}$/rGel and rGel for 72 h as described in Experimental Procedures. The cytotoxicity experiment was performed in triplicate, and data points represent the means.

Fig. 2. **Decreased KDR and increased p-KDR levels in PAE/KDR cells and HUVECs treated with $VEGF_{121}$/rGel at IC_{50} doses for 24 h.** To determine the effects of $VEGF_{121}$/rGel on the levels of KDR and activated KDR levels, samples were prepared as described in Experimental Procedures and probed with anti-KDR and anti-p-KDR antibodies. Actin levels were used as a loading control. *A*, total KDR and p-KDR levels in PAE/KDR cells show an increase within 2 h after the start of treatment and gradually level off by 48 h. *B*, at 24h after the start of treatment of HUVECs with $VEGF_{121}$/rGel, KDR levels are decreased slightly but p-KDR levels are increased. NT, not treated.

Fig. 3. **TUNEL assay of endothelial cells treated with $VEGF_{121}$/rGel.** After PAE/KDR cells were grown overnight, and 1 nM $VEGF_{121}$/rGel was added, the cells were further incubated for 24, 48, and 72 h. The cells were then analyzed by TUNEL. Positive control cells were incubated with 1 mg/ml DNAse for 10 min at 37°C. The results show that cytotoxicity of $VEGF_{121}$/rGel in PAE/KDR cells does not result in apoptosis. NT, not treated.

Fig. 4. **Lack of effect of $VEGF_{121}$/rGel on apoptotic markers in endothelial cells.** To understand the mechanism of cytotoxicity of $VEGF_{121}$/rGel, protein levels of key markers of apoptosis were assessed 24 h after treatment. Protein levels of Bax, Bcl-XL and caspase-3 remained unchanged, suggesting that the mechanism of cell death induced by the construct is not apoptotic. Levels of cytochrome C, caspase-6, and Bcl-2 were undetectable (data not shown). NT, not treated.

Fig. 5. **Analysis of HUVECs treated with $VEGF_{121}$/rGel.** *A*, validation of the microarray analysis by PCR is shown. Upregulation of genes for E-selectin, TNFAIP3, NF-κBIα and SCYA2 were validated by RT-PCR. GAPDH levels were assessed as a control. *B*, protein levels of E-selectin in HUVECs treated with $VEGF_{121}$/rGel are shown. NT, not treated.

Fig. 6. **Inhibition of translation of upregulated E-selectin RNA by $VEGF_{121}$/rGel.** *A*, RNA from PAE/KDR cells that were untreated or treated with $VEGF_{121}$/rGel for the periods indicated were examined by PCR for upregulation of E-selectin, one of the genes identified by microarray analysis. GAPDH primers were used as a control for loading. RNA levels of E-selectin were all upregulated in PAE/KDR cells, as in HUVECs. *B*, protein levels of E-selectin are also upregulated.

Fig. 7. **$VEGF_{121}$/rGel-mediated inhibition of tube formation in PAE/KDR cells.** PAE/KDR and PAE/Flt-1 cells were added to Matrigel-coated plates, treated with $VEGF_{121}$/rGel and rGel at the concentrations indicated, and analyzed for tube formation after 24 h. *A*, A 1 nM dose of $VEGF_{121}$/rGel was sufficient to inhibit tube formation by 50%, whereas the same degree of

inhibition was seen with rGel only at 100 nM. *B*, up to 100 nM $VEGF_{121}$/rGel was needed to inhibit tube formation in PAE/Flt-1 cells, the same concentration as the untargeted gelonin toxin.

Fig. 8. **Time-dependent inhibition of tube formation of PAE/KDR cells by $VEGF_{121}$/rGel.** PAE/KDR cells were treated with 1 nM $VEGF_{121}$/rGel for the periods indicated, detached, incubated on Matrigel-coated plates for 24 h, and assessed for tube formation. Incubation of PAE/KDR cells with $VEGF_{121}$/rGel for as little as 9 h was sufficient to abolish the ability of these cells to form tubes by 50%.

Fig. 9. **$VEGF_{121}$/rGel-mediated inhibition of angiogenesis in chicken embryo CAMs.** Shown are vessels in representative CAMs treated with bFGF alone (50 ng), bFGF in combination with $VEGF_{121}$/rGel (1 nM), or bFGF in combination with rGel (10 nM) (x0.5 objective). Angiogenesis was induced on CAMs from 9-day-old chicken embryos by filter disks saturated with bFGF. Disks were simultaneously treated with $VEGF_{121}$/rGel or rGel. At 72 h, CAMs were harvested and examined using an Olympus stereomicroscope. Experiments were performed twice per treatment, with 6 to 10 embryos per condition in every experiment. *A*, the photograph shows the vasculature of a CAM after stimulation with bFGF alone. *B*, the photograph shows that rGel had no effect on angiogenic stimulation of bFGF at either 1 nM or 10 nM. *C*, the photograph shows that 1 nM $VEGF_{121}$/rGel in the presence of 50 ng of bFGF inhibited angiogenesis.

Fig. 10. **$VEGF_{121}$/rGel-mediated reduction of the vascular area and number of vascular branches in the CAM assay.** Quantitative evaluation of $VEGF_{121}$/rGel-mediated inhibition of

angiogenesis in the CAM model was determined, after the indicated treatments, by image analyses, and the results were normalized to CAMs treated with buffer (PBS; equal to 100%). *A*, $VEGF_{121}$/rGel at both 1 and 10 nM decreased the vascular area. As expected, rGel alone had no effect. Data represent the means ± standard deviations from replicated experiments. *, $P < 0.001$; *t*-test, double-sided. *B*, $VEGF_{121}$/rGel decreased the number of newly sprouting vessels. $VEGF_{121}$/rGel at a concentration of 1 nM dramatically affected the formation of the neovasculature, completely inhibiting bFGF-mediated stimulation of the neovasculature. As expected, rGel did not affect the number of newly sprouting vessels. Data shown represent the means ± standard deviations from replicated experiments. *, $P < 0.001$; *t*-test, double-sided.

Acknowledgments— We thank Kate Ó Súilleabháin (UT MD Anderson Cancer Center Department of Scientific Publications) for editing the manuscript.

[1]The abbreviations used are: VEGF-A, vascular endothelial growth factor-A; $VEGF_{121}$, 121-amino-acid splice variant of VEGF-A; rGel, recombinant toxin gelonin; bFGF, basic fibroblast growth factor; p-KDR, phosphorylated KDR; PAE, porcine aortic endothelial; FBS, fetal bovine serum; HUVEC, human umbilical vein endothelial cell; PBS, phosphate-buffered saline; SDS-PAGE, sodium dodecyl sulfate-polyacrylamide gel electrophoresis; CAM, chorioallantoic membrane; SCYA2, cytokine A2; TNFAIP3, tumor necrosis factor alpha-induced protein 3; NF-κBIα, NF-κB inhibitor alpha.

REFERENCES

1. Folkman, J. (1993) *C. R. Acad. Sci. III* **316,** 909-918

2. Schultz, G. S. and Grant, M. B. (1991) *Eye* **5 (Pt 2),** 170-180

3. Sebag, J. and McMeel, J. W. (1986) *Surv. Ophthalmol.* **30,** 377-384

4. Rand, L. I. (1981) *Am. J. Med.* **70,** 595-602

5. Koch, A. E. (1998) *Arthritis Rheum.* **41,** 951-962

6. Szekanecz, Z., Szegedi, G., and Koch, A. E. (1998) *J. Investig. Med.* **46,** 27-41

7. Oliver, S. J. and Brahn, E. (1996) *J. Rheumatol. Suppl* **44,** 56-60

8. Brown, R. A. and Weiss, J. B. (1988) *Ann. Rheum. Dis.* **47,** 881-885

9. Verheul, H. M., Voest, E. E., and Schlingemann, R. O. (2004) *J. Pathol.* **202,** 5-13

10. Bogenrieder, T. and Herlyn, M. (2003) *Oncogene* **22,** 6524-6536

11. Aoun, E. and Taher, A. (2002) *J. Med. Liban.* **50,** 32-38

12. Folkman, J. (2002) *Semin. Oncol.* **29,** 15-18

13. Bergers, G., Song, S., Meyer-Morse, N., Bergsland, E., and Hanahan, D. (2003) *J. Clin. Invest* **111,** 1287-1295

14. Klohs, W. D., Fry, D. W., and Kraker, A. J. (1997) *Curr. Opin. Oncol.* **9,** 562-568

15. Manley, P. W., Martiny-Baron, G., Schlaeppi, J. M., and Wood, J. M. (2002) *Expert. Opin. Investig. Drugs* **11,** 1715-1736

16. Rosen, L. S. (2002) *Hematol. Oncol. Clin. North Am.* **16,** 1173-1187

17. Ruegg, C., Dormond, O., and Foletti, A. (2002) *Endothelium* **9,** 151-160

18. Veronese, M. L. and O'Dwyer, P. J. (2004) *Eur. J. Cancer* **40,** 1292-1301

19. Zondor, S. D. and Medina, P. J. (2004) *Ann. Pharmacother.* **38,** 1258-1264

20. Kim, E. S., Serur, A., Huang, J., Manley, C. A., McCrudden, K. W., Frischer, J. S., Soffer, S. Z., Ring, L., New, T., Zabski, S., Rudge, J. S., Holash, J., Yancopoulos, G. D., Kandel, J. J., and Yamashiro, D. J. (2002) *Proc. Natl. Acad. Sci. U. S. A.* **99,** 11399-11404

21. Holash, J., Davis, S., Papadopoulos, N., Croll, S. D., Ho, L., Russell, M., Boland, P., Leidich, R., Hylton, D., Burova, E., Ioffe, E., Huang, T., Radziejewski, C., Bailey, K., Fandl, J. P., Daly, T., Wiegand, S. J., Yancopoulos, G. D., and Rudge, J. S. (2002) *Proc. Natl. Acad. Sci. U. S. A.* **99,** 11393-11398

22. Wulff, C., Wilson, H., Rudge, J. S., Wiegand, S. J., Lunn, S. F., and Fraser, H. M. (2001) *J. Clin. Endocrinol. Metab.* **86,** 3377-3386

23. Cavallaro, U. and Christofori, G. (2000) *J. Neurooncol.* **50,** 63-70

24. Shinkaruk, S., Bayle, M., Lain, G., and Deleris, G. (2003) *Curr. Med. Chem. Anti.-Canc. Agents* **3,** 95-117

25. Verheul, H. M. and Pinedo, H. M. (2000) *Clin. Breast Cancer* **1 Suppl 1,** S80-S84

26. Arora, N., Masood, R., Zheng, T., Cai, J., Smith, D. L., and Gill, P. S. (1999) *Cancer Res.* **59,** 183-188

27. Backer, M. V., Budker, V. G., and Backer, J. M. (2001) *J. Control Release* **74,** 349-355

28. Hotz, H. G., Gill, P. S., Masood, R., Hotz, B., Buhr, H. J., Foitzik, T., Hines, O. J., and Reber, H. A. (2002) *J. Gastrointest. Surg.* **6,** 159-166

29. Masood, R., Kundra, A., Zhu, S., Xia, G., Scalia, P., Smith, D. L., and Gill, P. S. (2003) *Int. J. Cancer* **104,** 603-610

30. Ramakrishnan, S., Wild, R., and Nojima, D. (2001) *Methods Mol. Biol.* **166,** 219-234

31. Veenendaal, L. M., Jin, H., Ran, S., Cheung, L., Navone, N., Marks, J. W., Waltenberger, J., Thorpe, P., and Rosenblum, M. G. (2002) *Proc. Natl. Acad. Sci. U. S. A.* **99,** 7866-7871

32. Waltenberger, J., Claesson-Welsh, L., Siegbahn, A., Shibuya, M., and Heldin, C. H. (1994) *J. Biol. Chem.* **269,** 26988-26995

33. Bussolati, B., Dunk, C., Grohman, M., Kontos, C. D., Mason, J., and Ahmed, A. (2001) *Am. J. Pathol.* **159,** 993-1008

34. Joki, T., Machluf, M., Atala, A., Zhu, J., Seyfried, N. T., Dunn, I. F., Abe, T., Carroll, R. S., and Black, P. M. (2001) *Nat. Biotechnol.* **19,** 35-39

35. Kroll, J. and Waltenberger, J. (1999) *Biochem. Biophys. Res. Commun.* **265,** 636-639

36. Brooks, P. C., Montgomery, A. M., and Cheresh, D. A. (1999) *Methods Mol. Biol.* **129,** 257-269

37. Jiang, B. H., Zheng, J. Z., Aoki, M., and Vogt, P. K. (2000) *Proc. Natl. Acad. Sci. U. S. A.* **97,** 1749-1753

38. Shmulevich, I., Hunt, K., El Naggar, A., Taylor, E., Ramdas, L., Laborde, P., Hess, K. R., Pollock, R., and Zhang, W. (2002) *Cancer* **94,** 2069-2075

39. Baggerly, K. A., Coombes, K. R., Hess, K. R., Stivers, D. N., Abruzzo, L. V., and Zhang, W. (2001) *J. Comput. Biol.* **8,** 639-659

40. Dobbin, K., Shih, J. H., and Simon, R. (2003) *J. Natl. Cancer Inst.* **95,** 1362-1369

41. Brogi, E., Schatteman, G., Wu, T., Kim, E. A., Varticovski, L., Keyt, B., and Isner, J. M. (1996) *J. Clin. Invest* **97,** 469-476

42. Rosenblum, M. G., Cheung, L. H., Liu, Y., and Marks, J. W., III (2003) *Cancer Res.* **63,** 3995-4002

43. Foss, F. M. (2000) *Clin. Lymphoma* **1,** 110-116

44. Hall, P. D., Kreitman, R. J., Willingham, M. C., and Frankel, A. E. (1998) *Toxicol. Appl. Pharmacol.* **150,** 91-97

45. Wang, L., Liu, B., Schmidt, M., Lu, Y., Wels, W., and Fan, Z. (2001) *Prostate* **47,** 21-28

46. Brinkmann, U. (2000) *In Vivo* **14,** 21-27

47. Baluna, R., Coleman, E., Jones, C., Ghetie, V., and Vitetta, E. S. (2000) *Exp. Cell Res.* **258,** 417-424

48. Burbage, C., Tagge, E. P., Harris, B., Hall, P., Fu, T., Willingham, M. C., and Frankel, A. E. (1997) *Leuk. Res.* **21,** 681-690

49. Ruggeri, B., Singh, J., Gingrich, D., Angeles, T., Albom, M., Yang, S., Chang, H., Robinson, C., Hunter, K., Dobrzanski, P., Jones-Bolin, S., Pritchard, S., Aimone, L., Klein-Szanto, A., Herbert, J. M., Bono, F., Schaeffer, P., Casellas, P., Bourie, B., Pili, R., Isaacs, J., Ator, M., Hudkins, R., Vaught, J., Mallamo, J., and Dionne, C. (2003) *Cancer Res.* **63,** 5978-5991

50. Aoki, M., Kanamori, M., Yudoh, K., Ohmori, K., Yasuda, T., and Kimura, T. (2001) *Tumour. Biol.* **22,** 239-246

51. Leopold, J. A., Walker, J., Scribner, A. W., Voetsch, B., Zhang, Y. Y., Loscalzo, A. J., Stanton, R. C., and Loscalzo, J. (2003) *J. Biol. Chem.* **278,** 32100-32106

52. Kim, K. Y., Kim, S. O., Lim, H., Yoo, S. E., and Hong, K. W. (2003) *Eur. J. Pharmacol.* **465,** 219-228

53. Itokawa, T., Nokihara, H., Nishioka, Y., Sone, S., Iwamoto, Y., Yamada, Y., Cherrington, J., McMahon, G., Shibuya, M., Kuwano, M., and Ono, M. (2002) *Mol. Cancer Ther.* **1,** 295-302

54. Favot, L., Keravis, T., Holl, V., Le Bec, A., and Lugnier, C. (2003) *Thromb. Haemost.* **90,** 334-343

55. Hembrough, T. A., Ruiz, J. F., Swerdlow, B. M., Swartz, G. M., Hammers, H. J., Zhang, L., Plum, S. M., Williams, M. S., Strickland, D. K., and Pribluda, V. S. (2004) *Blood* **103,** 3374-3380

56. Ribatti, D., Nico, B., Vacca, A., Roncali, L., and Presta, M. (1999) *Angiogenesis* **3,** 89-95

57. Wang, F. S., Wang, C. J., Chen, Y. J., Chang, P. R., Huang, Y. T., Sun, Y. C., Huang, H. C., Yang, Y. J., and Yang, K. D. (2004) *J. Biol. Chem.* **279,** 10331-10337

58. Yang, S., Toy, K., Ingle, G., Zlot, C., Williams, P. M., Fuh, G., Li, B., de Vos, A., and Gerritsen, M. E. (2002) *Arterioscler. Thromb. Vasc. Biol.* **22,** 1797-1803

59. Kim, F. and Corson, M. A. (2000) *Biochem. Biophys. Res. Commun.* **273,** 539-545

60. Kim, W., Moon, S. O., Lee, S., Sung, M. J., Kim, S. H., and Park, S. K. (2003) *Arterioscler. Thromb. Vasc. Biol.* **23,** 1377-1383

61. Kim, I., Moon, S. O., Kim, S. H., Kim, H. J., Koh, Y. S., and Koh, G. Y. (2001) *J. Biol. Chem.* **276,** 7614-7620

62. Nubel, T., Dippold, W., Kleinert, H., Kaina, B., and Fritz, G. (2004) *FASEB J.* **18,** 140-142

63. Takada, A., Ohmori, K., Yoneda, T., Tsuyuoka, K., Hasegawa, A., Kiso, M., and Kannagi, R. (1993) *Cancer Res.* **53,** 354-361

64. Sawada, R., Tsuboi, S., and Fukuda, M. (1994) *J. Biol. Chem.* **269,** 1425-1431

65. Kobayashi, K., Matsumoto, S., Morishima, T., Kawabe, T., and Okamoto, T. (2000) *Cancer Res.* **60,** 3978-3984

66. Laferriere, J., Houle, F., Taher, M. M., Valerie, K., and Huot, J. (2001) *J. Biol. Chem.* **276,** 33762-33772

67. Laferriere, J., Houle, F., and Huot, J. (2002) *Ann. N. Y. Acad. Sci.* **973,** 562-572

68. Khatib, A. M., Kontogiannea, M., Fallavollita, L., Jamison, B., Meterissian, S., and Brodt, P. (1999) *Cancer Res.* **59,** 1356-1361

69. Zetter, B. R. (1993) *Semin. Cancer Biol.* **4,** 219-229

70. Kadl, A., Huber, J., Gruber, F., Bochkov, V. N., Binder, B. R., and Leitinger, N. (2002) *Vascul. Pharmacol.* **38,** 219-227

71. Johnston, C. J., Williams, J. P., Okunieff, P., and Finkelstein, J. N. (2002) *Radiat. Res.* **157,** 256-265

72. Lu, B., Rutledge, B. J., Gu, L., Fiorillo, J., Lukacs, N. W., Kunkel, S. L., North, R., Gerard, C., and Rollins, B. J. (1998) *J. Exp. Med.* **187,** 601-608

73. Wagner, K., Dendorfer, U., Chilla, S., Schlondorff, D., and Luckow, B. (2001) *Genomics* **78,** 113-123

74. Guo, C. J., Lai, J. P., Luo, H. M., Douglas, S. D., and Ho, W. Z. (2002) *J. Neuroimmunol.* **131,** 160-167

75. Guo, C. J., Douglas, S. D., Lai, J. P., Pleasure, D. E., Li, Y., Williams, M., Bannerman, P., Song, L., and Ho, W. Z. (2003) *J. Neurochem.* **84,** 997-1005

76. Chung, I. Y., Kim, Y. H., Choi, M. K., Noh, Y. J., Park, C. S., Kwon, d. Y., Lee, D. Y., Lee, Y. S., Chang, H. S., and Kim, K. S. (2004) *Biochem. Biophys. Res. Commun.* **314,** 646-653

77. Brown, K., Park, S., Kanno, T., Franzoso, G., and Siebenlist, U. (1993) *Proc. Natl. Acad. Sci. U. S. A.* **90,** 2532-2536

78. Sun, S. C., Ganchi, P. A., Ballard, D. W., and Greene, W. C. (1993) *Science* **259,** 1912-1915

79. Scott, M. L., Fujita, T., Liou, H. C., Nolan, G. P., and Baltimore, D. (1993) *Genes Dev.* **7,** 1266-1276

80. de Martin, R., Vanhove, B., Cheng, Q., Hofer, E., Csizmadia, V., Winkler, H., and Bach, F. H. (1993) *EMBO J.* **12,** 2773-2779

81. Schwamborn, J., Lindecke, A., Elvers, M., Horejschi, V., Kerick, M., Rafigh, M., Pfeiffer, J., Prullage, M., Kaltschmidt, B., and Kaltschmidt, C. (2003) *BMC. Genomics* **4,** 46

82. Wuyts, W. A., Vanaudenaerde, B. M., Dupont, L. J., Demedts, M. G., and Verleden, G. M. (2003) *Respir. Med.* **97,** 811-817

83. Ai, W., Liu, Y., Langlois, M., and Wang, T. C. (2004) *J. Biol. Chem.* **279,** 8684-8693

84. Van Huffel, S., Delaei, F., Heyninck, K., De Valck, D., and Beyaert, R. (2001) *J. Biol. Chem.* **276,** 30216-30223

85. Shiozaki, E. N., Chai, J., Rigotti, D. J., Riedl, S. J., Li, P., Srinivasula, S. M., Alnemri, E. S., Fairman, R., and Shi, Y. (2003) *Mol. Cell* **11,** 519-527

Table I

HUVEC genes that increase following treatment with $VEGF_{121}$/rGel for 24 hours, compared to untreated cells

Gene classification	Accession number	Symbol Gene		Mean fold change
Cell adhesion	H39560	SELE	E-selectin (endothelial adhesion molecule 1)[a]	94.6
	H07071	VCAM	Vascular cell adhesion molecule 1	4.9
	AA284668	PLAU	Plasminogen activator, urokinase	2.3
Apoptosis	AA476272	TNFAIP3	Tumor necrosis factor alpha-induced protein 3[a]	13.5
	H48706	BIRC3	baculoviral IAP repeat-containing 3	3.3
Transcription regulation	T99236	JUNB	jun B proto-oncogene	4.9
	W55872	NF-κBIα	nuclear factor of kappa light polypeptide gene enhancer in B-cells inhibitor, alpha[a]	4.8
	AA451716	NF-κB1	nuclear factor of kappa light polypeptide gene enhancer in B-cells 1 (p105)	2.3
	H45711	KLF4	Kruppel-like factor 4	2.3
Chemotaxis	AA425102	SCYA2	small inducible cytokine A2 (MCP-1)[a]	20.2
	H62985	SCYA4	small inducible cytokine A4 (MIP-1β)	5.8
	AA040170	SCYA7	small inducible cytokine A7 (MCP-3)	5.5
	T62491	CXCR4	chemokine (C-X-C motif), receptor 4 (fusin)	1.85
Structural organization	NM004856	KNSL5	kinesin-like 5 (mitotic kinesin-like protein 1)	6.4
	AA479199	NID2	nidogen 2	3.1
	AA453105	H2AFL	H2A histone family, member L	2.5
Inflammatory response	W69211	SCYA11	small inducible cytokine A11 (Cys-Cys) (eotaxin	8.4
	NM_001964	EGR1	early growth response 1	3.9
	NM_000963	PTGS2	prostaglandin-endoperoxide synthase 2 (COX-2)	3.3
	AA148736	SCD4	syndecan 4 (amphiglycan, ryudocan)	3.2
Signalling	W65461	DUSP5	dual specificity phosphatase 5 (MKP-1)	2.7
Metabolic	AA011215	SAT	spermidine/spermine N1-acetyltransferase	2.1

[a] Confirmed by RT-PCR at 4 and 24 h posttreatment

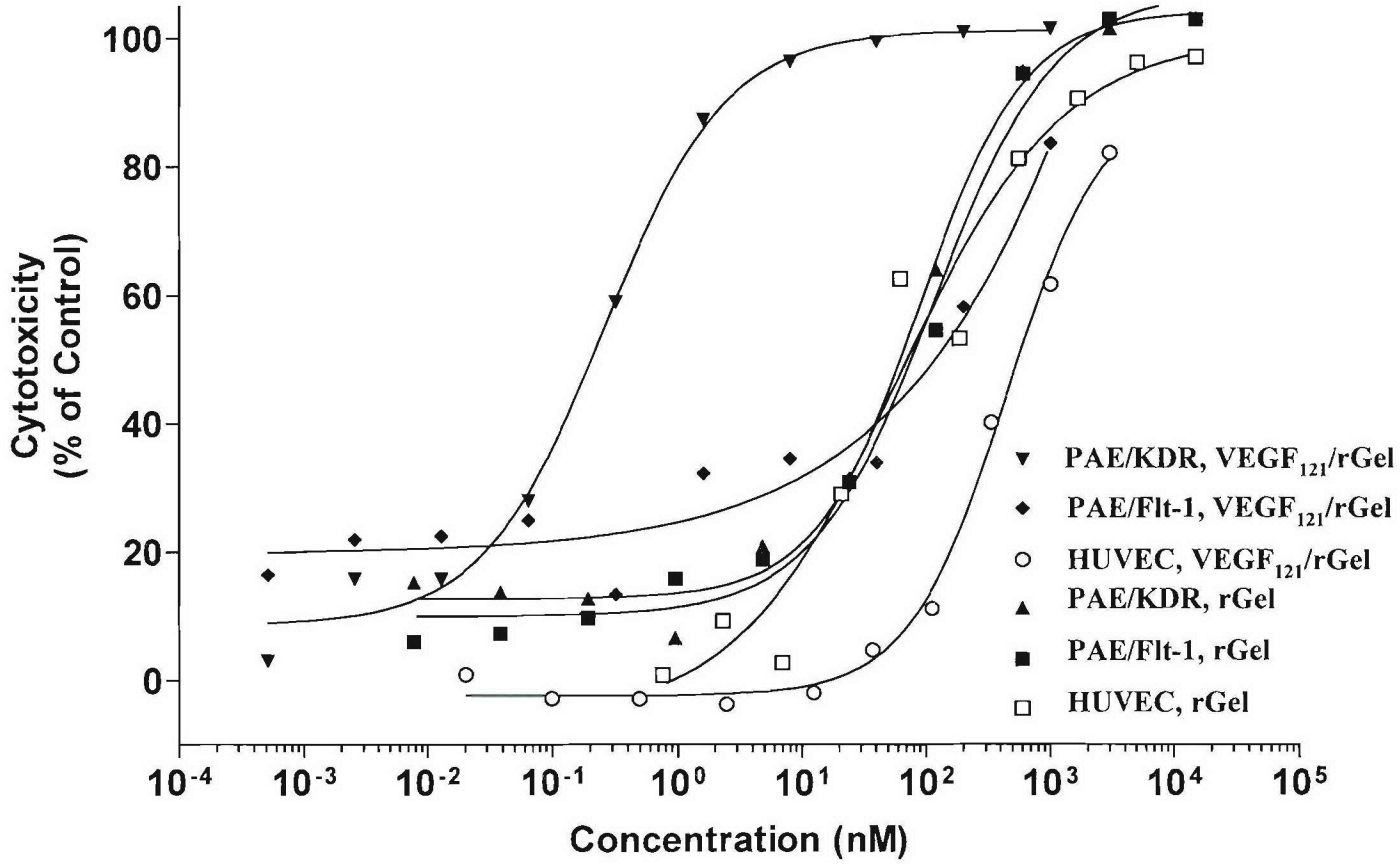
Cytotoxicity
(% of Control)
100
80
60
40
20
0
10^{-4}
10^{-3}
10^{-2}
10^{-1}
10^{0}
10^{1}
10^{2}
10^{3}
10^{4}
10^{5}
Concentration (nM)
PAE/KDR, $VEGF_{121}$/rGel
PAE/Flt-1, $VEGF_{121}$/rGel
HUVEC, $VEGF_{121}$/rGel
PAE/KDR, rGel
PAE/Flt-1, rGel
HUVEC, rGel

Figure 1

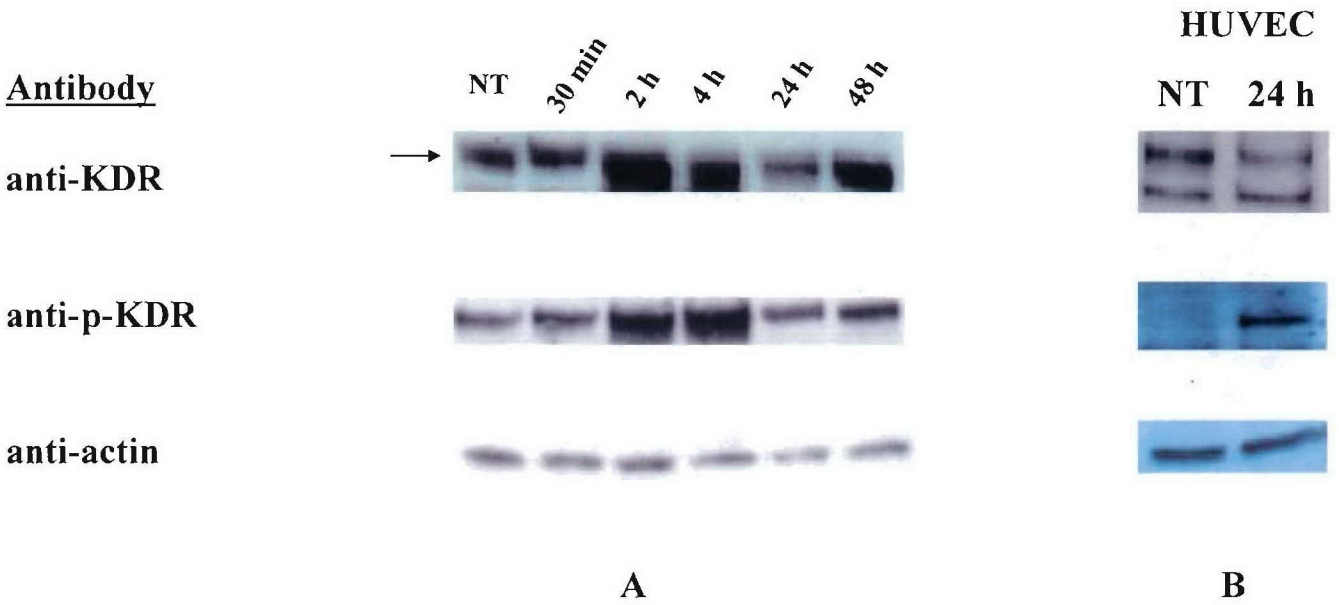
Antibody
anti-KDR
anti-p-KDR
anti-actin
NT
30 min
2 h
4 h
24 h
48 h
A
HUVEC
NT
24 h
B

Figure 2

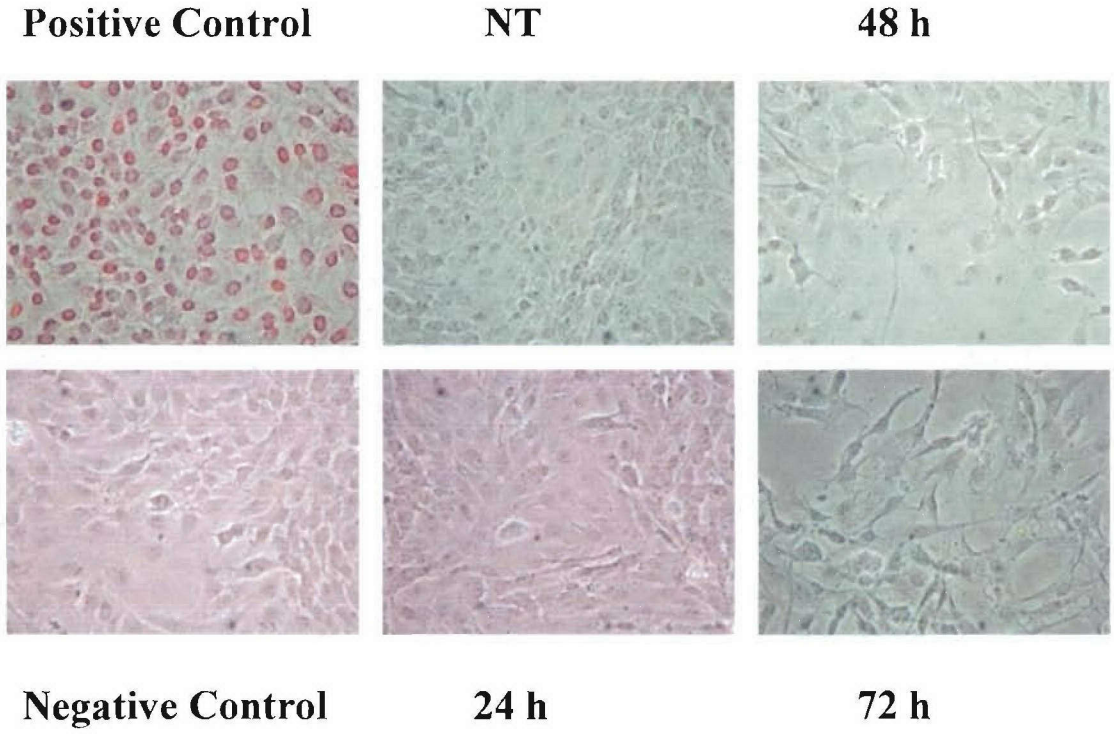

Figure 3

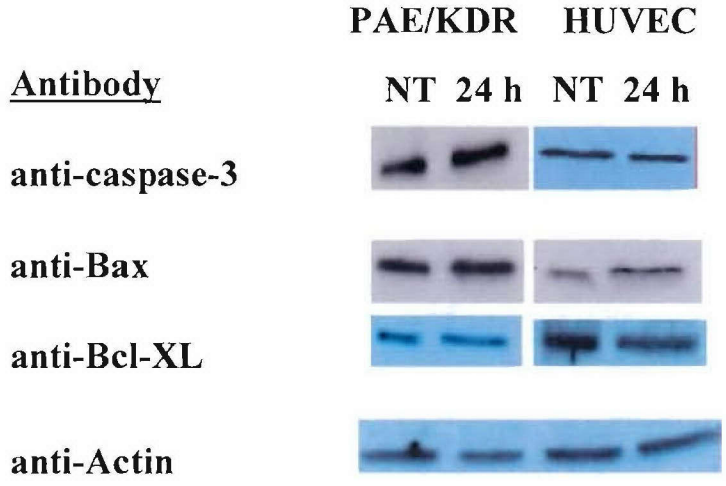
PAE/KDR
HUVEC
Antibody
NT 24 h NT 24 h
anti-caspase-3
anti-Bax
anti-Bcl-XL
anti-Actin

Figure 4

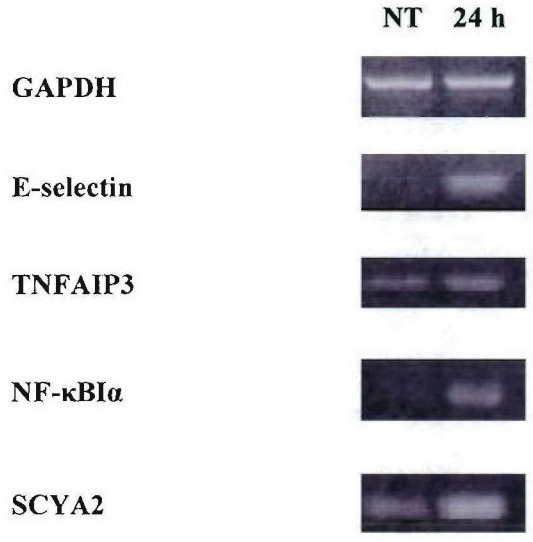
NT 24 h
GAPDH
E-selectin
TNFAIP3
NF-κBIα
SCYA2

A

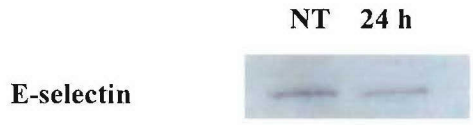
NT 24 h
E-selectin

B

Figure 5

PCR

A

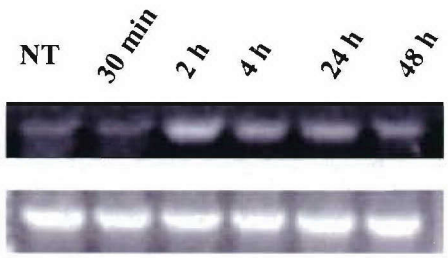

Western Blot

B

Figure 6

A

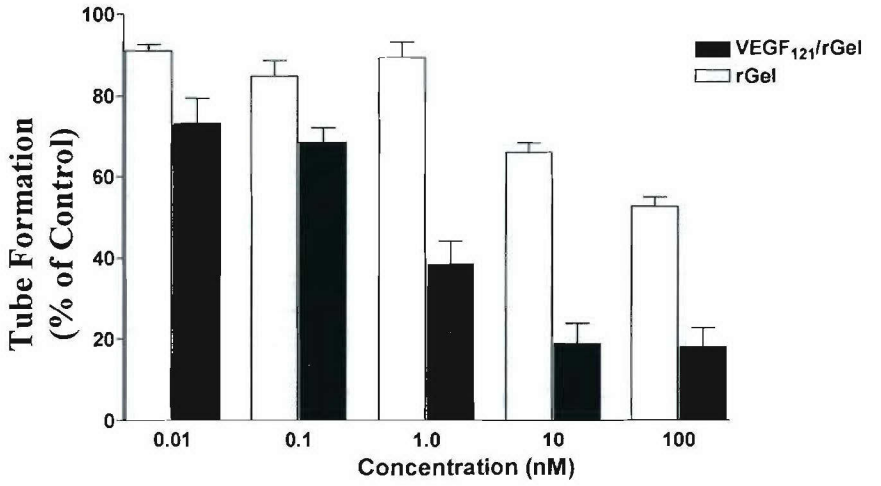
100
80
60
40
20
0
Tube Formation
(% of Control)
VEGF121/rGel
rGel
0.01
0.1
1.0
10
100
Concentration (nM)

B

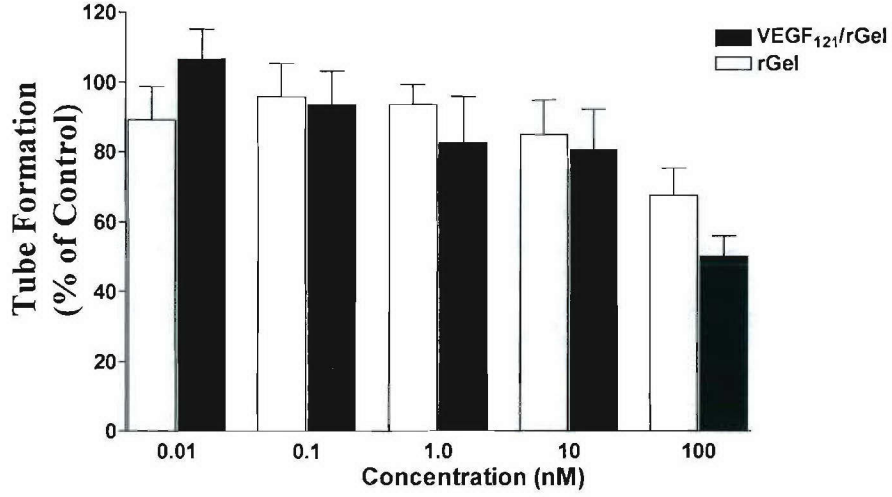
120
100
80
60
40
20
0
Tube Formation
(% of Control)
VEGF121/rGel
rGel
0.01
0.1
1.0
10
100
Concentration (nM)

Figure 7

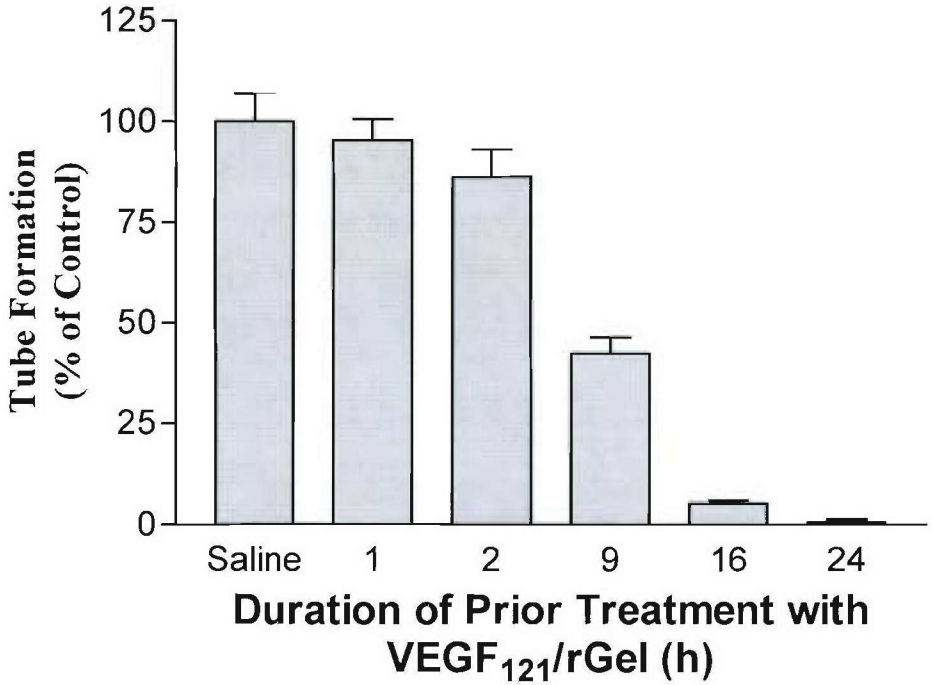
125
100
75
50
25
0
Tube Formation
(% of Control)
Saline
1
2
9
16
24
Duration of Prior Treatment with
VEGF121/rGel (h)

Figure 8

A

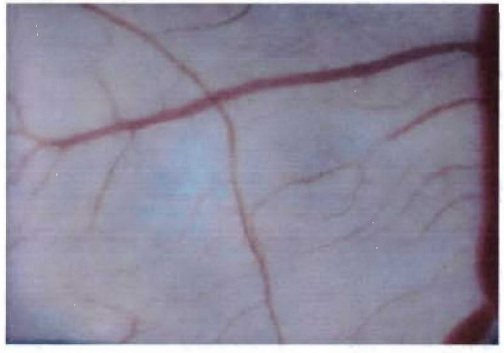

B

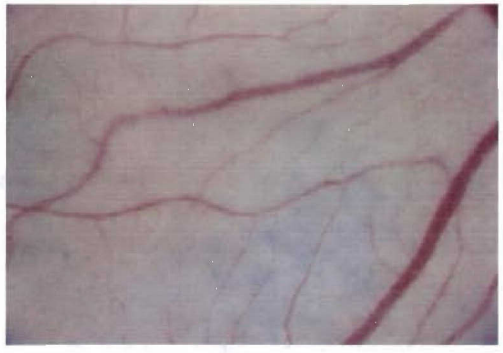

C

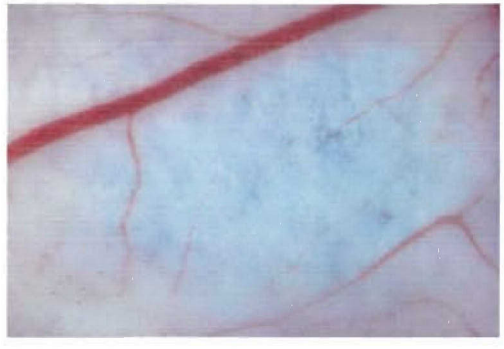

Figure 9

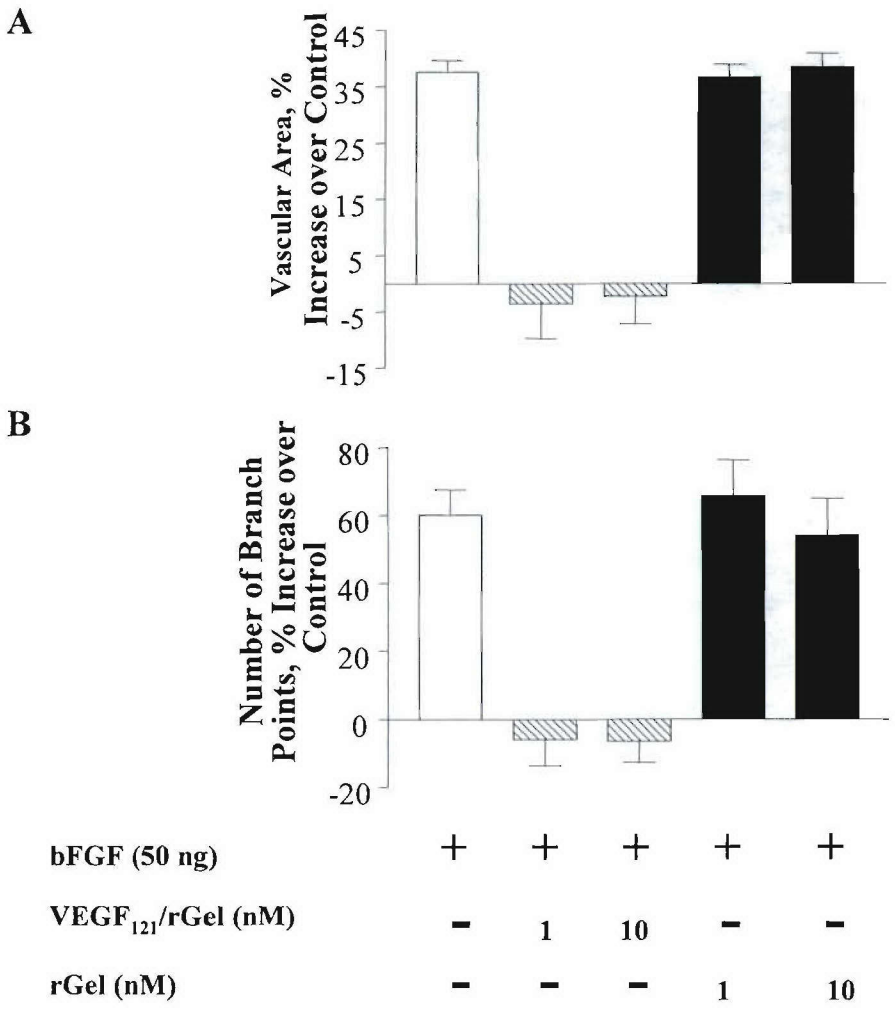
A
Vascular Area, % Increase over Control
45
35
25
15
5
-5
-15
B
Number of Branch Points, % Increase over Control
80
60
40
20
0
-20
bFGF (50 ng)
+ + + + +
VEGF121/rGel (nM)
- 1 10 - -
rGel (nM)
- - - 1 10

Figure 10